THALASSAEMIA AND IRON-INDUCED CARDIAC FAILURE: DEVELOPMENT OF A METHOD TO QUANTIFY MYOCARDIAL IRON AND ITS APPLICATION FOR CLINICAL MANAGEMENT

MD THESIS

LISA JUDITH ANDERSON

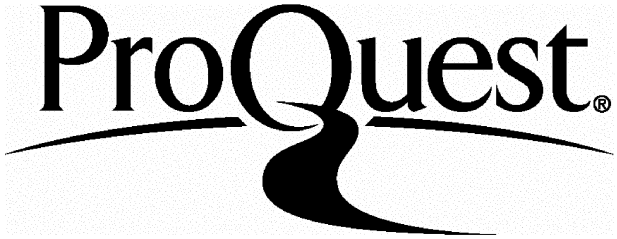

ABSTRACT

BACKGROUND Iron-induced heart failure is the commonest cause of death in thalassaemia major. The cardiomyopathy is reversible when treated early, but once heart failure is established it is often rapidly progressive, and unresponsive to treatment. Our aim was to develop and validate a non-invasive measurement of myocardial iron in order to allow earlier diagnosis and treatment.

METHODS AND RESULTS We have developed and validated a new magnetic resonance (MR) T2* technique for the measurement of tissue iron. There was a highly significant, inverse correlation between iron concentration by liver biopsy and liver T2* ($r=0.93$, $p<0.0001$). Inter-study reproducibility was 5.0% in the heart and 3.3% in the liver. As myocardial iron increased, there was a progressive decline in ejection fraction ($r= 0.61$, $P<0.0001$), associated with a progressive increase in left ventricular mass and end systolic volume. Myocardial iron content cannot be predicted from serum ferritin or liver iron, the conventional markers of tissue iron deposition, and assessments of cardiac function alone detect only those with advanced disease. Multivariate analysis to relate left ventricular ejection fraction to clinical parameters including age, liver iron and serum ferritin identified myocardial T2* as the only independent predictor (odds ratio 7.0, $p<0.0001$). In a small, prospective study of patients with cardiac involvement we demonstrated that intensification of iron-chelation therapy leads to removal of iron from the heart and reversal of the cardiomyopathy. A controlled comparison study of the iron-chelating agents, deferiprone and desferrioxamine, suggests that deferiprone is more effective in removing iron from the heart than standard treatment with desferrioxamine.

CONCLUSIONS This MR T2* technique provides a simple, robust assessment of myocardial iron deposition. Early identification and treatment of patients with myocardial iron overload should reduce the excess mortality and morbidity from this reversible cardiomyopathy.

CONTENTS

RESULTS

CHAPTER 1: SUMMARY AND OBJECTIVES

Thalassaemia major is an inherited anaemia, which is fatal without recurrent transfusions. Although relatively rare in the UK, the beta-thalassaemias are the commonest single gene disorders world-wide. As socio-economic conditions in developing countries improve, more children are being transfused, and are developing normally only to die from iron overload in their teens and early twenties [Weatherall 1996a]. Even in the UK, where iron-chelation therapy was first introduced and treatment has been uninterrupted from the early 1970s to the present day, only 50% of patients currently survive to the age of 35 [Modell 2000]. The major cause of death is iron-induced heart failure, a potentially reversible condition provided it is detected early and appropriate augmentation of iron-chelation treatment is instituted in time. Until now, detection of the cardiomyopathy has been problematic as only indirect markers of cardiac iron were available and systolic dysfunction detected by echocardiography is known to be a poor and late marker of cardiac involvement [Henry 1978, Nienhuis 1980]. Once heart failure develops the outlook is poor and many patients die within the first few months of diagnosis [Ehlers 1981]. Myocardial biopsy has never been routinely practised due to the invasive nature of the technique and the potential for sampling error in the case of inhomogeneous iron deposition. A method for quantifying myocardial iron would allow earlier diagnosis and treatment and has the potential to reduce the mortality from this reversible cardiomyopathy, but until now an established technique has not existed.

For the purposes of studying iron-induced cardiomyopathy, thalassaemic patients form a unique model. They are a genetically pre-defined group, and cardiac involvement is regrettably common, resulting in death from heart failure in more than 60% of patients [Zurlo 1989]. In addition, transfusional iron-overload progresses at such a rapid rate that the cardiomyopathy presents at a young age when cardiac disease due to other causes (once congenital anomalies are excluded) is extremely rare. Finally, two major centres of expertise for thalassaemia are based in London, at the Whittington Hospital (Dr Beatrix Wonke) and University College Hospital (Professor John Porter), which supervise the care of more than

half of UK thalassaemic patients. Advice and close collaboration from these two centres has been an important factor in the progress of this study.

Early in the development of clinical magnetic resonance it was noticed that iron-loaded tissues appear blackened or dark on magnetic resonance (MR) images [Stark 1983, Brasch 1984]. These findings have triggered a series of efforts to quantify the relationship between tissue iron concentration and decreased image signal intensity. Gradient-echo techniques have recently been shown to quantify iron over limited ranges in the liver. As expertise in cardiovascular MR (CMR) imaging is rapidly developing and as it is theoretically possible to quantify tissue iron with MR, we attempted to develop a non-invasive technique for the measurement of iron in the heart. The following chapters describe the development of the T2* technique and our subsequent clinical findings in a large cohort of thalassaemic patients.

In Chapter 4, I describe the development and validation of the new T2* technique for the measurement of myocardial iron. In Chapter 5, the technique is applied to 106 thalassaemic patients, and the relation between myocardial iron and ventricular remodelling is examined. In Chapter 6, we investigated the relation between ventricular function and the conventional markers of myocardial iron; serum ferritin and liver iron. In Chapter 7, the variability of iron deposition between organs is examined. Chapter 8 incorporates the results of a prospective trial of intensive iron-chelation in a small group of patients with cardiac iron involvement. Chapter 9 illustrates the outcome after long-term iron chelation with the oral iron-chelator, deferiprone, in a small cohort of patients compared to a control group treated with standard subcutaneous desferrioxamine. In summary, the work suggests that conventional measurements of myocardial iron are inadequate, and early detection of cardiac iron with the T2* technique should improve mortality from this reversible cardiomyopathy.

CHAPTER 2: THALASSAEMIA AND IRON-INDUCED CARDIOMYOPATHY

2.1 HISTORY, DISTRIBUTION AND PREVALENCE

Thalassaemia major is characterised by chronic severe anaemia, responsive only to transfusions, and by increased iron deposition in the tissues. The disorder was first recognised in 1925 by Thomas Cooley, who described a series of infants who became profoundly anaemic and developed splenomegaly over the first year of life. In 1936, the pathological changes were described by Whipple and Bradford, who observed that many of their patients came from the Mediterranean region and coined the word thalassaemia from the Greek *'thalassa'*, meaning 'the sea'. More recently it has become clear that the disorder is not localised to this area, but occurs widely in a broad belt ranging from the Mediterranean and parts of north and West Africa through the Middle East and Indian subcontinent to Southeast Asia (figure 2.1). The thalassaemias are the commonest single-gene disorders worldwide and estimates of gene frequencies range from 3 to 10% in some areas. Globally, there are approximately 94 million heterozygotes for beta thalassaemia and up to 60,000 affected homozygote infants are born each year [Weatherall 1996b]. As social conditions improve in developing countries and childhood mortality from infection and malnutrition declines, children with thalassaemia are now surviving long enough to require treatment. This makes the management of the disease of increasing importance not only in parts of the world where the disease is particularly common but for any country which has an immigrant population from these regions. In a British study of Asian children in Northwest London, 4% were found to be heterozygous carriers for beta thalassaemia, [Earley 1990] and there are estimated to be 800 homozygotes in the UK. Beta thalassaemia also arises sporadically in every racial group [Trent 1990, Hall 1992].

Figure 2.1 Global Distribution of Thalassaemia Major

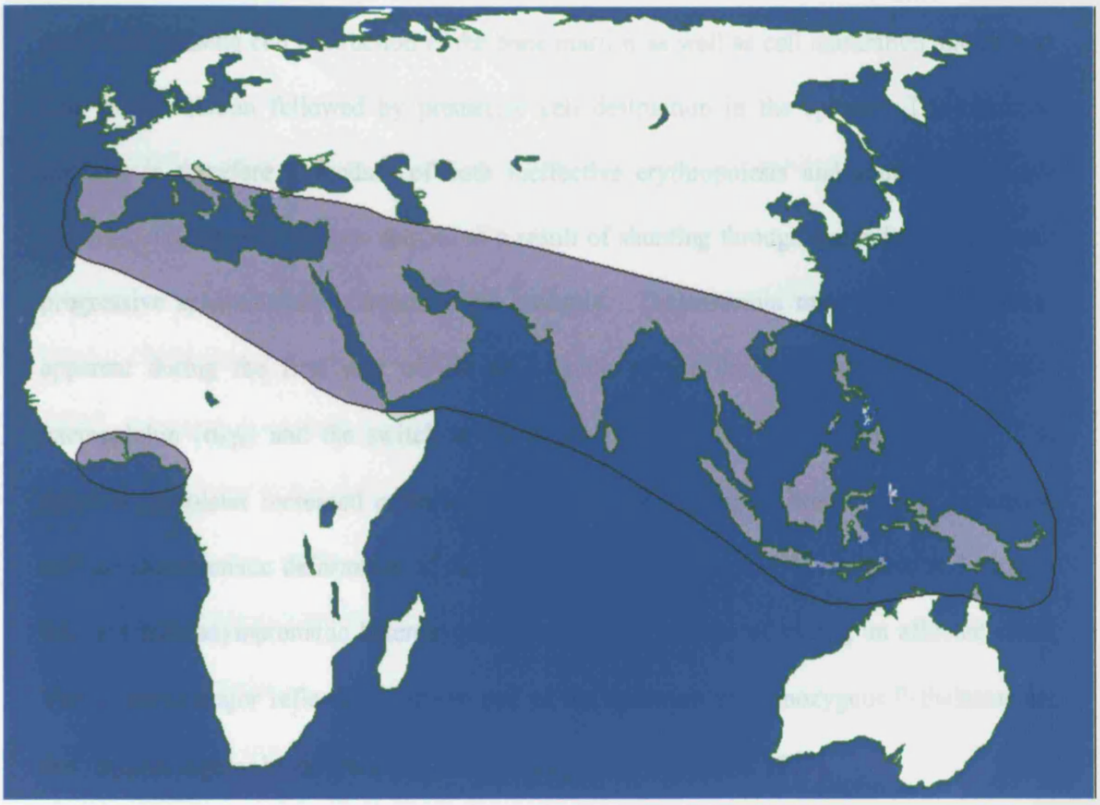

2.2 Molecular Pathology and Pathophysiology of β-Thalassaemia

Within each population at risk for β-thalassaemia a small number of common mutations are found and it is therefore believed that β-thalassaemia arose independently in several different populations [Flint 1993]. There is some evidence for enhanced protection against falciparum malaria in heterozygote symptomless carriers [Weatherall 1987], which may account for the continued transmission of these genes. Nearly 200 different mutations can produce the phenotype of β-thalassaemia. These mutations result either in the absence of β-globin chains (β^0 thalassaemia) or a reduction in their output (β^+ thalassaemias). Most mutations are nucleotide substitutions within the β-globin cluster although a few are deletions [Weatherall 1994]. Because so many different β-thalassaemia mutations exist, many patients who are apparently homozygotes are actually compound heterozygotes for two different mutations.

Despite absent or reduced β-chain production, α-chain synthesis proceeds at a normal rate, resulting in an excess of α-chains. These α-chains are unstable and precipitate in the red cell precursors causing cell destruction in the bone marrow as well as cell maturation and release into the circulation followed by premature cell destruction in the spleen. The resulting anaemia is therefore a product of both ineffective erythropoiesis and shortened red-cell survival. Increases in plasma volume as a result of shunting through expanded marrow and progressive splenomegaly exacerbate the anaemia. Thalassaemia major usually becomes apparent during the first year of life as a result of the decline in synthesis of foetal haemoglobin ($\alpha_2\gamma_2$) and the switch to the production of adult haemoglobin ($\alpha_2\beta_2$). The anaemia stimulates increased erythropoietin production leading to bone marrow expansion and the characteristic deformities of the skull and face. Inheritance is recessive and couples who are both asymptomatic heterozygotes have a 25% chance of having an affected child. Thalassaemia major reflects the severe end of the spectrum of homozygous β-thalassaemia and requires regular blood transfusions to prolong life [Weatherall 1997].

2.3 Iron Overload

Iron overload of tissue is the most important complication of β-thalassaemia [Olivieri 1997]. When the anaemia is corrected by blood transfusion, the erythropoietic drive is switched off and thalassaemic children grow normally without bone deformities. However, the combination of transfusional iron (200mg per transfusion) and an inappropriate increase in intestinal absorption [Brittenham 1994a], leads to an inexorable accumulation of iron in the body tissues. Eventually, extensive iron-induced injury develops in the heart [Buja 1971], liver [Risdon 1973], pancreas [Lassman 1974] and endocrine system [Grundy 1994].

The human body has no mechanism for excreting excess iron, which is stored as crystalline iron oxide within ferritin and haemosiderin in the body. At normal body iron levels, plasma iron is bound to transferrin, preventing catalytic activity and free radical production [Hershko 1987a]. The combination of excess gastrointestinal iron absorption and catabolic iron from

red cell breakdown in the reticulo-endothelial system exhausts the iron binding capacity of transferrin resulting in the emergence of non-transferrin bound plasma iron (NTBI) [Hershko 1978]. The toxicity of NTBI is much higher than bound iron, and promotes hydroxyl radical formation resulting in peroxidative damage to membrane lipids and proteins [Gutteridge 1985]. NTBI is taken up more readily by cardiac myocytes than transferrin bound iron [Link 1985] and whereas transferrin bound iron uptake is reduced by the down regulation of transferrin receptors, NTBI uptake is increased in the presence of high levels of tissue iron [Parkes 1993]. In the heart, intracellular iron results in impaired Na-K-ATPase activity [Link 1994], increased lysosomal fragility [Link 1993] and impaired mitochondrial respiratory chain activity [Link 1996], and is manifested clinically as heart failure [Hershko 1998].

2.4 Iron Deposition in the Heart

2.4.1 Pathophysiology

Iron deposition in the heart has been reported to follow a characteristic pattern [Buja 1971]. The ventricular walls contain the most iron, and the atria and conduction system contain less amounts [James 1964, Schellhammer 1967]. The presence of supraventricular tachycardia correlates with the extent of iron deposition found in the atria [Buja 1971]. There is also a marked difference in the extent of iron deposition in the ventricular wall, with the epicardial layer containing the most iron [Buja 1971, Fitchett 1980, Olson 1987]. The degree of cardiac dysfunction is considered to depend on the quantity of iron deposited in individual myocardial fibres and the number of fibres affected. In patients with only mild cardiac dysfunction, iron deposits are usually limited to the perinuclear areas, with only a few fibre cells involved, whereas in patients with significant cardiac dysfunction, iron deposits occupy large areas of the of myocardial fibre cells [Buja 1971]. The relatively mild degree of fibrosis in most autopsy studies suggests that even when advanced, the cardiomyopathy may be potentially reversible [Buja 1971, Olson 1987 and 1989]. The iron is stored in intracellular lysosomes in the relatively non-toxic forms of ferritin or haemosiderin but once a critical concentration is reached, NTBI is released and the cell begins to fail. The toxicity of iron to heart cells does

not depend on intracellular iron concentration alone. It is also highly dependent on oxidative state. Reduction of ferric to ferrous iron promotes hydroxyl radical formation via the Haber-Weiss reaction [Halliwell 1990]. Ascorbic acid, a natural reducing agent, accelerates iron-induced lipid peroxidation at low concentrations but acts as an antioxidant at high concentrations [Link 1985], and it has been reported that ascorbate supplementation may be associated with clinical deterioration in patients with overt cardiac failure due to iron overload [Nienhuis 1981]. Conversely, α-tocopheryl reduces iron-induced lipid peroxidation initiated by free radicals [Hershko 1987b, Link 1989a]. In addition, intracellular acidosis causes increased quantities of NTBI to be released from ferritin [Voogd 1992].

2.4.2 Clinical Presentation

Cardiac failure secondary to transfusional iron overload remains the commonest cause of death in patients with thalassaemia major [Zurlo 1989, Olivieri 1994]. In the United Kingdom, approximately 50% of patients die before reaching the age of 35, figure 2.2 [Modell 2000]. The cardiomyopathy is reversible if iron chelation treatment is intensified in time, but the diagnosis is often delayed by the unpredictability of cardiac iron deposition and the late development of symptoms and echocardiographic abnormalities [Henry 1978, Nienhuis 1980]. Once heart failure develops, the outlook is usually poor [Felker 2000] despite intensive chelation, figure 2.3.

The cardiac complications of thalassaemia major were first described prior to the introduction of chelation therapy [Engle 1964]. Engle described an increase in heart size after 10 years of age with first-degree heart block in a third of the patients. Episodes of pericarditis occurred in half of the patients after 11 years of age. Congestive cardiac failure developed at a mean age of 16 years. As heart failure progressed, AV block worsened and either complete heart block, right or left bundle branch block occurred in a third of patients. Atrial arrhythmias were noted in half and repetitive ventricular tachycardia was present in a minority. The duration of life after the onset of failure was less than 3 months in over half of the patients. There has been

little improvement in prognosis once cardiac complications occur, despite advances in diagnostic cardiology and chelation therapy [Ehlers 1991].

Figure 2.2 Survival Curves for Thalassaemia Major in the UK

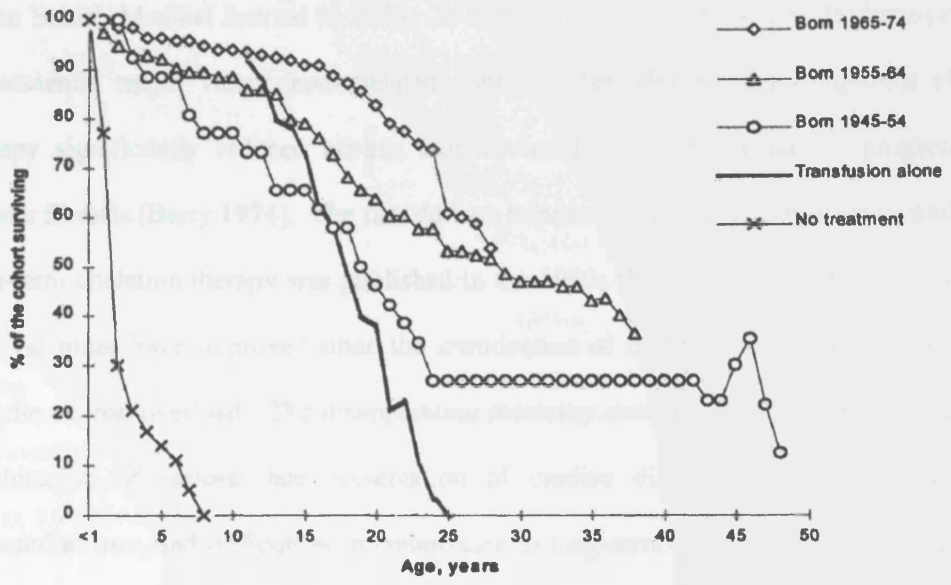

From Modell et al, Lancet 2000: 355: 2051-2. Prior to transfusion therapy patients died in early childhood. Following the introduction of chelation therapy, patients died in their teens from iron-induced heart failure. The cohort born between 1945-54 died from iron overload until the introduction of desferrioxamine. The cohort born 1965-74 should demonstrate the results of chelation therapy. Initial survival was promising but there has been 25% mortality in the last 5 years: survival for this cohort is only 50% to age 30.

Figure 2.3 Late Presentation of Thalassaemic Cardiomyopathy

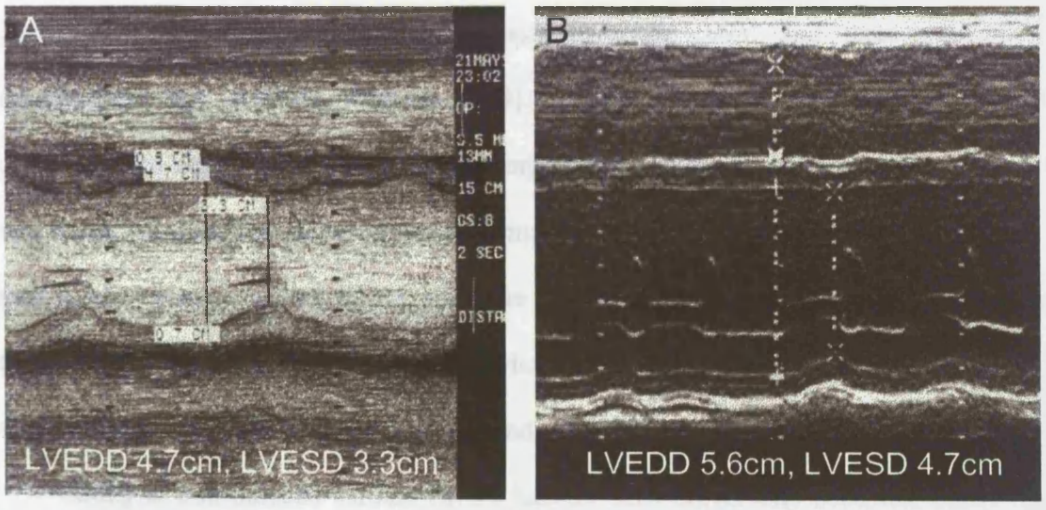

Panel A. Routine echocardiogram of a 27 year-old female with thalassaemia major.
Panel B. Eighteen months later the patient presented with severe fatigue, and despite continuous intravenous iron chelation, died five weeks later in low output cardiac failure.

2.4.3 Iron Chelation Therapy and the Reversibility of Iron-induced Cardiomyopathy

The iron chelator desferrioxamine was first introduced more than 30 years ago [Sephton-Smith 1964], but its value was not recognised until the publication of findings by Barry et al in the British Medical Journal in 1974. In a trial of daily intramuscular desferrioxamine in thalassaemia major versus non-chelated controls, they showed that long-term chelation therapy significantly reduced hepatic iron accumulation and slowed the progression of hepatic fibrosis [Barry 1974]. The first data on improved survival in thalassaemic patients on long-term chelation therapy was published in the 1980s [Modell 1982]. However, although survival times have improved since the introduction of chelation treatment, many patients still die of iron overload. The disappointing mortality statistics [Modell 2000] are due to a combination of factors: late presentation of cardiac disease, difficulties in assessing myocardial iron, and difficulties in compliance to long-term treatment with daily parenteral iron chelation regimes.

The potential reversibility of iron induced cardiomyopathy was first documented in case reports of patients with hereditary haemochromatosis treated with recurrent venesection [Easley 1972, Short 1981, Rivers 1987]. Subsequently, improvement of ventricular dysfunction with chelation therapy have been reported in a patient with megaloblastic anaemia [Rahko 1986], thalassaemia major [Wacker 1993] and three patients with transfusional iron overload [Marcus 1984]. It has also been reported that intensified chelation with high dose subcutaneous desferrioxamine reversed subtle exercise-induced left ventricular dysfunction detected by radionuclide ventriculography [Freeman 1983]. In studies of cardiac myocytes, desferrioxamine has been shown to remove iron from the cells, reverse lipid peroxidation [Link 1985, Hershko 1987b], and reverse the iron-induced abnormalities of cellular contractility and rhythmicity [Link 1989b]. However, the reversibility of iron-induced cardiac failure has not been universally accepted, partly due to the high mortality of patients presenting with advanced cardiac failure despite chelation treatment [Marcus 1984] and more recently by those questioning the role of iron in thalassaemic cardiomyopathy [Krematinos 1995 and 1999].

Figure 2.4 Reversibility of Iron-induced Cardiomyopathy

A 22 year old patient presented with a non-sustained ventricular tachycardia after 5 minutes of exercise testing and a dilated, poorly functioning left ventricle. Left ventricular end diastolic dimension (LVEDD) 5.5cm, left ventricular end systolic dimension (LVESD) 4.7cm. An indwelling central venous line was inserted and continuous intravenous desferrioxamine commenced. By the following year ventricular function had significantly improved (LVEDD 5.3cm, LVESD 4.4cm) and by 1998 ventricular dimensions had normalised and the patient completed 12 minutes of Bruce protocol exercise testing (LVEDD 4.6cm, LVESD 2.8cm).

2.4.4 Pre-clinical Diagnosis of Iron Induced Cardiomyopathy

The diagnosis of iron-induced cardiomyopathy is challenging. Detection of absolute cardiac iron levels is difficult, and overt systolic dysfunction presents late in the disease process [Henry 1978, Nienhuis 1980] when intensive chelation therapy is less likely to improve the prognosis. Many attempts have been made to develop a non-invasive means of detecting those patients who are most at risk. Increased left ventricular mass, volume and left atrial dimensions were described in a group of 56 thalassaemic patients compared to normal controls using M-mode echocardiography, and the authors found this method to be more sensitive than chest Xray or electrocardiography in detecting abnormalities [Henry 1978]. However only four patients had abnormal left ventricular ejection fractions, all of whom died within a 6-month follow-up period, illustrating that systolic dysfunction is a late marker of cardiac involvement and associated with a poor prognosis. Lewis et al described similar findings in 23 thalassaemic patients [Lewis 1978]. All had normal left ventricular ejection fractions yet one died of heart failure within 3 months of the echocardiographic examination. Valdes-Cruz described slower left ventricular posterior wall relaxation in 13 patients with thalassaemia major compared to healthy normal controls [Valdes-Cruz 1982]. However

Kremastinos et al found no significant differences in segmental left ventricular systolic or diastolic function between thalassaemic patients and controls or between thalassaemic patients with or without symptoms of heart failure [Kremastinos 1985]. Spirito et al described abnormal diastolic filling in thalassaemia major patients [Spirito 1990], and diastolic filling parameters have been reported to be predictors of cardiac outcome in thalassaemia major [Hou 1994]. However Kremastinos et al found that doppler diastolic indexes in β-thalassaemia major patients were similar to those seen in conditions with an increased preload, and attributed these changes to chronic anaemia [Kremastinos 1993]. Using M-mode, two-dimensional and doppler-echocardiography, Ceccheti et al found increased thickness of the left ventricle to be the only preclinical finding in 36 patients with iron overload secondary to haemochromatosis [Cecchetti 1991]. Systolic dysfunction was present in only three of these patients, two of whom died rapidly from cardiovascular complications. Increased myocardial reflectivity on echocardiographic images has also been reported [Lattanzi 1993], but no significant correlation was found between myocardial reflectivity and total number of transfusions or the left ventricular mass index. In summary to date, no clear echocardiographic criteria have been established for the pre-clinical detection of iron-induced cardiomyopathy.

Using exercise radionuclide angiography, Leon et al established that in 24 patients with transfusional iron overload, 21 had normal ejection fractions at rest but ejection fraction during exercise was normal in only 11 patients. Significantly more patients in the abnormal group had received in excess of 100 units of blood [Leon 1979]. The drawbacks of this method are the inability to specify the aetiology of the cardiac abnormality [Rozanski 1983], and the requirement for intravenous administration of the radionuclide agent, which is unpopular with these young patients. Despite the availability of echocardiography and radionuclide stress angiography, cardiological evaluation of thalassaemic patients remains problematic, and the progression from mildly abnormal echocardiographic parameters to fulminant cardiac failure is often rapid and relentless.

2.5 Assessment of Tissue Iron Stores

Due to the variability in iron deposition between and within different organs, there is no single measurement of body iron that is entirely satisfactory. The measurement of serum ferritin is the most commonly used indirect estimate of body iron stores [Finch 1986, Pippard 1989]. In normal individuals, the amount of plasma ferritin synthesised and secreted is proportional to the intracellular ferritin produced during iron storage, so that plasma ferritin concentration is related to the magnitude of body iron stores [Addison 1972, Cazzola 1983]. However, serum ferritin only reflects the proportion of stored iron that is in transition in the blood, representing only 1% of the total iron storage pool. In addition, interpretation of ferritin values may be complicated by a variety of conditions that alter concentrations independently of iron burden, including inflammation [Baynes 1986], ascorbic acid deficiency [Chapman 1982], hepatic dysfunction and ineffective erythropoiesis. All these factors are common in thalassaemic patients, in whom iron status has been shown to account for only 57% of the variation in plasma ferritin concentration [Brittenham 1993]. As a consequence, reliance on serum ferritin alone can lead to an inaccurate assessment of body iron stores in individual patients.

To date, measurement of hepatic iron concentration by liver biopsy is considered the most quantitative and sensitive method for determining the body iron burden [Overmoyer 1987]. However, this is an invasive technique with a low but recognised complication rate and hepatic fibrosis (common in thalassaemics as a result of increased liver iron and hepatitis C infection) is known to cause considerable variability in measured iron concentrations from small liver biopsies [Villeneuve 1996, Edmond 1999]. Iron has been shown to be unevenly distributed in the thalassaemic liver even in the non-cirrhotic stages [Ambu 1995]. Therefore a single liver biopsy cannot be assumed to reliably represent the mean hepatic iron concentration. Furthermore, measurement of liver iron can only be an effective indicator of cardiac iron stores if iron is assumed to be stored predictably and homogeneously throughout the body.

Endomyocardial biopsy has been used to evaluate iron deposition in the heart in thalassaemia [Barosi 1989, Lombardo 1995], but has never become a routine part of patient management. This is partly due to the invasiveness of the technique in an ostensibly healthy patient group, and partly due to inhomogeneous deposition of iron in the heart [Buja 1971, Fitchett 1980]. In addition, iron has been reported to be absent from the right ventricular subendocardium in some patients with cardiac iron overload [Olson 1987].

Because of these problems, we decided to investigate the possibility of developing a new MR technique to measure myocardial iron.

CHAPTER 3: MAGNETIC RESONANCE AND THE DETECTION OF TISSUE IRON DEPOSITION

3.1 BASIC PRINCIPLES OF IMAGE CREATION

3.1.1 The Hydrogen Nucleus

The hydrogen nucleus contains a single proton and is widely used for clinical magnetic resonance imaging due to its abundance in living tissues and because the solitary proton has a relatively large magnetic moment. The positively charged proton spins and induces a small magnetic field around itself.

3.1.2 Proton Alignment

In the absence of an applied magnetic field the magnetic vectors or moments of the hydrogen nuclei are randomly orientated. When placed in an external, applied magnetic field the magnetic moments of the hydrogen nuclei align with the field (figure 3.1). More protons align in the direction of the magnetic field than against it resulting in a net magnetic vector parallel to the field, B_0, and it is this net magnetisation vector (NMV) that is used to generate clinical MR images. The protons aligned parallel to the magnetic field are in a low energy state and the protons aligned anti-parallel to the magnetic field are in a high energy state.

Figure 3.1 Alignment to the external magnetic field

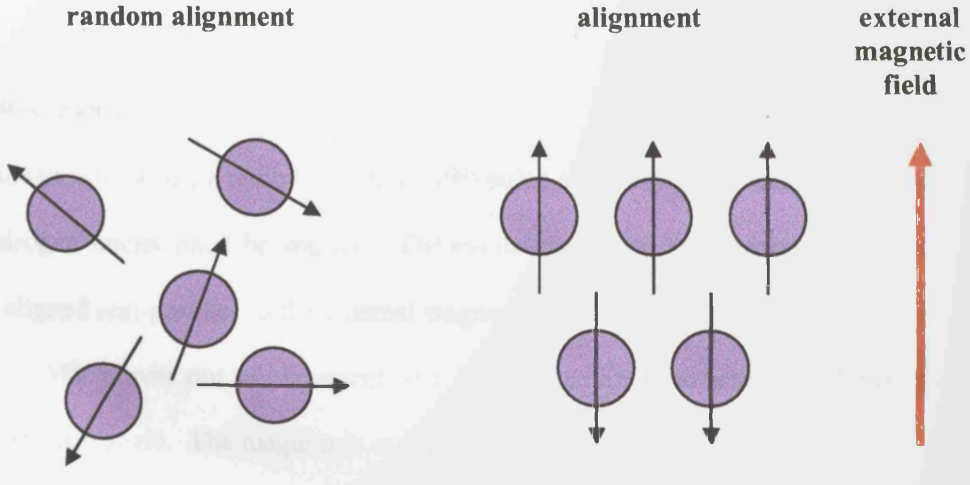

3.1.3 Precession

When aligned with the external magnetic field, the protons follow a circular path about B_0 called precession (figure 3.2). The speed with which the net magnetisation vector precesses about B_0 is called the precession frequency, which can be calculated from the Larmor equation:

$$\omega_0 = \gamma B_0$$

Where ω_0 is the precessional frequency in megahertz (MHz), B_0 is the field strength of the magnet in tesla (T) and γ is the gyro-magnetic ratio (MHz/T). The gyro-magnetic ratio is a constant and is expressed as the precessional frequency of an MR active nucleus at 1.0T.

Figure 3.2 Precession

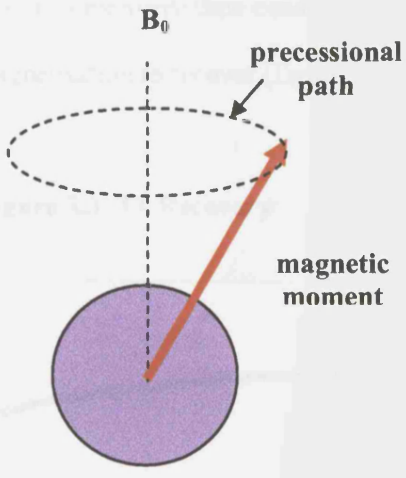

3.1.4 Resonance

For resonance to occur, a radio frequency (RF) pulse at exactly the precessional frequency of the hydrogen nuclei must be applied. The excitation causes an increase in the number of nuclei aligned anti-parallel to the external magnetic field, B_0. The result of this excitation is that the NMV moves out of alignment with B_0, and the angle to which the NMV moves is termed the flip angle. The magnitude of the flip angle depends on the amplitude and duration of the RF pulse. If the flip angle is 90^0, the NMV is flipped from a longitudinal plane, in line

with B_0, to a transverse plane, where it precesses at the Larmor frequency. The RF pulse causes the magnetic moments of all the hydrogen nuclei to precess in phase with each other. The NMV in the transverse plane induces a voltage in the receiver coil, producing the MR signal. The frequency of the MR signal is also at the Larmor frequency.

3.1.5 Relaxation

When the RF pulse is switched off, the NMV starts to realign with B_0. In order to do so, the NMV loses the energy absorbed from the RF pulse. This process is termed relaxation. As relaxation occurs, the amount of magnetisation in the longitudinal plane recovers as the NMV realigns with B_0, and the magnetisation in the transverse plane decays as the nuclei lose phase coherence. The recovery of longitudinal magnetisation is termed T1 recovery and is caused by the nuclei transferring energy to the surrounding tissue or lattice (spin-lattice relaxation). The rate of recovery is exponential, with a recovery time constant T1 that represents the time taken for 63% of the longitudinal magnetisation to recover (figure 3.3).

Figure 3.3 T1 Recovery

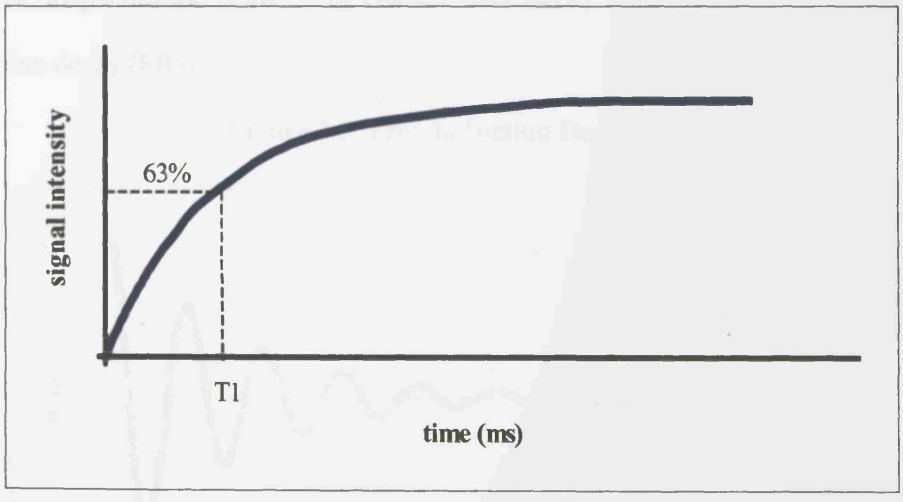

The decay of transverse magnetisation in a perfectly homogenous field is termed T2 decay and is caused by nuclei exchanging energy with other nuclei (spin-spin relaxation). The rate of decay is also exponential with a time constant T2 that represents the time taken for 63% of the transverse magnetisation to be lost (figure 3.4).

Figure 3.4 T2 Relaxation

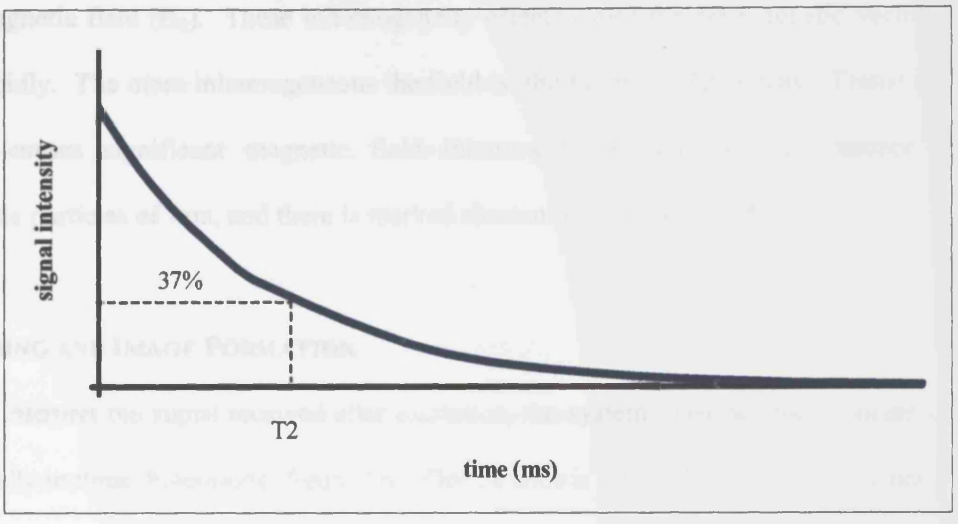

3.1.6 T2* Decay and the Free Induction Decay Signal

When the RF pulse is turned off, the alternating signal from the receiver coil decays rapidly, as transverse magnetisation is lost. The characteristic decay signal (figure 3.5) is termed the free induction decay (FID).

Figure 3.5 Free Induction Decay

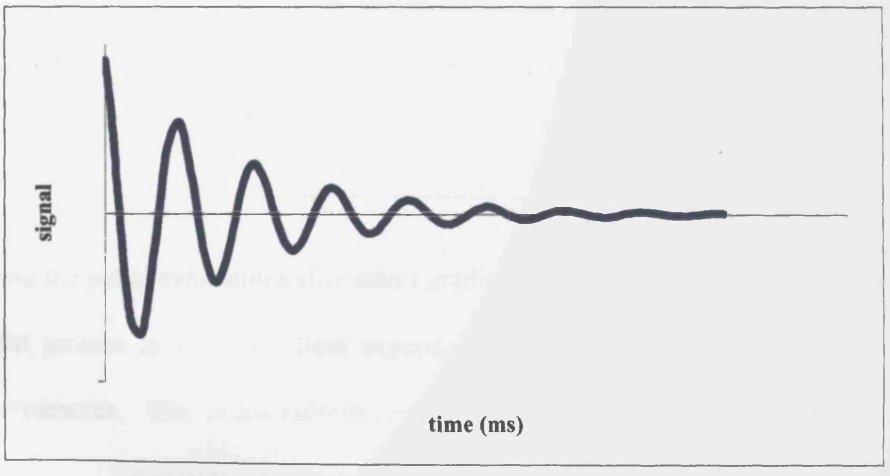

The rate of decay of the FID signal is determined by T2* relaxation time. T2* decay is faster than T2 decay because it results from the combination of T2 (spin-spin) relaxation and dephasing due to magnetic field inhomogeneities. As stated by the Larmor equation, nuclei in an area of slightly higher magnetic field will precess at a higher frequency and nuclei in an area of lower magnetic field will precess at a lower frequency than nuclei elsewhere in the external magnetic field (B_0). These inhomogeneity effects cause the net magnetic vector to dephase rapidly. The more inhomogeneous the field is, the faster the T2* decay. Tissue iron deposition causes significant magnetic field inhomogeneities due to the presence of paramagnetic particles of iron, and there is marked shortening of T2 and T2*.

3.2 Encoding and Image Formation

In order to interpret the signal received after excitation, the system must be able to locate the signal spatially in three dimensions (figure 3.6). Once a slice is selected, the signal is located or encoded along both axes of the image slice. Spatial encoding is performed by magnetic gradients.

Figure 3.6 The X, Y and Z gradient axes

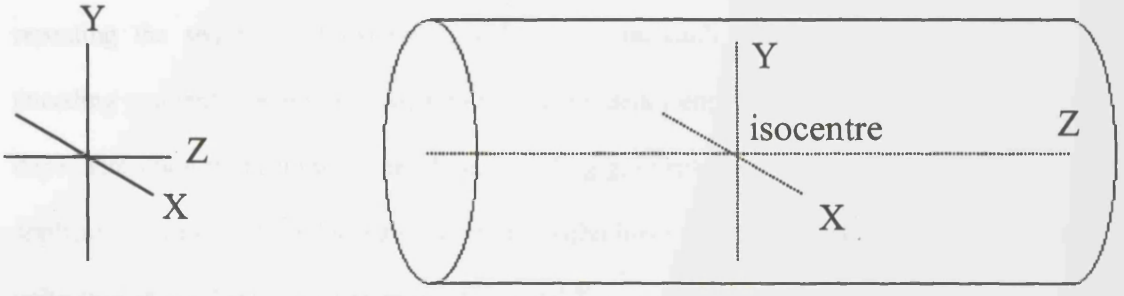

Firstly, during the initial excitation a slice select gradient is applied perpendicular to the imaging plane so that protons in different slices experience different magnetic fields and precess at different frequencies. The initial radiofrequency pulse of a single frequency will then only excite a thin slice of the patient, and any resulting signal will come only from that slice. When a patient lies in the long-axis of the scanner, the Z gradient will therefore select axial slices, the X

gradient selects sagittal slices and the Y gradient selects coronal slices. Oblique slices are formed by employing a combination of gradients. The slice thickness depends on the slice select bandwidth and the slope of the slice select gradient. In spin-echo sequences, the slice select gradient is switched on during the application of both the 90^0 and the 180^0 pulses, to excite and rephase each slice. In gradient-echo sequences, the slice select gradient is switched on during the excitation pulse only.

Once a slice has been selected, the signal must be located along both axes of the image. While the signal is being received, another magnetic gradient called the frequency encoding or read-out gradient is applied perpendicular to the slice select gradient, which forces different lines within the plane to emit signals at different frequencies. The amplitude at each frequency is determined by a technique called Fourier transformation, which resolves the signal in the read-out gradient direction. This is equivalent to the transformation of signal strength against time curve into one representing signal strength versus frequency. Spatial encoding in the third dimension is achieved using a magnetic gradient called the phase encoding gradient, which is applied just before signal acquisition. This is repeated many times (typically 128 or 256 steps for cardiac imaging) and its magnitude is raised from negative through zero to positive, in a series of small increments. This has the effect of altering the phase of precession of the protons by an amount dependent upon their position in each line that is frequency encoded. By repeating the sequence of excitation and acquisition each time with an increasing phase encoding gradient, the phase of each point in a frequency encoded line varies with a frequency dependent upon its position. The phase encoding gradient is usually switched on just before application of the 180^0 rephasing pulse in spin-echo imaging and between excitation and signal collection in gradient-echo imaging. A second Fourier transformation in the phase encoding direction then extracts the amplitude information along this third dimension, and amplitude can be assigned to individual points in the image.

3.3 DATA COLLECTION

The application of all the gradients selects a slice and produces a frequency shift along one axis and a phase shift along another. When data of each signal position is collected, the information is stored in K space before being converted into the final image. K space is rectangular with two axes perpendicular to each other. The phase axis is horizontal and the frequency axis is vertical. Both axes are centred in the middle of K space. In order to fill out different lines of K space, the slope of the phase encoding gradient must be altered after each repeat time. The number of lines of K space that are filled is determined by the number of different phase encoding slopes that are applied. The slope of the phase encoding gradient determines the magnitude of the phase shift between two points in the patient. The lines nearest to the phase axis are the central lines, which are filled after the application of shallow phase encoding gradients. Shallow phase encoding slopes do not produce a large phase shift along their axis. The resultant signal has large amplitude but low spatial resolution. The lines furthest away from the phase axis both positively and negatively are filled after the application of steep phase encoding gradients. The resultant signal has small amplitude but high spatial resolution. The vertical axis of K space corresponds to the frequency encoded axis. The centre of an echo (with maximum amplitude as all the protons are in phase) is placed central to the frequency axis and the rephasing and dephasing portions of an echo are placed either side of the frequency axis.

3.4 MAGNETIC RESONANCE PULSE SEQUENCES USED IN IMAGING

3.4.1 Spin-Echo Sequences

The spin-echo pulse sequence uses a 90^0 RF excitation pulse to flip the net magnetic vector into the transverse plane. After the RF pulse a free induction decay signal is produced. After a time delay t, a 180^0 RF pulse is applied which moves the net magnetic vector through 180^0, reversing the direction of precession of the NMV in the transverse plane. The magnetic moments of the nuclei immediately begin to rephase and signal increases in the receiver coil until a maximum signal at a time 2t after the initial 90^0 pulse when the magnetic moments are precessing in phase once again. This maximum signal is called the spin-echo (figure 3.7). As

the 180^0 pulse compensates for the magnetic field inhomogeneities – T2* effects – the resulting decay in a spin-echo signal is due to T2 effects alone.

Figure 3.7 The spin-echo sequence

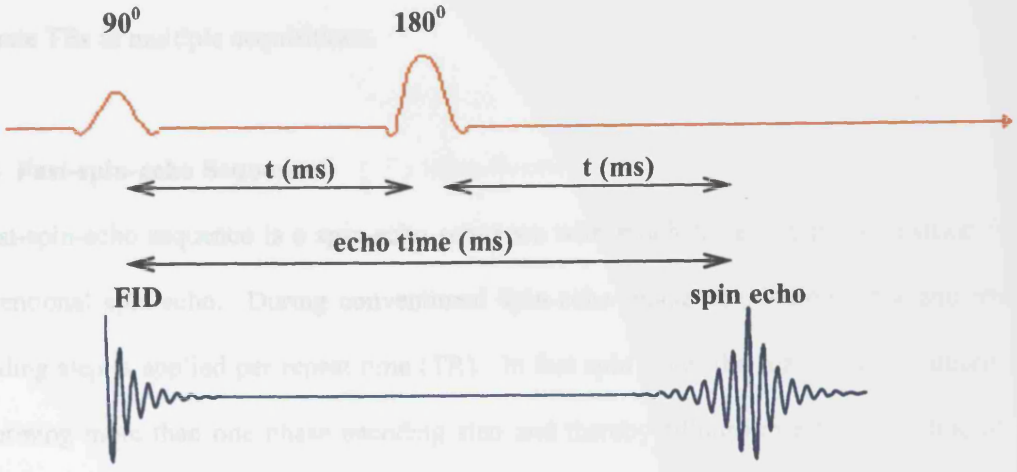

3.4.2 Multi-Echo Spin-Echo Sequences

Multiple echoes with increasing echo times (TE) can be generated from a spin-echo sequence by using a succession of 180^0 rephasing pulses (figure 3.8).

Figure 3.8 Multi-echo spin-echo sequence

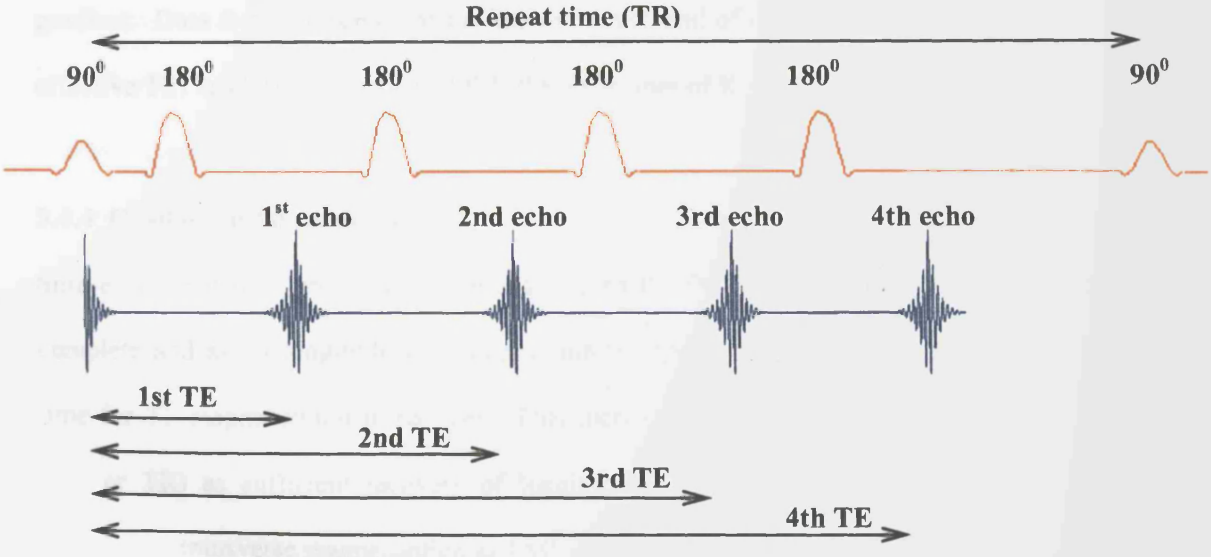

As T2 decay increases with increasing echo time, the T2 contrast increases as image signal intensity decreases with each sequential echo. This type of sequence can be used in the measurement of T2 relaxation times, using multiple TEs in a single acquisition rather than separate TEs in multiple acquisitions.

3.4.3 Fast-spin-echo Sequences

A fast-spin-echo sequence is a spin-echo sequence with much faster image acquisition than conventional spin-echo. During conventional spin-echo image acquisition, only one phase encoding step is applied per repeat time (TR). In fast spin echo, the scan time is reduced by performing more than one phase encoding step and thereby filling more than one line of K space per TR. This is achieved by using a train of 180^0 rephasing pulses. After each rephasing pulse an echo is produced and a different phase encoding step is performed. Data from each echo is placed into one image. If 16 echoes are used, scanning time is reduced to $1/16^{th}$ of the original time. Although the rephasing pulses are repeated in rapid succession, each echo has a slightly different TE. In order to minimise the effect of using multiple echo times, maximum signal is centred on the effective TE selected and amplitude from the echoes furthest from this effective echo time is reduced by increasing the slope of the phase encode gradient. Data from the echoes at the beginning and end of the echo train (furthest from the effective TE) has less amplitude and fills the outer lines of K space.

3.4.4 Gradient-echo sequences

Spin-echo sequences are time consuming. Both the 90^0 and the 180^0 pulse take time to complete and as all longitudinal magnetisation is flipped into the transverse plane, it takes time for T1 magnetisation to recover. This increases the time between excitations (repeat time or TR) as sufficient recovery of longitudinal magnetisation is required in order to produce the transverse magnetisation and MR signal following the next excitation. A gradient echo sequence usually employs an initial RF pulse with a lower flip angle (often between 10 to 35^0), therefore requiring an RF pulse of a shorter duration. In this case only part of the

longitudinal magnetisation is flipped into the transverse plane, which results in a smaller MR signal but a shorter repeat time as complete T1 recovery is not necessary. Even if a very short TR is used there is sufficient longitudinal magnetisation to generate a transverse signal after the next excitation.

Figure 3.9 The Gradient-echo Sequence

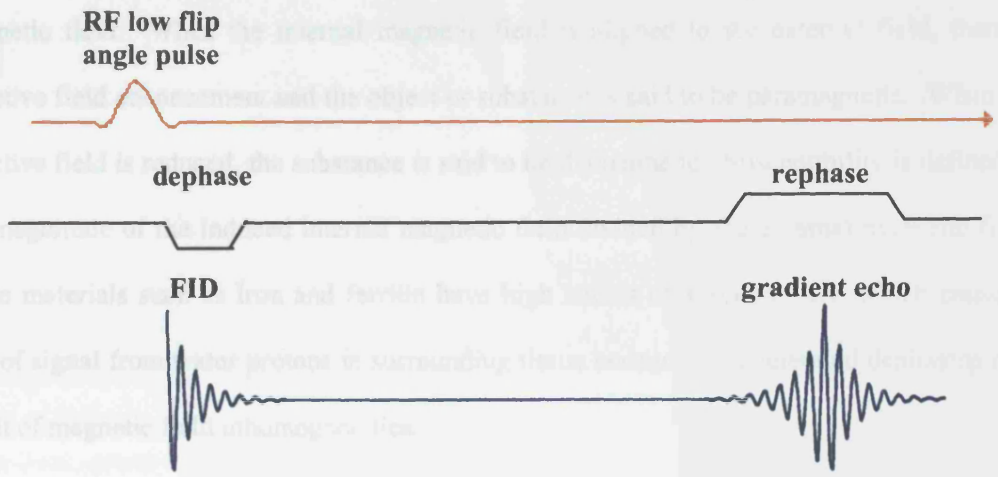

In addition, the dephasing protons are not rephased with a 180^0 pulse but with a magnetic field gradient (figure 3.9). Following the RF excitation a gradient is superimposed on the existing magnetic field for a short time, and resulting in an increase in the magnetic field inhomogeneities. The protons therefore dephase more quickly (due to T2* relaxation). After a short time a gradient of the same strength but opposite direction is switched on, causing the protons to rapidly rephase. The signal increases to a maximum called the gradient echo. The drawbacks of gradient-echo imaging are the sensitivity to field inhomogeneities, which cause susceptibility artefacts and the lower signal to noise ratio. However the susceptibility to field inhomogeneities and the rapid image acquisitions make gradient-echo imaging suitable for the assessment of myocardial iron deposition.

3.5 Magnetic Resonance for the Detection of Tissue Iron

3.5.1 Susceptibility

Magnetic susceptibility is a measure of the extent to which a substance becomes magnetised when it is placed in the field of the scanner. Whenever an object is placed in a magnetic field, electromagnetic interactions take place, which induce internal magnetisation in the object. The direction of this internal magnetisation is either aligned or opposed to the external magnetic field. When the internal magnetic field is aligned to the external field, there is effective field enhancement and the object or substance is said to be paramagnetic. When the effective field is reduced, the substance is said to be diamagnetic. Susceptibility is defined as the magnitude of the induced internal magnetic field divided by the external magnetic field. Some materials such as iron and ferritin have high values of susceptibility, which causes a loss of signal from water protons in surrounding tissue because of accelerated dephasing as a result of magnetic field inhomogeneities.

3.5.2 Magnetic Resonance Properties of Iron and Ferritin

The human body has no mechanism for excreting excess iron, which is stored as crystalline iron oxide within ferritin and haemosiderin in the body. The complexed iron within ferritin is mostly in the oxidized ferric (Fe^{3+}) state. There are approximately 1800 to 2400 iron atoms per molecule of ferritin (molecular weight 450,000). Each ferric iron is paramagnetic, with an average magnetic moment of 3.5 Bohr magnetons (Joules per Tesla), less than the magnetic moment for simple aqueous Fe^{3+} ion (5.9 Bohr magnetons).

The proton magnetic resonance signal observed from a static tissue is largely dependent on the T1 and T2 relaxation times of the protons in that tissue [Hinshaw 1977, Herfkens 1981]. T1 and T2 relaxation times are, in turn, dependent upon the chemical microenvironment surrounding the protons [Floyd 1975, Brasch 1983]. Paramagnetic substances, such as iron which itself does not create any signal with hydrogen MR imaging, produce an enhancement of proton relaxation resulting in shortening of T1 and T2 relaxation times of nearby hydrogen nuclei [James 1975]. This effect causes a reduction of signal intensity in the affected tissue

and is strongly dependent on inter-nuclear distance (figure 3.10). Early in the development of clinical MRI it was noted that iron overload caused a reduction in signal intensity of the liver [Doyle 1982].

Figure 3.10 The Magnetic Resonance Appearances of Tissue Iron Overload

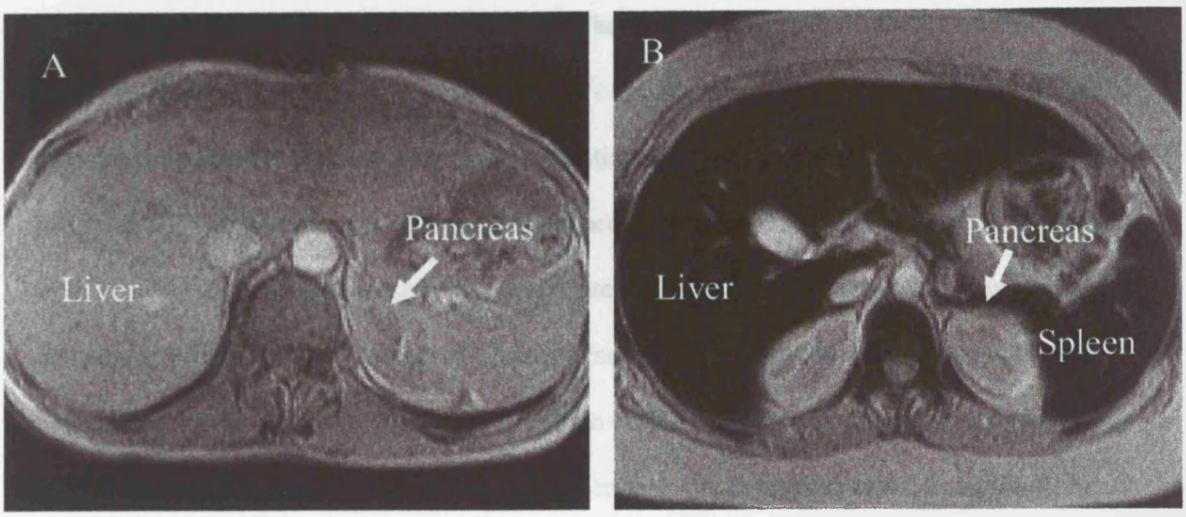

Panel A. Normal volunteer. Panel B. Iron overloaded thalassaemic patient. Iron deposition in the liver, spleen and pancreas causes loss of MR signal and the tissue appears black.

However it was not known whether this was due to the iron or a related tissue alteration such as fibrosis. It was apparent from the equation for spin echo signal intensity that proton density, T1 or T2 must be altered.

$$\text{Signal Intensity} = N_H*(1-e^{-TR/T1})*e^{-TE/T2}$$

Where N_H=proton density, TR=repeat time, TE=echo time

Stark et al investigated the relaxation times of experimental animals with hepatic iron overload in vivo with MR and in vitro with spectroscopy [Stark 1985]. They showed that increased tissue iron led to extreme decreases in T2 but only moderate decreases in T1 and that both 1/T2 and 1/T1 increased linearly with hepatic iron levels. With spectroscopy they showed that the in vitro T2 relaxivity of ferritin in solution did not appear sufficient to account for the extreme decrease in T2 observed in tissue iron overload and postulated that the difference may be due to the additional effect of low molecular weight free cytosol iron.

Alternatively, Gomori and Grossman suggested that the intracellular storage of ferritin in large lysosomes (siderosomes) caused a coarser cellular field gradient and may account for the extreme decreases in T2 observed in vivo [Gomori 1988].

Ferritin and haemosiderin are said to be paramagnetic because they become strongly magnetised when placed in a magnetic field. The ratio of this induced field over the applied magnetic field is termed the susceptibility. Localised regions of increased magnetic susceptibility shorten T2 relaxation time by creating regions of magnetic field non-uniformity. Transverse T2 relaxation is thought to be enhanced by diffusion of solvent water through the magnetic field gradients caused by particulates having a large magnetic susceptibility. Transverse relaxation (de-phasing of protons) caused by the diffusion of water in a gradient will not be refocused by the 180^0 pulse of a spin echo sequence and therefore will contribute (along with dipole-dipole relaxation) to the observed 1/T2 relaxation rate. In addition, fixed gradients will dephase stationary protons. De-phasing caused by static field inhomogeneity is refocused by the 180^0 pulse of a spin-echo sequence. When this pulse is absent, such as in a gradient echo sequence, these contributions to transverse relaxation are additive. Therefore gradient echo sequences are more sensitive than spin-echo sequences to paramagnetic particulates such as ferritin [Stark 1991].

3.5.3 Spin-Echo Techniques Used for the Quantification of Tissue Iron

Using early spin-echo sequences, it was noted that iron overload resulted in darkening of the affected tissue on spin-echo images. Stark et al reported a decrease in MR signal intensity in four rats with experimentally induced iron overload [Stark 1983]. Brasch et al noted that in three children with thalassaemia major, the liver and bone marrow showed very low signal intensities and appeared black on MR images [Brasch 1984]. Decreased signal intensities were subsequently demonstrated in the spleen and hearts of patients with transfusional iron overload [Johnston 1989]. These observations stimulated research to develop a non-invasive diagnostic test to quantitate tissue iron concentration. Initial attempts employed spin-echo sequences and measured either the T2 value of the liver or signal intensity ratios (SIR)

between the liver and skeletal muscle. Different research groups explored the advantages and disadvantages of these two methods. Measuring transverse relaxation rates, a close linear correlation between 1/T2 and hepatic iron concentration by biopsy was found [Kaltwasser 1990]. However, Chezmar et al reported difficulty in measuring T2 accurately due to the low signal intensities at long echo times and had more success using liver to skeletal muscle signal intensity ratios [Chezmar 1990]. In order to overcome this difficulty, Gomori et al used shorter echo times for their images and confirmed Kaltwasser's results by demonstrating a close linear relationship between liver iron concentration and 1/T2 relaxation rate [Gomori 1991]. Jensen et al found a highly significant correlation between SIRs and chemically determined liver iron [Jensen 1994], but over a broad range of liver iron concentrations, Papakonstantinou et al demonstrated a better correlation to T2 than to signal intensity measurements [Papakonstantinou 1995].

Due to the limited sensitivity of the spin echo techniques, only moderate to severe iron overload could be quantified and it was not possible to distinguish between normal and mild degrees of liver iron loading. In addition, spin echo images rely on slow acquisitions over several minutes, and are therefore sub-optimal for imaging of the beating heart. Despite this, gross iron overload of the heart was demonstrated by reduced myocardial intensity [Steudel 1987, Waxman 1994], and in excised mouse hearts, Liu et al showed a close relationship between myocardial 1/T2 and cardiac iron content [Liu 1996]. However, in practice there were difficulties in measuring T2 in-vivo due to both low signal intensities [Mavrogeni 1998a] and cardiac motion artefacts.

3.5.4 Gradient-Echo Techniques Used for the Quantification of Tissue Iron

The newer gradient-echo T2* sequences have two major theoretical advantages to spin-echo T2 sequences for the determination of tissue iron concentration. Firstly, gradient echo images are more sensitive to the paramagnetic effects of tissue iron deposition because they do not have a rephasing 180^0 pulse [Stark 1991]. Secondly, due to the rapid acquisition times,

cardiac-gated images can be acquired during a single breath-hold, minimizing motion artefact caused by myocardial contraction and respiratory movement.

Gandon et al were first to use gradient-echo techniques for the assessment of tissue iron [Gandon 1994]. Using gradient-echo SIRs and spin-echo T2 measurements at 1.0 Tesla they showed that the correlation to liver iron was better for gradient-echo sequences. For severe iron overload, short echo-time (TE) gradient-echo sequences gave the best correlation and for mild iron overload, long TE gradient-echo sequences gave the best correlation to tissue iron. The sensitivity of this gradient-echo sequence was confirmed by Ernst et al who demonstrated that it was capable of detecting iron loading between 2.8 and 16mg/g dry liver weight at 1.0 Tesla [Ernst 1997]. To increase the sensitivity to mild liver iron overload, Bonkovsky et al scanned patients at a field strength of 1.5 Tesla [Bonkovsky 1999]. They acknowledged the potential inaccuracies of measuring small regions of skeletal muscle, and measured background noise to generate liver to noise SIRs. Comparing spin-echo and gradient-echo techniques they found gradient-echo sequences to be more accurate for predicting tissue iron concentrations. The optimal technique studied was a breath-hold gradient-echo sequence with a short echo-time of 5ms, with which liver iron could be reliably estimated between 2.5 and 10mg/g dry weight. Above this level, signal intensities of liver tissue were very low and the coefficient of variation increased to between 13-20%.

Until now, these gradient-echo sequences have all employed SIRs for the quantification of liver iron and the method has not been tested in the heart. The disadvantages of SIRs are firstly that the ratios are highly sequence dependent and vary with the scanning parameters used such as echo-time and repeat-time. Each new sequence would therefore require validation against tissue iron biopsy to calibrate the SIR measurements. Secondly, the range over which iron can be reliably quantified is limited and depends upon the echo-time used. A short echo-time will ensure accurate iron quantification in severe iron overload but will be less accurate for mild tissue iron levels and vice-versa. An ideal MR technique would offer a wide range over which iron could be accurately quantified in order to allow monitoring of

therapy. Quantification would be reproducible on different machines, simple to implement and fast to perform.

One case report has described the appearances of siderotic cardiomyopathy using of gradient-echo imaging [Blankenberg 1994]. No attempt at iron quantification was made.

Figure 3.11 MR Appearances of Myocardial Iron Deposition in Gradient-echo Images

Normal Myocardial Iron

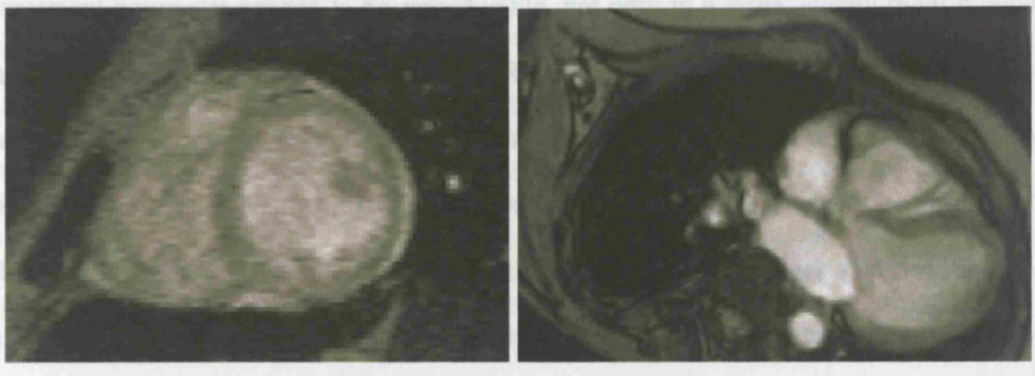

Severe Myocardial Iron Overload

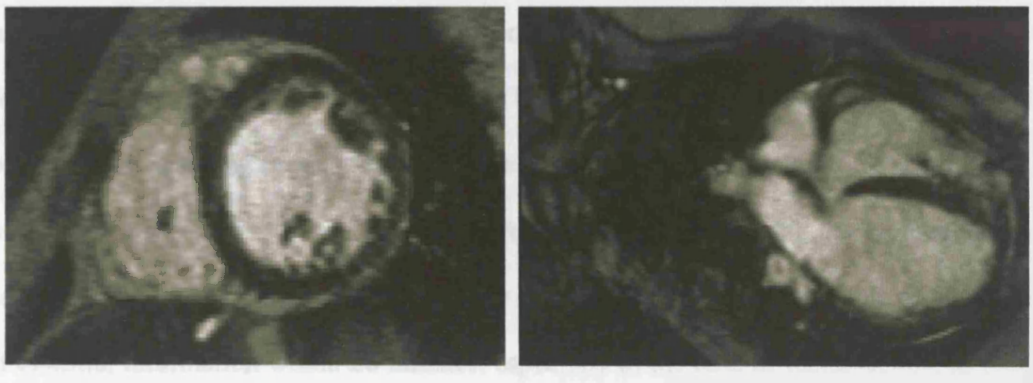

CHAPTER 4: DEVELOPMENT OF THE T2* TECHNIQUE FOR THE QUANTIFICATION OF TISSUE IRON CONCENTRATION

4.1 SEQUENCE REQUIREMENTS

We evaluated the potential of fast-spin-echo, spin-echo and gradient-echo imaging sequences for the quantification of myocardial iron. In order for a technique to be of value, the measurement parameter needed to be reproducible, not only in a large, slowly mobile organ such as the liver, but also in the beating heart. Reproducibility of an MR parameter such as a signal intensity ratio, or a tissue T2 measurement, is inextricably linked to the quality of the original MR images. To measure an area of myocardial signal intensity requires high resolution, as myocardial wall thickness is usually less than 1cm. Images also need to have high definition – even a cardiac-gated breath-hold image will demonstrate blurring of the myocardial edges if the acquisition time is long, allowing cardiac motion during image data collection. For clinical application, the sequence must be reliable and relatively quick to perform. Complex adjustments of the sequence between patients is undesirable as this results in longer overall scanning times and may reduce the ability of the protocol to be readily taken up by other centres. If the scan is likely to have a high clinical demand, the protocol should be easy for MR technologists to learn and carry out. It should also be possible to obtain the most essential information within 20 minutes, especially in the case of thalassaemia, as many of the patients are less than 10 years old. A sequence should not place unrealistic demands on the patient – long breath-hold times may yield interesting information in the research setting with motivated normal controls, but cannot be achieved by a sick patient or a young child. Ideally, the sequence should also be robust and produce adequate images even in sub-optimal conditions – such as imperfect breath holding or in the presence of common arrhythmias such as atrial fibrillation or sinus arrhythmia.

4.2 Spin-Echo (SE) and Fast-Spin-Echo (FSE) Sequences

4.2.1 Background

The spin-echo parameters that have been shown in the medical literature to provide semi-quantitative assessments of tissue iron were signal intensity ratios (SIR) and tissue T2 time. Both had been shown to be inversely proportional to iron concentration by liver biopsy. However, a significant disadvantage of spin-echo images for the heart is the long acquisition times required resulting in both impaired image quality due to respiratory motion and prolongation of overall scanning time. Fast-spin-echo imaging would theoretically overcome this problem as images can be acquired in breath-hold scans, decreasing respiratory artefact and speeding up the total scanning time. A potential drawback is the reduced signal-to-noise ratio in fast-spin-echo imaging which may be important in the setting of low tissue signal due to iron overload.

T2 is calculated from spin-echo and fast-spin-echo images in the same way. A set of images is acquired at increasing echo times. The signal intensity of all tissues in the image decreases with increasing echo time. The T2 relaxation time of the tissue under study can be derived by plotting the signal intensity against the echo-time, which forms a decay curve with the equation, $y=Ke^{-x/T2}$, where y represents the image signal intensity, K represents a constant, and x represents the echo time.

4.2.2 Imaging Parameters

We evaluated three sequences: a single echo FSE sequence where the T2 relaxation time was calculated from six images with six different echo times, each acquired during separate breath-holds; a standard spin echo sequence with four echo times from four separate acquisitions; and a multi-echo spin-echo sequence where four images with four different echo times were generated from a single acquisition. The advantage of a multi-echo sequence is reduced scan time and simplification of subsequent analysis as the region of interest is in the identical position on each image (compared to repeated acquisitions where the position of the heart can vary considerably with the depth of each breath-hold).

The sequence parameters for the standard echo FSE sequence were as follows: Echo times: 22.9ms, 34.3ms, 46.7ms, 57.1ms, 68.6ms and 80.0ms. Repeat time varied with the heart rate, matrix 128 x 128 pixels, field of view 40cm, echo train length 8. An initial double inversion pulse was positioned immediately after the R wave in order to allow black blood imaging after a subsequent delay of 650ms. Each image was acquired during a 15-22 second breath-hold. The sequence parameters for the standard SE sequence were as follows: Echo times: 8ms, 16ms, 20ms and 30ms. Repeat time varied with the heart rate, matrix 128 x 128 pixels, field of view 35cm. The sequence parameters for the multi-echo SE sequence were as follows: Echo times: 30ms, 60ms, 90ms and 120ms. Repeat time varied with the heart rate, matrix 128 x 128 pixels, field of view 35cm.

The T2 relaxation time for normal myocardium is reported as 57ms [Bottomley 1984], for which the echo times of all three sequences are likely to provide accurate results. However myocardial T2 relaxation times below 20ms have been reported in the presence of myocardial iron overload [Mavrogeni 1998b], shorter than the earliest echo time of either the FSE or the multi-echo SE sequence, which could render the measurement of severe cardiac iron overload impossible.

4.2.3 In-vivo reproducibility of FSE and SE techniques in skeletal muscle

Before testing the single echo FSE sequence in the heart – where image quality is affected by a variety of factors such as respiratory and cardiac motion and blood flow – we assessed the reproducibility of the sequence in skeletal muscle (table 4.1).

Table 4.1 Mean T2 Measurements and Reproducibility in Skeletal Muscle

Technique	Mean Quadriceps T2 Relaxation Time (ms)	Coefficient of Variation (%)
Single-echo FSE	44.1	2.9
Multi-echo SE	32.6	1.7
Spin-echo	39.2	3.4

We compared the single-echo FSE sequence, the multi-echo SE sequence and a standard spin-echo sequence in six healthy volunteers, measuring T2 relaxation times in the quadriceps

muscles of the thigh. A large area of muscle was measured distant from any flow artefacts arising from the femoral artery. The reproducibility of each method would be considered sufficient for measurement of T2 relaxation times in stationary skeletal muscle. However it was noted that the multi-echo T2 values were significantly lower than the single-echo FSE and the spin-echo T2 measurements ($p<0.001$, paired t-test).

4.2.4 Accuracy

We tested the in vitro capability of these techniques to measure known T2 values. We compared the known T2 values of a commercial multi-gel MR phantom (Eurospin Relaxation Times, Diagnostic Sonar, UK) with T2 measurements recorded using the FSE, multi-echo SE and the standard SE sequences.

As shown in figure 4.1, there was close agreement between the known T2 relaxation times and the times measured by either standard spin-echo or FSE techniques. The multi-echo sequence correlated less well with the known T2 values and tended to underestimate the T2 relaxation time. The coefficients of variation between the known T2 values and our measurements were as follows: single echo FSE 7.6%, multi-echo SE 27.8%, standard SE 0.7%. As the multi-echo sequence appeared inadequate for accurate T2 measurements we proceeded to in-vivo cardiac assessment with the standard SE and the FSE sequences only.

Figure 4.1 Comparison of Known Phantom T2 Times With Measured T2 Times

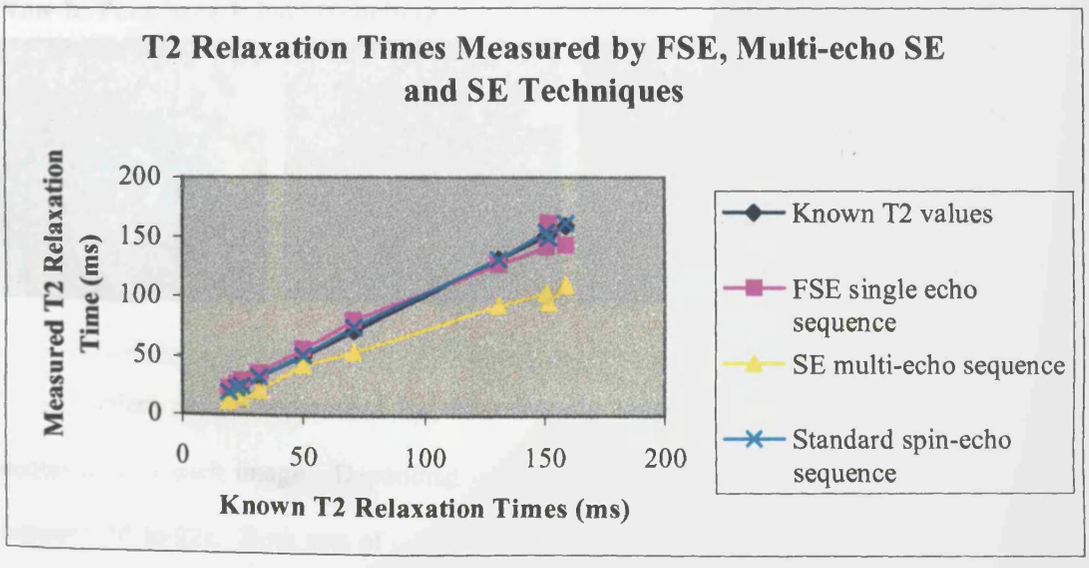

4.2.5 Reproducibility of T2 Measurements in Normal Myocardium

Spin-echo image quality was poor, particularly at longer echo times, making myocardial T2 measurement impracticable with this technique (figure 4.2).

Figure 4.2 Spin-echo short axis images for calculation of T2

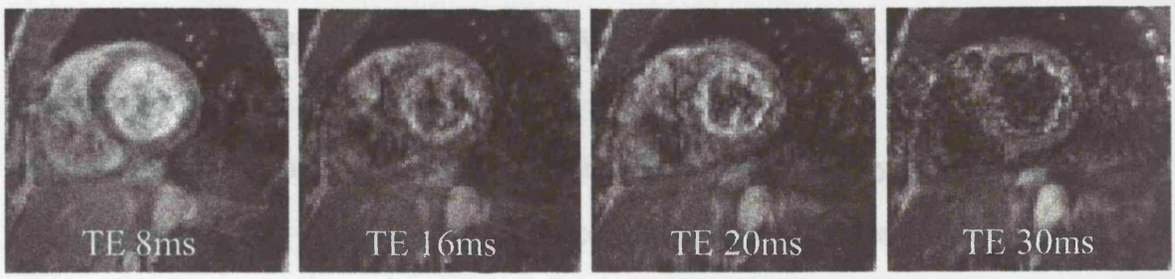

The breath-hold FSE images were better but strongly dependent on the compliance of the volunteer and easily degraded by even minimal respiratory artefact (figure 4.3).

Figure 4.3 Fast-Spin-Echo Short Axis Images of the Heart

Row A: Good breath-hold technique

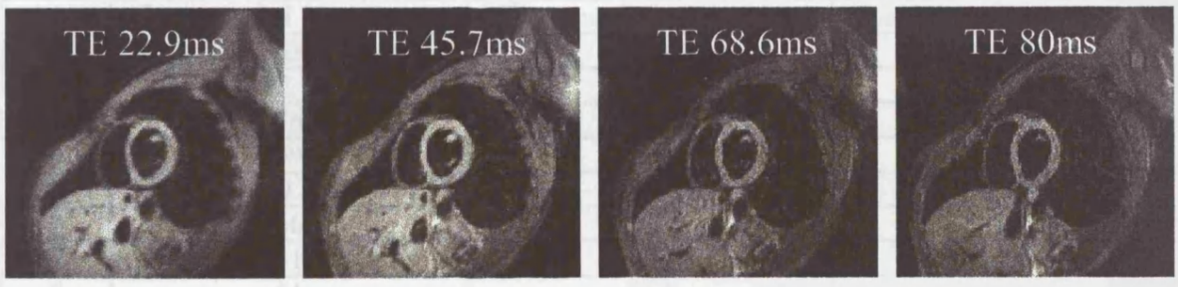

Row B: Poor breath-hold technique

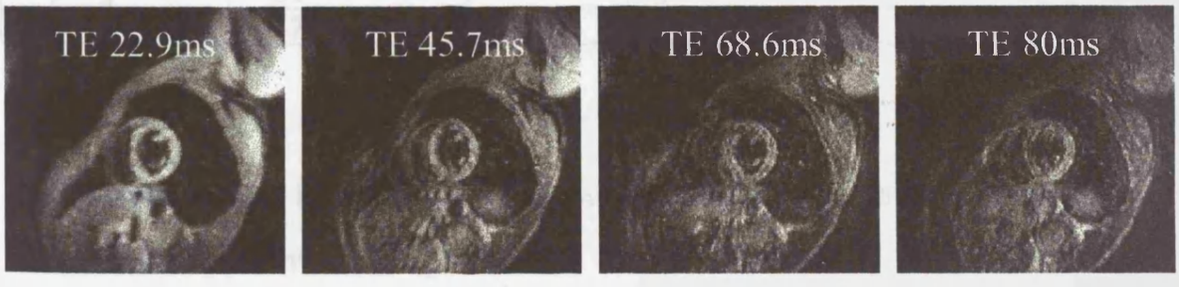

This problem was compounded by the relatively long breath-hold time required for the acquisition of each image. Depending on heart rate, the duration of the breath-hold varied between 16 to 22s. Both sets of images are from the same subject at the echo times shown.

Image quality is good in the first study (row A) but deteriorates in the second study (row B) due to motion artefact related to poor breath holding technique.

A further drawback of the FSE sequence used was the requirement for adjustment of the inversion time for each breath-hold. The optimum inversion time following the double inversion pulse for black blood imaging was estimated as 650ms but this was not achievable if the heart rate was more than 70 beats per minute and shortening of the inversion time was frequently required.

Table 4.2 shows that there is considerable variation in the reproducibility of myocardial T2 measurement using the single-echo FSE sequence. The coefficient of variation is as low as 0.6% in a volunteer with two high quality sets of cardiac images, but as high as 44.7% when breath-holding technique was imperfect. The overall coefficient of variation was 15.7% and was not considered satisfactory for use as a clinical tool, where high-quality images and good reproducibility are necessary for monitoring clinical progress.

Table 4.2 Reproducibility of FSE Myocardial T2 Measurements in Normal Volunteers

Patient	1st myocardial T2 time (ms)	2nd myocardial T2 time (ms)	Coefficient of variation (%)
1	63	62.5	0.6
2	62.5	32.5	44.7
3	76	63	13.2
4	69	66	3.1
5	70.5	41	37.4
6	66	58	9.1
7	41	56	21.9
8	51	53.5	3.4
9	64	57.5	7.6
10	47	59	16.0

4.3 Gradient-Echo Imaging and T2* Measurement for the Determination of Tissue Iron Content

4.3.1 Advantages of Gradient-Echo Techniques for Myocardial Iron Measurement

Neither spin-echo nor fast-spin-echo techniques were sufficiently reliable or reproducible for in-vivo T2 measurements of the heart. Gradient-echo imaging had been used in the liver to

produce signal intensity ratios which had been shown to be inversely proportional to iron concentration [Gandon 1994, Ernst 1997, Bonkovsky 1999]. However, the range over which iron could be reliably quantified was limited, with short echo-time images providing quantification for high iron content and long echo-time images providing quantification for mild, not severe iron overload [Gandon 1994].

To avoid the restrictive ranges associated with signal intensity ratios, we explored the possibility of employing T2* tissue measurements for the quantification of iron. Although this method had not been tried before, it was to be expected from relaxation theory that T2* should also be inversely related to tissue iron. Like T2, T2* is measured over a series of echo times, and we would theoretically have a wide range over which iron could be quantified. Gradient-echo images are also known to be more sensitive to the paramagnetic properties of iron and are ideal for cardiac imaging because of their swift acquisition times, which reduce artefact from respiration and cardiac motion. T2* is calculated from gradient-echo images of increasing echo time in the same way as T2 is calculated from spin-echo images. As the echo time of the images increases, the signal intensity of all tissues decreases and this rate of decay is strongly enhanced in the presence of iron deposition, reducing the T2* relaxation time. A concern however was that at the high field strength of our scanner (1.5 T), iron-loaded tissues would appear black at even the shortest echo times, making T2* calculations impossible.

4.3.2 The T2* sequence – Choice of Imaging Parameters

Cardiac Images: As T2* is sensitive to tissue iron deposition, we required an imaging sequence with a short initial echo time. The sequence also needed to be robust to the motion artefacts present at longer echo times. A balance was found using a motion artefact suppression sequence, which allowed a minimum echo time of 5.6ms and longer echo times to 20ms and above. From experience we now know that an ideal sequence would permit even shorter echo times to improve the accuracy of evaluation of very severe cardiac iron overload. In order to maximise reproducibility we employed a large number of echo times – 9 in total (at 5.6ms, 6.6ms, 7.6ms, 8.6ms, 9.6ms, 11.6ms, 13.6ms, 15.6ms and 17.6ms). Although echo

times greater than 17.6ms were possible, the image quality decayed rapidly above this echo time. In order to minimise T1 effects we chose a low flip angle of 35^0. To reduce breath-hold time, the phase encode group was set at 8 and the image matrix was set at 128 x 256 pixels. Although a matrix of 256 x 256 pixels would produce an image of higher definition, the scanning time would be doubled. Using this sequence, breath-hold times (which vary with heart rate and size of the patient) averaged at 10 seconds – and in children who are smaller and frequently have higher pulse rate - the breath-hold time was usually less than 8 seconds. A gating delay of 0ms after the R-wave was chosen in order to obtain myocardial images in a consistent position in the cardiac cycle irrespective of the heart rate. The resulting image is therefore acquired in early systole. An end-systolic image would have offered the benefits of decreased wall motion and thicker ventricular myocardium in which to draw the region of interest. However the delay time would require alteration to end-systole for each patient and also between breath-holds if there was any variation in the patient's heart rate. The fixed delay time of 0ms simplifies the scanning procedure and ensures that images were taken at the same part of the cardiac cycle for each follow-up scan. This may be significant because relaxation times have been shown to vary during different phases of the cardiac cycle [Baron 1987, DeRees 1988], which may be explained by alterations in myocardial blood content during systole and diastole [Judd 1991]. A short axis mid-ventricular slice was chosen to minimise artefacts from blood flow. The region of interest was drawn in the ventricular septum, encompassing all layers of the myocardium from the right through to the left ventricular endocardium. The region was drawn away from the cardiac veins which are known to cause susceptibility artefacts and would artificially decrease the T2* measurement if included [Reeder 1998].

To calculate the myocardial T2*, the signal intensity of the myocardial region of interest and the signal intensity of the background noise were measured in each of the nine images using in-house software (CMRtools, © Imperial College, London). Background noise was subtracted from the myocardial signal intensity, and the net value was plotted against the echo time for each image. A trendline was fitted to the resulting exponential decay curve, with an

equation of the form $y=Ke^{-x/T2^*}$ where K represents a constant, x represents the echo time and y represents the image signal intensity (Figure 4.4).

Figure 4.4 Calculation of Myocardial T2* from Nine Images at Increasing Echo Times

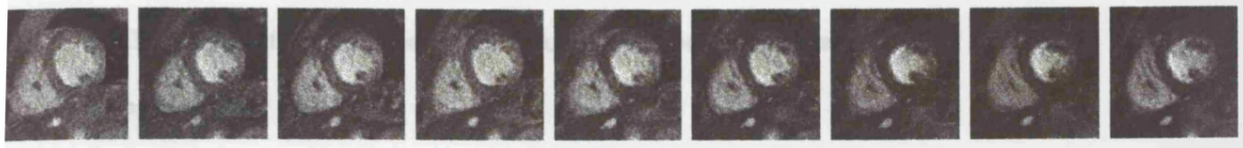

5ms 6ms 7ms 8ms 9ms 11ms 13ms
15ms 17ms

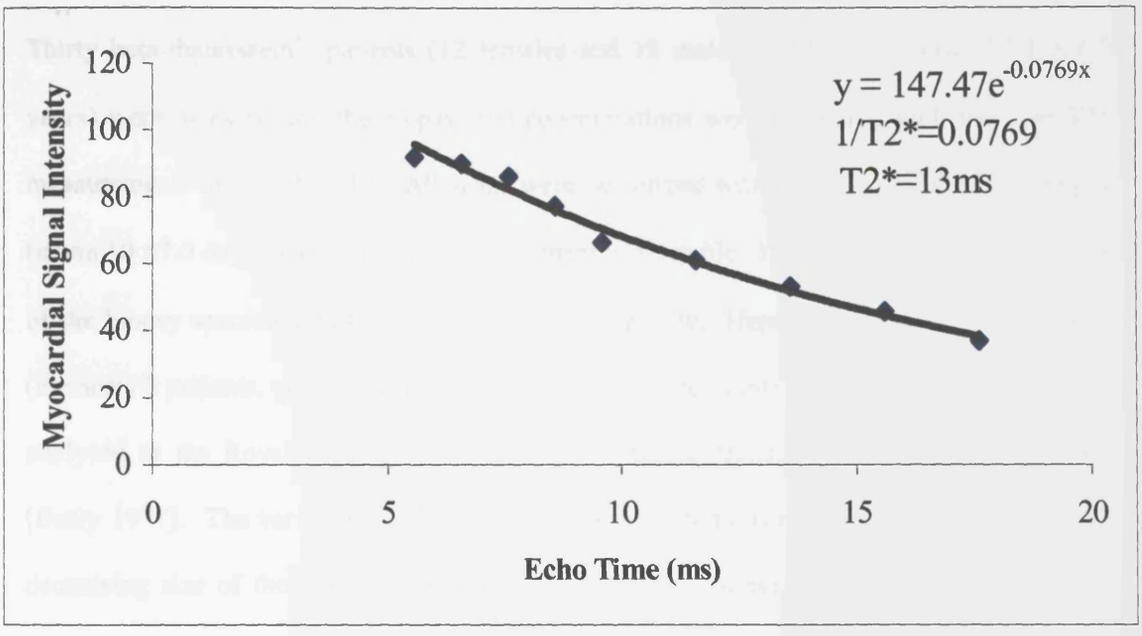

Liver Images: As gating of the images to cardiac contraction is not necessary for liver imaging, a simpler sequence was used. Eight images at 8 separate echo times were used (2.24, 3.36, 4.47, 6.71, 8.95, 10.07, 15.66 and 20.13ms). This sequence allowed a lower initial echo time of 2.24ms, which is valuable because liver iron deposition can often exceed 15mg/g dry liver weight in thalassaemic patients. Each image was acquired during a 9-13 second breath-hold with a repetition time 200ms and a low flip angle of 20° to minimise T1 effects. As the liver is a large organ through which iron is deposited relatively uniformly [Overmoyer 1987], we could afford to reduce image resolution to a matrix of 96 x 128 pixels in order to reduce breath-hold duration. A transverse slice was used to minimise respiratory artefact, positioned through the centre of the liver (and spleen if present). A region of interest

was drawn in the periphery of the liver away from the large central vessels. Liver T2* was then calculated in the same way as in the heart.

4.3.3 Validation of the T2* Technique for the Measurement of Tissue Iron Concentration

To investigate the relationship between tissue iron and T2* relaxation, we prospectively studied all patients undergoing liver biopsy as part of their routine clinical management. Thirty beta-thalassaemic patients (12 females and 18 males, aged 18-38, mean 27.1 ± 6.7 years) were assessed and the biopsy iron concentrations were compared with the liver T2* measurements derived by MR. All scans were performed within 21 days of the liver biopsy (mean 10 ±7.0 days) and iron-chelation treatment were stable. In all but three cases, a section of the biopsy specimen was also examined histologically. Hepatic fibrosis was found in 13 (cirrhosis 3 patients, peri-portal fibrosis 10 patients). The biopsy specimens were chemically analysed at the Royal Free Hospital, London using the technique of Barry and Sherlock [Barry 1971]. The variability of biopsy iron determination has been shown to increase with decreasing size of the biopsy [Villeneuve 1996] so we ensured that the dry weights of all specimens in this study exceeded 0.5mg (mean 1.33 ± 0.59 mg).

We found a significant, curvilinear, inverse correlation between liver T2* and the liver iron content for all samples ($r=0.81$, figure 4.5). As predicted from the known variatiability of biopsy iron determination in the presence of hepatic fibrosis [Villeneuve 1996, Edmond 1999], there was a better correlation with the non-fibrotic liver samples ($r=0.93$, $p<0.0001$) than the fibrotic samples ($r=0.68$, $p<0.0001$). Therefore we subsequently employed non-fibrotic samples to generate predictions of liver iron content from the measured T2* values. As liver iron concentration and liver T2* measurements were positively skewed, the values were $\log_e$ transformed for analysis (Figure 4.6).

Figure 4.5 Correlation between Liver T2* and Liver Biopsy Iron Concentration.

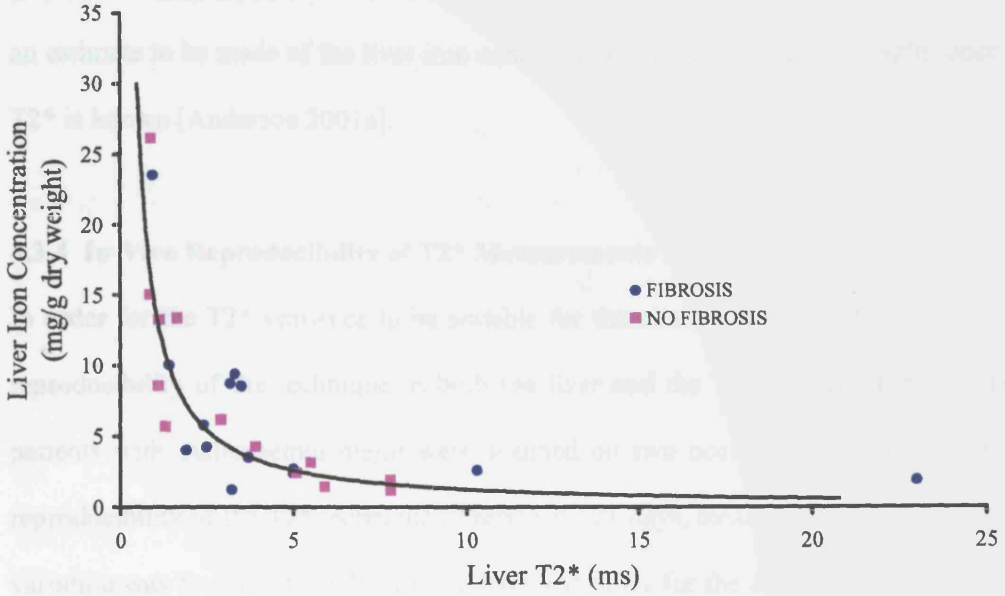

Figure 4.6 Regression Curve for Liver T2* and Liver Iron Concentration in the Nonfibrotic Samples

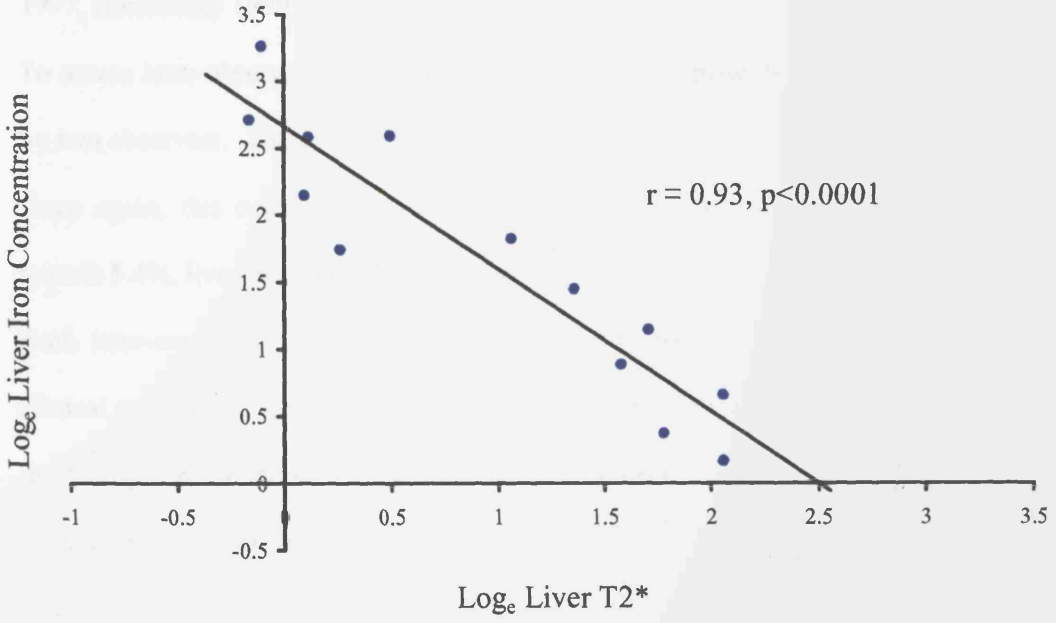

For the non-fibrotic samples, both Pearson's and Spearman's tests gave a correlation coefficient of 0.93 which is highly significant ($p<0.0001$). Regression analysis shows that a

one unit increase in $\log_e$ T2* is associated with a 1.07 unit increase in $\log_e$ iron concentration (95% confidence interval 0.78 to 1.35 unit decrease). This correlation to liver biopsy allows an estimate to be made of the liver iron concentration in mg/g liver dry weight, once the liver T2* is known [Anderson 2001a].

4.3.4 In-Vivo Reproducibility of T2* Measurements

In order for the T2* sequence to be suitable for the clinical assessment of tissue iron, good reproducibility of the technique in both the liver and the heart is required. Therefore ten patients with thalassaemia major were scanned on two occasions to assess the inter-study reproducibility of the T2* technique (interval 1 – 21 days, mean 7.1 days). The coefficient of variation was found to be 3.3% for the liver and 5.0% for the heart [Anderson 2001a]. This compared favourably with coefficients of variation for signal intensity ratio measurements from these same images (liver-to-muscle 7.9%, liver-to-noise 8.8%, heart-to-muscle 12.6%, and heart-to-noise 14.1%), techniques that have previously been used [Gandon 1994, Ernst 1997, Bonkovsky 1999].

To assess inter-observer variability, the images from 10 patients were studied independently by two observers. The coefficient of variation was 4.5% for the liver and 6.4% for the heart. Once again, this compared favourably with signal intensity ratio measurements (liver-to-muscle 5.4%, liver-to-noise 6.1%, heart-to-muscle 10.8%, and heart-to-noise 7.5%).

Both inter-study and inter-observer reproducibility were considered sufficiently good for clinical application. The improved reproducibility of these gradient-echo T2* techniques over the fast-spin-echo and spin-echo techniques results principally from improved quality of the original images from which T2* is measured.

4.3.5 Normal Ranges for T2* Relaxation Times

To determine normal ranges for T2* values in the liver, heart, spleen and skeletal muscle we scanned 15 healthy volunteers using the same protocol (9 males, 6 females, aged 26-39, mean 31±3.7 years). The normal values for T2* were myocardium 52±16ms, liver 33±7ms, skeletal

muscle 30±5ms and spleen 56±22ms. There is limited literature with which to compare these results. Li et al studied 13 normals and reported a myocardial T2* of only 33 ±6.5ms, but only 2 echo times were used [Li 1996]. Wacker et al reported the normal myocardial value in 6 patients with coronary disease (remote from ischaemia) as 48±9 ms using a 10 echo time technique [Wacker 1999]. Reeder reported normal T2* values of 38±6ms in the mid septum in 5 normal volunteers, and showed reduced values adjacent to the cardiac veins due to their local susceptibility effect [Reeder 1998].

4.4 Cardiovascular MR (CMR) for the Determination of Ventricular Volumes and Mass

4.4.1 Background

CMR measurements of left and right ventricular function, volumes and mass were made during each patient study in addition to myocardial and liver T2*. Volume studies use a series of contiguous short-axis cines to construct a three-dimensional representation of the ventricles, allowing direct measurement of mass and volume (figure 4.7). Compared to echocardiography and cine-angiography, CMR does not rely on geometric assumptions or calculations based on partial sampling of the cardiac volume. The technique has been shown to be accurate [Longmore 1985, Sechtem 1987], and the reproducibility of this technique is superior to echocardiography and cine-angiography [Semelka 1990, Pattynama 1994, Bellenger 2000].

4.4.2 Imaging Technique and Analysis

A diastolic, horizontal-long-axis image of the left ventricle was used as the pilot onto which the stack of short-axis slices were positioned, commencing at the atrio-ventricular ring and extending to the ventricular apex. A segmented FLASH breath-hold cine was used for each contiguous 10mm short-axis slice (TE 3.8ms, repeat time gated to RR interval, field of view 35x35cm, matrix 128x256 pixels, flip angle 35^0, phase encode group 8, 12 frames). On

average 10 short-axis segments were required to encompass the entire left ventricle. The endocardial and epicardial borders of the right and left ventricle were traced manually in each diastolic short-axis slice. The endocardial borders alone were traced in the systolic slices. End diastolic volume (EDV) was determined as the sum of the endocardial diastolic regions of interest in all slices. End systolic volume (ESV) was determined as the sum of the systolic endocardial regions of interest from all slices. Ejection fraction (EF) was calculated from the equation EF%=100x(EDV-ESV)/EDV. Left ventricular mass was determined by subtracting the left ventricular endocardial from the left ventricular epicardial region of interest in each slice. The sum of the net myocardial volume from each slice was multiplied by 1.05g/ml (the density of normal myocardial tissue) to calculate the total LV mass.

Figure 4.7 Three dimensional measurement of left ventricular volumes and mass

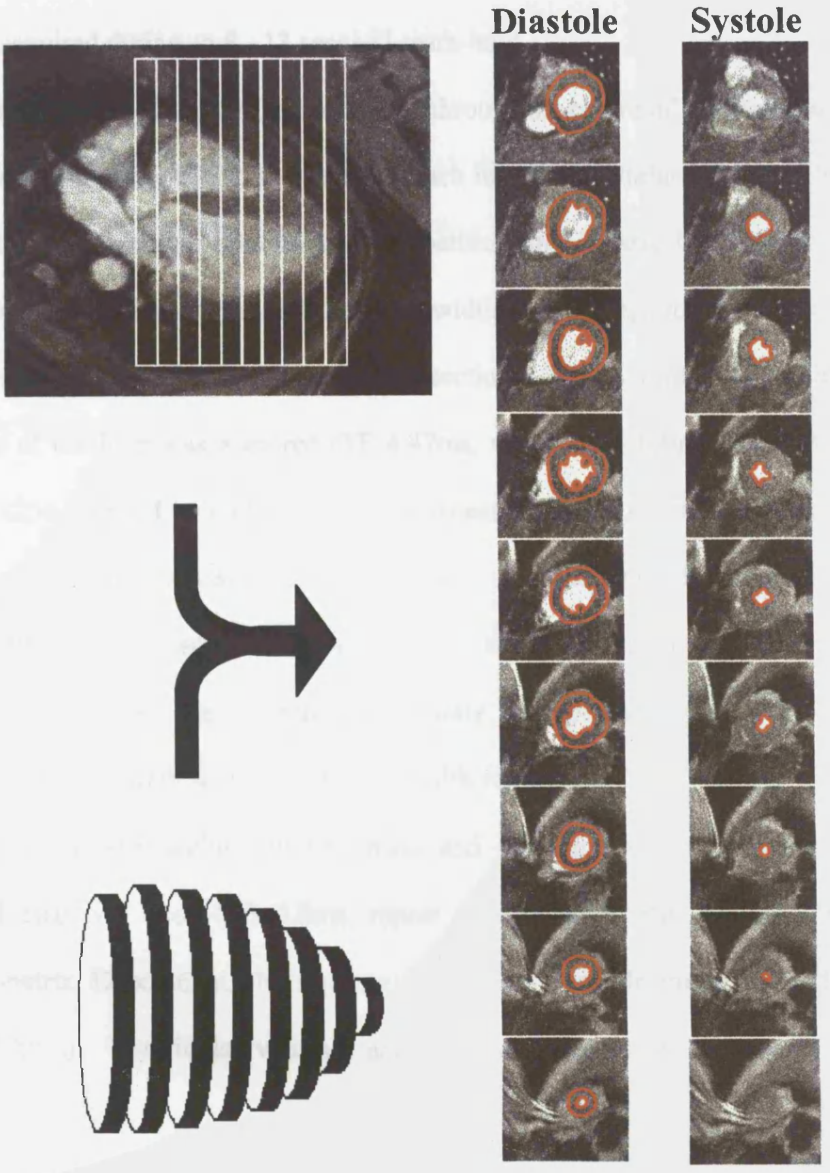

4.5 IMAGING PROTOCOL

All patients were scanned using the same imaging protocol, which was applied in all the work described in this thesis. A Picker 1.5T Edge Scanner was used (Marconi Medical Systems, Ohio, USA). Each scan lasted approximately 45 minutes and included the measurement of liver and heart T2*, and left and right ventricular function, volumes and mass.

For the measurement of myocardial T2*, a single short axis mid-ventricular slice was acquired at nine separate echo times (TE 5.6 – 17.6ms). The repetition time between radio-frequency pulses was between 11.8 - 23.8ms, depending on the echo time used. A gradient-echo sequence was used (flip angle 35°, matrix 128 x 256 pixels, phase encode group 8, field of view 35cm, sampling bandwidth of 250kHz, slice thickness 10mm). The repetition time was adjusted to the patient's heart rate, with a gating delay of 0ms after the R wave. Each image was acquired during an 8 - 13 second breath-hold.

For the measurement of liver T2*, a single slice through the centre of the liver was acquired at eight different echo times (TE 2.2 - 20.1ms). Each image was attained during a 10-13 second breath-hold using a gradient-echo sequence (repetition time 200ms, flip angle 20°, matrix 96 x 128 pixels, field of view 35cm, sampling bandwidth of 125kHz, slice thickness 10mm). T2* measurements were calculated as described in section 4.3.2. A further multi-slice gradient-echo image of the liver was acquired (TE 4.47ms, repeat time 100ms, field of view 40cm, matrix 128x256 pixels, flip angle 20^0, slice thickness 8mm, 16 slices in 2 10 second breath-hold batches) in order to visualise the pancreas. A signal intensity ratio of pancreas to paravertebral skeletal muscle was calculated, as we were unable to accurately measure pancreatic T2*, because the pancreas could rarely be captured on every T2* breath-hold acquisition due to its small size and movement with respiration.

For calculation of ventricular volumes, mass and ejection fraction, a segmented FLASH breath-hold cine was used (TE 3.8ms, repeat time gated to RR interval, field of view 35x35cm, matrix 128x256 pixels, flip angle 35^0, phase encode group 8, 12 frames, slice thickness 10mm). Ventricular volumes and mass were calculated as described in section 4.4.2.

CHAPTER 5: T2* MR FOR THE EARLY DIAGNOSIS OF MYOCARDIAL IRON OVERLOAD – THE RELATIONSHIP BETWEEN MYOCARDIAL IRON AND VENTRICULAR FUNCTION

5.1 INTRODUCTION

Although heart failure secondary to transfusional iron overload remains the commonest cause of death in patients with thalassaemia major [Zurlo 1989, Olivieri 1994], the relationship between myocardial iron deposition and cardiac function is unknown. In addition the prediction of cardiac risk has hitherto relied upon associations between other markers of iron overload such as serum ferritin and liver iron and prognosis [Olivieri 1994, Brittenham 1994b]. A direct measurement of myocardial iron would allow earlier diagnosis and treatment and help to reduce the excess mortality from this cardiomyopathy.

We applied our T2* MR method in the assessment of myocardial iron deposition in 106 patients with thalassaemia major and related the results to ventricular function.

5.2 METHODS

5.2.1 Study Population

A total of 109 regularly transfused patients with thalassaemia major were scanned. Three patients were excluded from comparison analysis of ventricular function due to cardiac anomalies (1 corrected tetralogy of Fallots, 1 sub-aortic shelf and 1 peripheral pulmonary artery stenosis). The residual cohort of 106 patients included 50 males and 56 females, aged 13-41, mean 27 ±7 years. All patients had received iron chelation therapy since the mid-to-late 1970s, or from early childhood in patients born after this time, with a broad range of compliance to treatment (serum ferritin 262 - 7624ng/l, mean 2095 ±1559ng/l). Seventeen patients required medication for ventricular dysfunction (antiarrhythmics or angiotensin-converting-enzyme inhibitors).

5.2.2 Serum Ferritin Measurements

Measurements of serum ferritin were carried out by enzyme immunoassay (WHO Ferritin 80/602 First International Standard, normal range 15-300μg/l).

5.2.3 Magnetic Resonance Assessments of Myocardial Iron and Ventricular Function

In order to quantify iron loading in the heart we used the T2* MR technique described in section 4.5. Myocardial T2* values measured in healthy volunteers showed a normal distribution with a mean value of 52ms, and a lower 95% confidence interval of 20ms. Myocardial T2* levels <20ms were taken to imply iron overload.

All patients were scanned using the same sequence with a Picker 1.5T Edge Scanner (Marconi Medical Systems, Cleveland, Ohio). Each scan included the measurement of heart iron using T2*, and the measurement of ventricular volumes, mass and ejection fraction using standard techniques [Pattynama 1994, Bellenger 2000] as described in section 4.4.

5.2.4 Statistical Analysis

Summary data are presented as mean ±1 standard deviation. Pearson's coefficient of correlation was used to assess the correlation between myocardial T2* and the indices of left ventricular function; left ventricular ejection fraction, left ventricular mass index and left ventricular end systolic volume index. As left ventricular volumes and mass vary with the height and weight of a patient, left ventricular volume and mass indices were calculated by dividing end systolic volumes and left ventricular mass by the patient's surface area. Pearson's coefficient of correlation was also used to assess the correlation between left and right ventricular ejection fractions. Logistic regression was performed to relate the requirement for cardiac medication to 7 clinical covariates. Multivariate backward stepwise regression analysis, with a cut off of $p=0.1$ for removing variables and $p=0.05$ for including variables was used to identify independent predictors for the requirement for cardiac medication. Stata statistical software was used for computations (Stata Corporation, Texas, USA).

5.3 RESULTS

5.3.1 Myocardial Iron and Parameters of Left Ventricular Function

As shown in figures 5.1,5.2 and 5.3, throughout the normal range of myocardial T2* (>20ms), parameters of ventricular function fall within normal limits [Lorenz 1999]. Only in the presence of excess cardiac iron, when myocardial T2* fell below 20ms, was there a progressive, linear decline in left ventricular ejection fraction ($r=0.61$, $p<0.0001$), and an increase in left ventricular end-systolic volume index ($r=0.50$, $p<0.0001$), and left ventricular mass index ($r=0.40$, $p<0.001$). Although 64 patients (60.3% of this cohort) had myocardial T2* values less than 20ms, significant ventricular abnormalities were detected in only 10 patients (9.4%). All of these 10 patients had severe myocardial iron deposition (myocardial T2*<12ms).

Figure 5.1 Relationship between Cardiac T2* and Left Ventricular Ejection Fraction

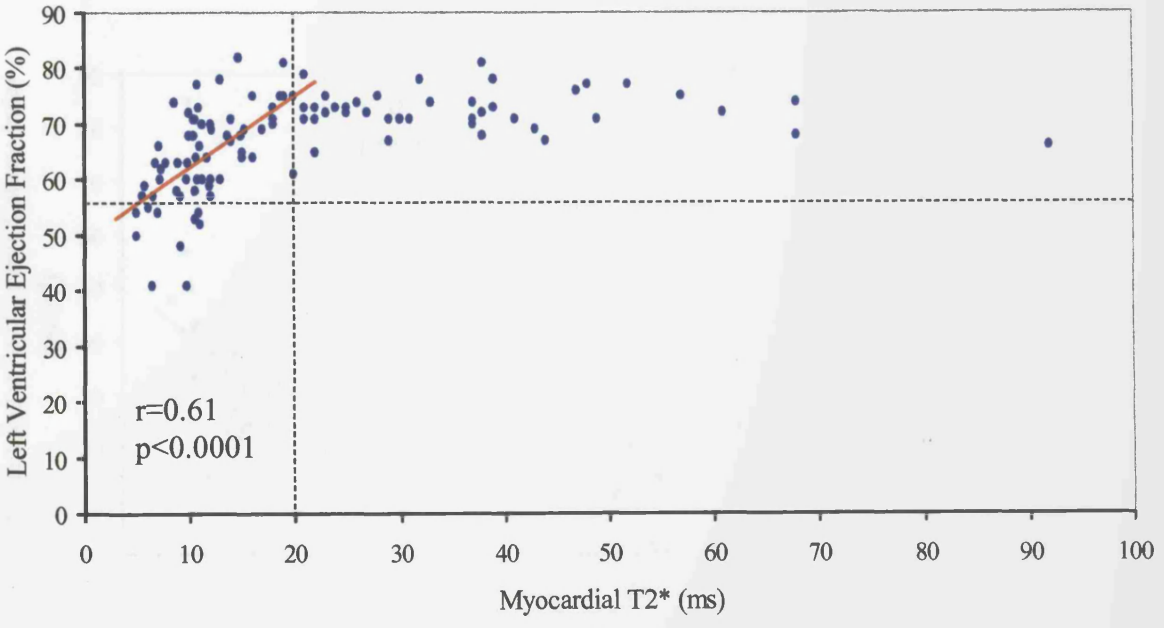

Figure 5.2 Relationship between Cardiac T2* and Left Ventricular Mass Index

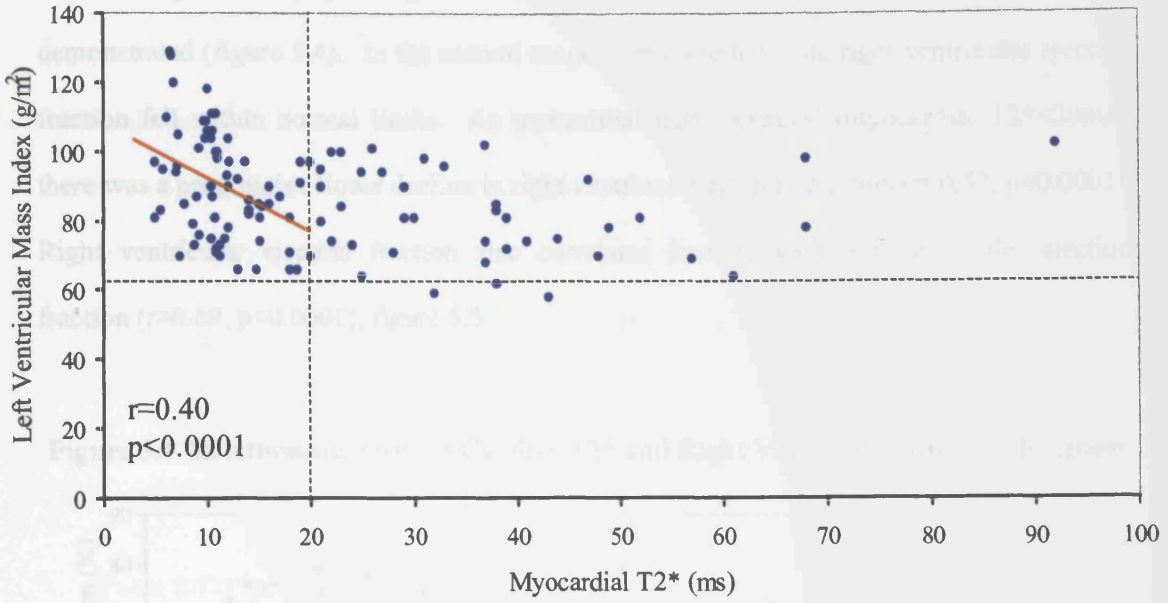

Figure 5.3 Relationship between Cardiac T2* and Left Ventricular End Systolic Index

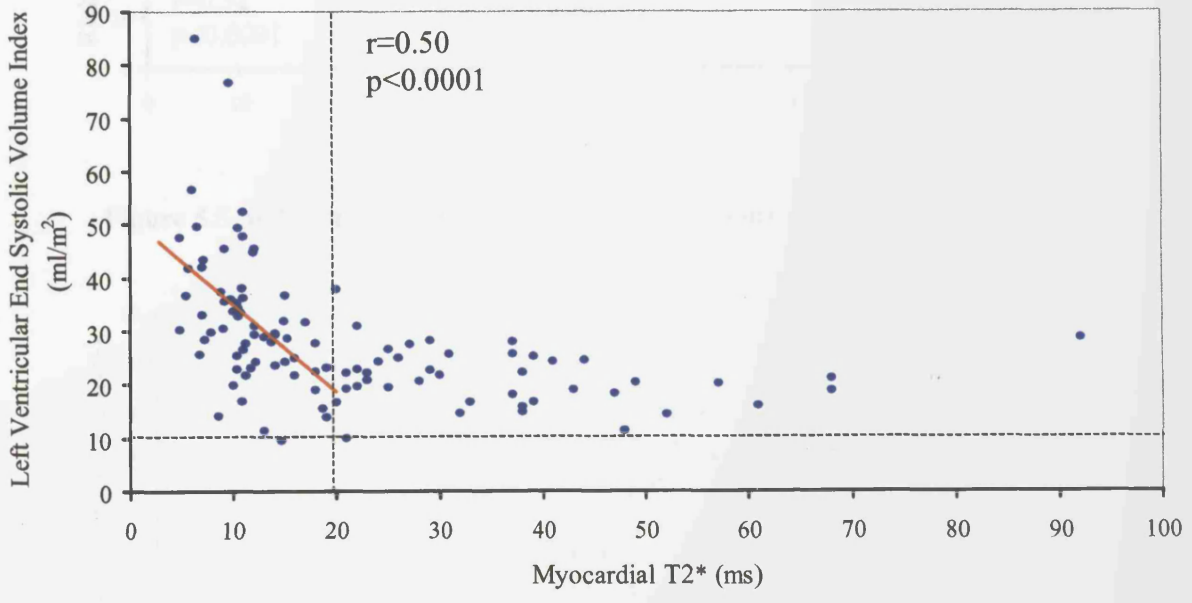

5.3.2 Myocardial Iron and Right Ventricular Ejection Fraction

A similar pattern between myocardial iron and right ventricular ejection fraction was demonstrated (figure 5.4). In the normal range of myocardial iron, right ventricular ejection fraction fell within normal limits. As myocardial iron increased (myocardial T2*<20ms), there was a progressive linear decline in right ventricular ejection fraction (r=0.52, p<0.0001). Right ventricular ejection fraction also correlated linearly with left ventricular ejection fraction (r=0.69, p<0.0001), figure 5.5.

Figure 5.4 Relationship between Cardiac T2* and Right Ventricular Ejection Fraction

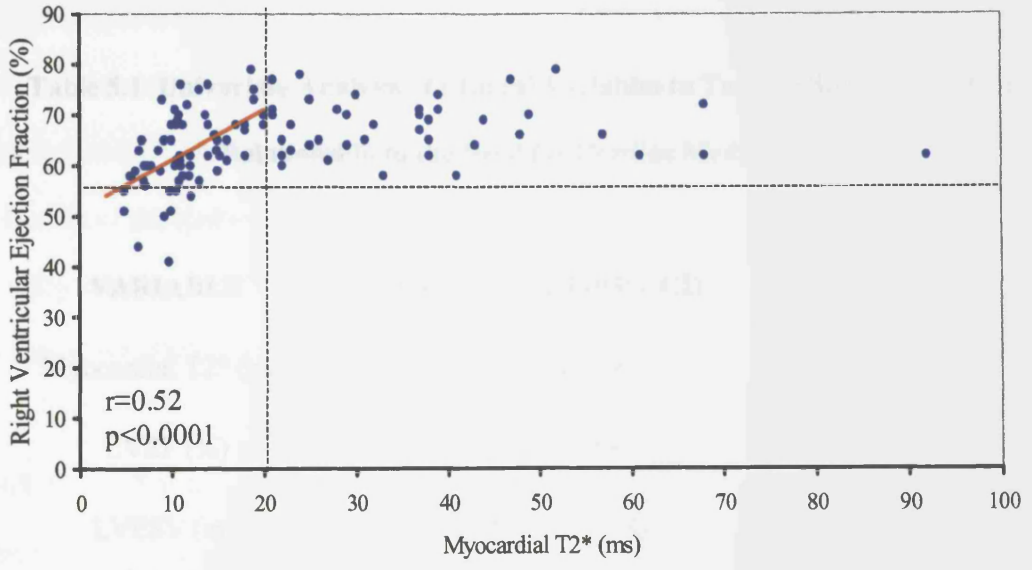

Figure 5.5 Relationship between Left and Right Ventricular Ejection Fraction

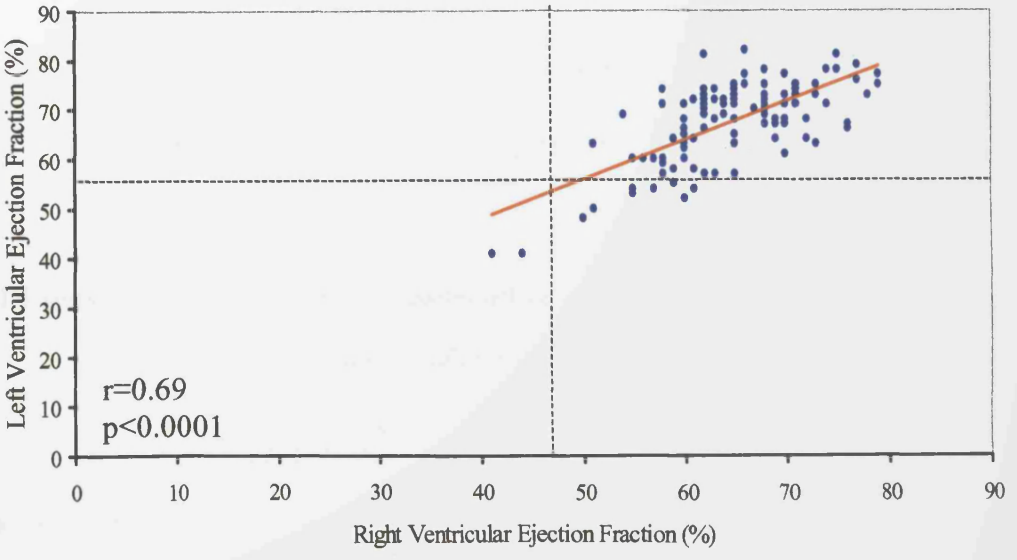

5.3.3 Myocardial T2* and Clinical Outcome

Logistic regression was performed to relate the clinical requirement for medication for heart failure to 7 clinical covariates. Of 106 patients, 17 patients required medication for ventricular dysfunction and univariate analysis identified myocardial T2*, left ventricular ejection fraction and left ventricular end systolic volume as significant variables (table 1). Using multivariate backward stepwise regression analysis, with a cut off of p=0.1 for removing variables and p=0.05 for including variables, only myocardial T2* (odds ratio 0.79, 95% confidence interval 0.67 - 0.92, p=0.002) and serum ferritin (odds ratio 0.95, 95% confidence interval 0.91 - 1.00, p=0.05) were significant.

Table 5.1 Univariate Analysis of Clinical Variables to Test the Strength of their Relationship to the Need for Cardiac Medication

VARIABLE	ODDS RATIO (95% CI)	P VALUE
Myocardial T2* (ms)	0.81 (0.71, 0.93)	0.003
LVEF (%)	0.88 (0.82, 0.94)	<0.001
LVESV (ml)	1.05 (1.02, 1.08)	0.001
Serum Ferritin (µg/l)	0.97 (0.93, 1.01)	0.17
Diabetes Mellitus	1.58 (0.56, 4.51)	0.39
Age	1.01 (0.94, 1.08)	0.85
Liver T2* (ml)	1.01 (0.91, 1.12)	0.85

CI denotes confidence interval, LVEF denotes left ventricular ejection fraction and LVESV denotes left ventricular end systolic volume.

5.4 DISCUSSION

5.4.1 Myocardial T2* measurement and ventricular function

There was a clear relation between deterioration in ventricular function and myocardial T2* values below the normal range (<20ms). As myocardial iron increased, the left ventricle dilated, LV mass increased and LV ejection fraction deteriorated. However, although 64 patients (60.3% of this cohort) had myocardial T2* values less than 20ms, significant ventricular abnormalities were detected in only 10 patients (9.4%). This lack of sensitivity of the absolute parameters of ventricular function indicates that ventricular dysfunction is a poor and late guide to ventricular iron loading. The lowest recorded ejection fraction was 41%, measured in two patients, both with severe myocardial iron overload (myocardial T2* of 3.2 and 5.9ms respectively). Although both patients were commenced on intravenous iron-chelation therapy, one has subsequently died in low output cardiac failure, reflecting the poor prognosis of iron induced cardiomyopathy [Felker 2000]. This suggests that myocardial iron imaging with the T2* MR technique would give a much earlier indication of the need for increased iron-chelation therapy.

5.4.2 Heart failure and causality

The reliance on indirect markers of myocardial iron loading such as serum ferritin and liver iron have made heart disease difficult to detect and treat in thalassaemia, and has raised controversy over the causal relationship between cardiac iron overload and cardiac failure. Some histochemical studies have indicated that cardiac iron deposits cause cardiac dysfunction and describe the increase in ventricular mass and the predominant epicardial deposition of iron, concurring with current MR findings (figure 5.6) [Engle 1964, Schellhammer 1967, Buja 1971]. However, others have suggested that iron deposits in the heart are of no functional significance [MacDonald 1960]. Recently, myocarditis rather than iron deposition has been proposed as an alternative etiology for heart failure in thalassaemic patients [Kremastinos 1995, 1999]. Furthermore, separate aetiologies for left and right ventricular dysfunction have been suggested [Mavrogeni 1997]. This study demonstrates the

Figure 5.6 MR gradient echo images in the short-axis (A) and horizontal long axis (B) of the heart, showing epicardial iron deposition.

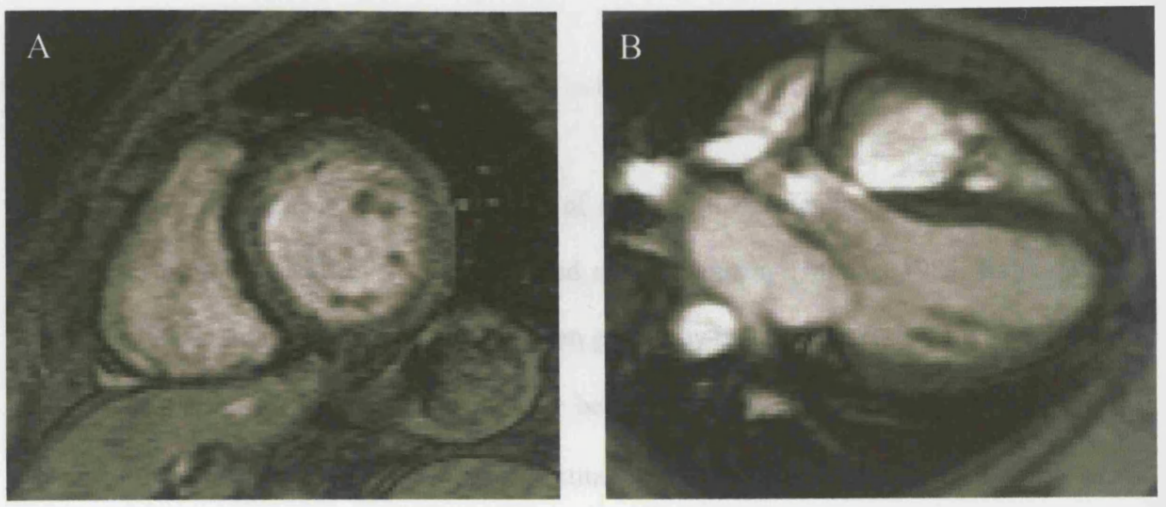

relation between deterioration in ventricular function and myocardial iron loading in both ventricles, compatible with a global cardiomyopathy, and illustrates clear evidence for the causality of iron overload in heart failure in thalassaemia patients.

5.4.3 Study limitations

It is not possible definitely to predict the myocardial iron concentration (mg/g) from the myocardial T2* value, because validation with cardiac tissue has yet to be performed. Nonetheless, the data presented demonstrates the strong relationship between declining myocardial T2* and impaired ventricular function indicating the empirical value of myocardial T2*, and the validation data from the liver biopsies supports the relationship between tissue iron and T2* (section 4.3.3).

5.4.4 Conclusions

Gradient-echo T2* MR provides a rapid, non-invasive, reproducible means for assessing myocardial iron. A myocardial T2* <20ms indicates incipient ventricular dysfunction. The early diagnosis of myocardial iron overload allows prompt intensification of iron-chelation therapy, and has the potential to prevent the mortality from heart failure associated with established ventricular dysfunction.

CHAPTER 6: CONVENTIONAL MARKERS OF IRON OVERLOAD CANNOT PREDICT CARDIAC RISK IN THALASSAEMIA MAJOR

6.1 INTRODUCTION

Heart failure remains the commonest form of death in thalassaemia major. Iron-chelation therapy can prevent and reverse iron-induced cardiomyopathy [Marcus 1984, Rahko 1986, Wacker 1993], but until now, therapy has been guided by indirect markers of myocardial iron overload. Serum ferritin levels consistently below 2500µg/l [Olivieri 1994] and liver iron levels lower than 15mg/g dry weight (80µmol/g wet weight) [Brittenham 1994b] were considered to indicate low cardiac risk in thalassaemic patients. With the emergence of advanced MR techniques it is now possible to assess myocardial and liver iron levels along with cardiac function in the same scan [Anderson 2001a]. We have analysed the data from 205 patients with thalassaemia major in order to examine the validity of using liver iron and serum ferritin to assess cardiac risk.

6.2 METHODS

6.2.1 Patient Cohort

Two hundred and ten thalassaemia major patients were assessed. Five patients were excluded from further analysis due to the presence of heart disease unrelated to iron overload (1 corrected fallots, 1 patent ductus arteriosus, 1 subaortic shelf, 1 aortic stenosis, 1 peripheral pulmonary stenosis). Of the remaining 205 patients, 103 were female and 102 were male (mean age 27 ± 7.8 years). All patients received transfusions at 2-4 week intervals to maintain the pre-transfusion haemoglobin concentration between 9- 9.5g/dl and all have received long-term iron chelation therapy with a broad range of compliance to treatment (serum ferritin 215-10341µg/l, mean 2111 ± 1527µg/l).

6.2.2 MR Assessments of Myocardial and Liver Iron and Ventricular Function

All patients were scanned using the same sequence with a Picker 1.5T Edge Scanner (Marconi Medical Systems, Cleveland, Ohio). Each scan included the measurement of liver and heart iron using T2*, and the measurement of ventricular volumes, mass and ejection fraction, as described in section 4.5.

As liver T2* has been validated against liver biopsy iron concentration, we have converted all liver T2* measurements into milligrams per gram liver dry weight as described in section 4.3.3. Myocardial T2* has not been converted into tissue iron concentrations because although the relationship is likely to be similar to that for liver iron, the precise correlation awaits confirmation with a ventricular biopsy study.

6.2.3 Serum Ferritin Measurements

Measurements of serum ferritin were carried out by enzyme immunoassay and all values are referable to the WHO Ferritin 80/602 First International Standard (normal range 15-300μg/l). As ferritin levels are known to fluctuate, all analyses have been made using the mean serum ferritin level for the year preceding the magnetic resonance scan.

6.2.4 Statistical Analysis

Summary data are presented as means ±1 standard deviation. Myocardial T2* was found to be highly positively skewed and was therefore log transformed to allow parametric analysis of the results. Pearson's coefficient of correlation was used to assess the degree of association between log myocardial T2* and both liver iron and serum ferritin and left ventricular ejection fraction and liver iron and serum ferritin. Pearson's coefficient of determination was used to estimate the proportion of variation in log myocardial T2* that could be accounted for by variation in either liver iron or serum ferritin. Unpaired Student's t-tests were used to compare left ventricular ejection fractions in patients with liver iron levels above and below 15mg/g dry weight and in patients with mean one-year serum ferritin levels above and below

2500µg/l. Stepwise backward multivariate analysis was used to detect predictors of left ventricular ejection fraction from five clinical covariates. A p value of less than 0.05 was considered to indicate statistical significance.

6.3 RESULTS

6.3.1 Relationships between Liver Iron and Serum Ferritin and log Myocardial T2*

Although the relationship between liver iron and log myocardial T2* achieves statistical significance in this large cohort (p=0.0002), the degree of association is weak (r=0.26) and only 6.5% of the variation in log myocardial T2* can be accounted for by variation in liver iron (figure 6.1).

Figure 6.1 The Relationship Between Liver Iron and Log Myocardial T2*

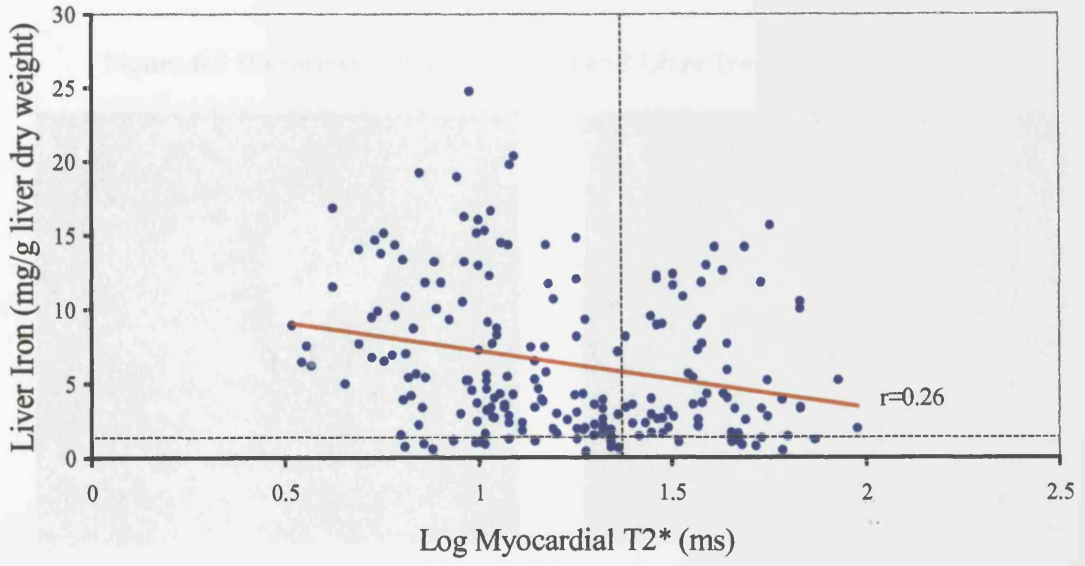

The relationship between serum ferritin and log myocardial T2* also achieves statistical significance (p=0.005) but the degree of association is negligible (r=0.19) and only 3.4% of the variation in log myocardial T2* can be accounted for by variation in serum ferritin (figure 6.2).

Figure 6.2 The Relationship Between Serum Ferritin and Log Myocardial T2*

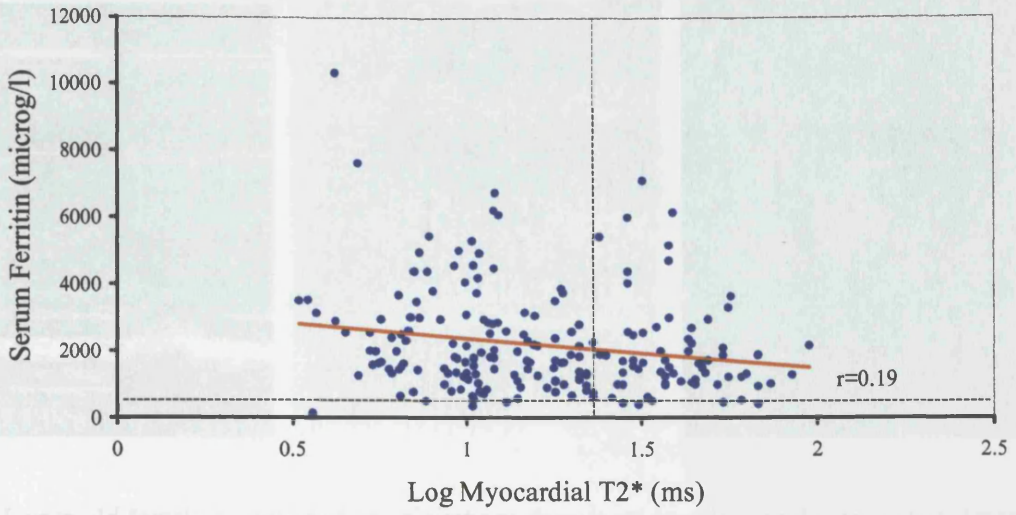

In many patients there were marked discrepancies between liver and heart iron concentration (figure 6.3), and serum ferritin and heart iron concentration (figure 6.4).

Figure 6.3 Discordance between Heart and Liver Iron Concentration

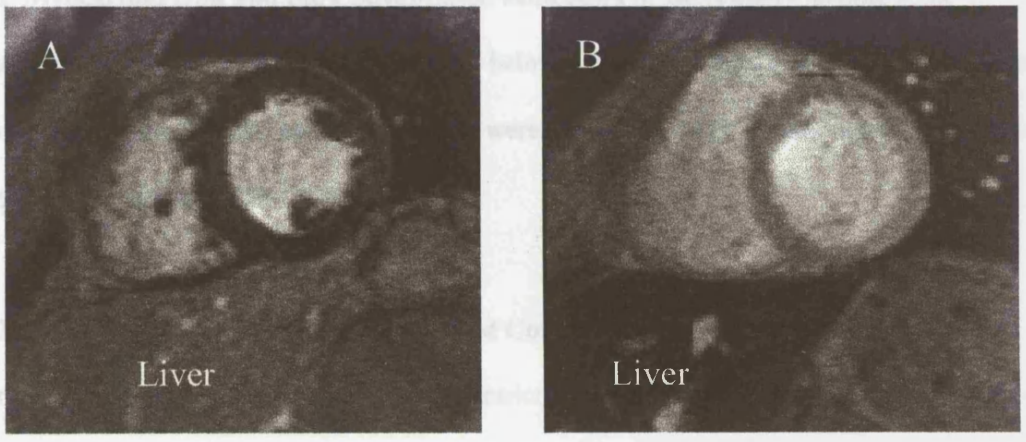

Panel A. Severe cardiac but minimal liver iron deposition (black heart, grey liver).
Panel B. Normal cardiac iron but severe liver iron overload (grey heart, black liver).

Figure 6.4 Discordance between Serum Ferritin and Myocardial Iron Deposition

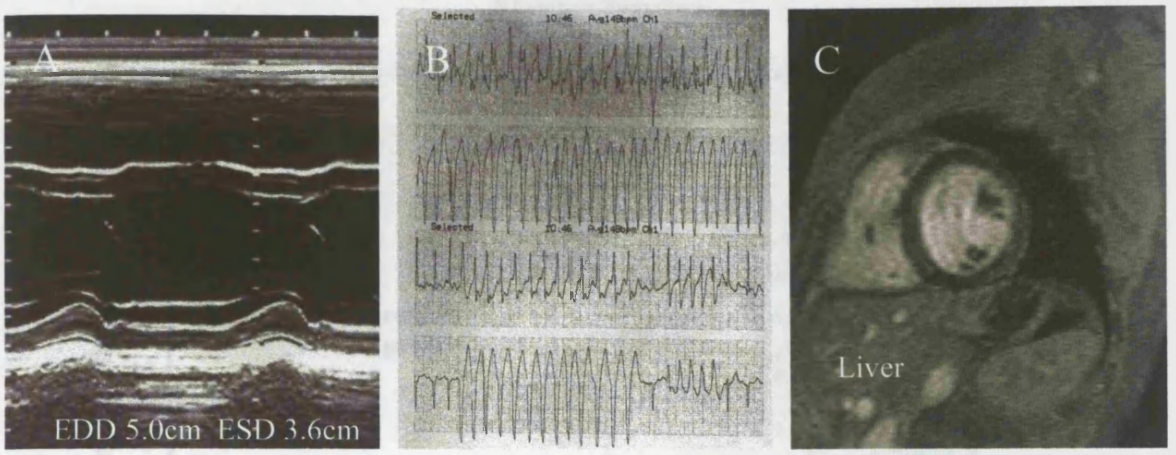

A 31-year-old female complained of palpitations despite an excellent chelation history (mean one year serum ferritin 504µg/l). Although the echocardiogram was within normal limits (panel A), the 24-hour tape revealed multi-focal, non-sustained ventricular tachycardia (panel B). A cardiac magnetic resonance scan was performed which confirmed significant myocardial iron deposition (myocardial T2*=7.6ms, panel C). The patient was commenced on amiodarone and continuous desferrioxamine chelation therapy and remains well and free of cardiac symptoms a year later.

6.3.2 Myocardial Iron and the Conventional Indicators of Increased Cardiac Risk

Fifty-seven percent of patients with liver iron below 15mg/g dry weight and 54% of patients with mean serum ferritin below 2500µg/l were found to have excess myocardial iron deposition (myocardial T2*<20ms).

6.3.3 Left Ventricular Ejection Fraction and Conventional Indicators of Cardiac Risk

There was no significant difference in left ventricular ejection fraction in patients with liver iron above 15mg/g (LVEF 66.1± 6.3%) or below 15mg/g (LVEF 66.2 ± 9.0%, p=0.96) or with serum ferritin levels above 2500µg/l (LVEF 65.1 ± 10.1) or below 2500µg/l (LVEF 66.6 ± 8.2, p=0.22). No significant correlation could be demonstrated between liver iron and left ventricular ejection fraction (r=0.13, p=0.07) or serum ferritin and left ventricular ejection fraction (r=0.08, p=0.27) in the cohort of 205 patients.

Figure 6.5 The Relationship between Liver Iron Concentration and Left Ventricular Ejection Fraction

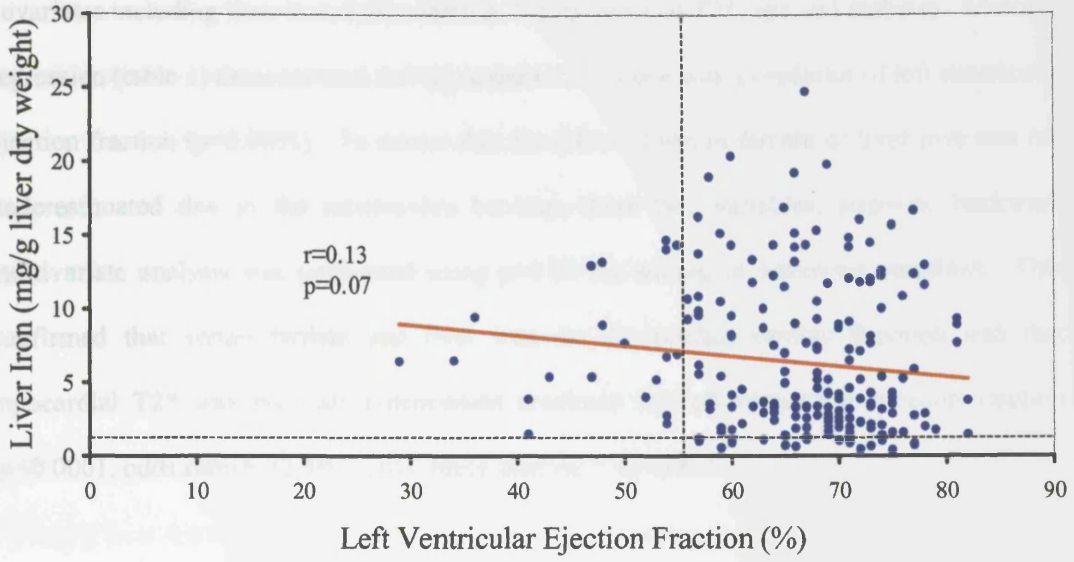

Figure 6.6 The Relationship between Serum Ferritin and Left Ventricular Ejection Fraction

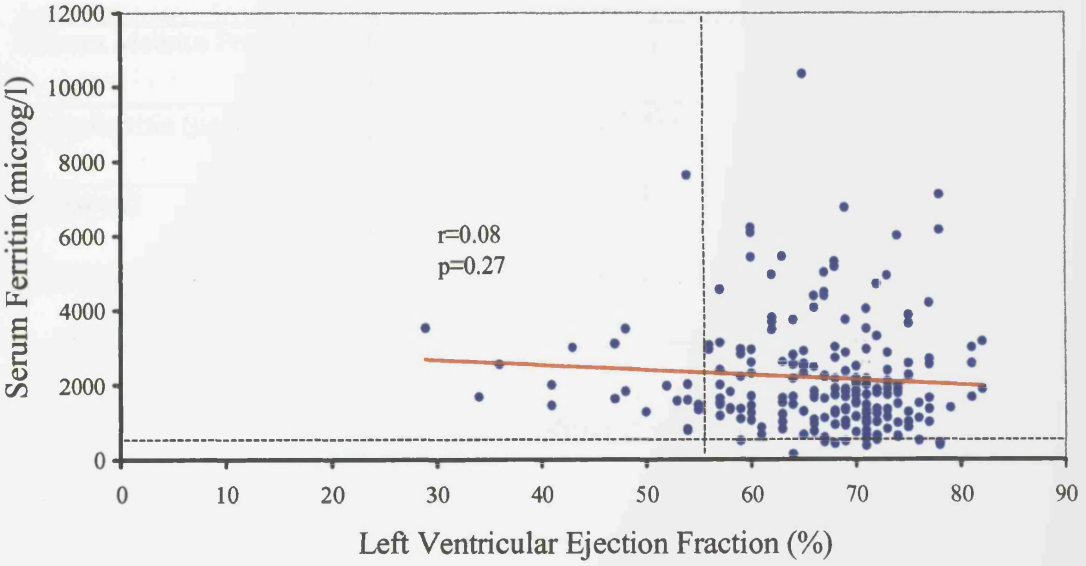

6.3.4 Assessment of Predictors of Cardiac Function

Logistic regression was performed to relate left ventricular ejection fraction to five clinical covariates including liver iron, serum ferritin, log myocardial T2*, age and diabetes. Multiple regression (table 1) demonstrated that myocardial T2* alone was a predictor of left ventricular ejection fraction ($p<0.0001$). To ensure that the effect of serum ferritin or liver iron was not underestimated due to the relationship between these two variables, stepwise backward multivariate analysis was performed using $p=0.05$ for adding or removing variables. This confirmed that serum ferritin and liver iron do not predict cardiac function and that myocardial T2* was the only independent predictor for left ventricular ejection fraction ($p<0.0001$, odds ratio 6.72, 95% confidence interval 5.42 to 8.01).

Table 6.1 Multivariate Analysis of Clinical Variables to Assess Predictors of Left Ventricular Ejection Fraction

VARIABLE	ODDS RATIO (95% CI)	P VALUE
Log Myocardial T2* (ms)	7.0 (5.64, 8.35)	<0.0001
Diabetes Mellitus Present	2.04 (-0.24, 4.32)	0.08
Serum Ferritin (µg/l)	0.0002 (-0.0005, 0.0001)	0.49
Age (years)	0.046 (-0.09, 0.18)	0.50
Liver Iron (mg/g dry weight)	0.03 (-0.23, 0.28)	0.84

CI denotes confidence interval

6.4 DISCUSSION

The measurement of liver iron has been considered the gold standard guide to the estimation of body iron stores [Pippard 1989]. It was believed that cardiac iron deposition was a late complication of iron overload and occurred only in the presence of severe liver iron loading [Buja 1971, Johnston 1989]. The benchmark value of 15mg/g liver dry weight (80μmol/g liver wet weight) above which a patient was assumed to have increased cardiac risk was adopted from a follow-up study of the effectiveness of chelation therapy in 59 patients with thalassaemia major [Brittenham 1994b]. Of interest, this was not a direct conclusion of the paper itself but of subsequent authors, inferred from a subset of 15 patients who developed cardiac complications. Liver iron was measured in 11 of these 15 patients and found to be >15mg/g liver dry weight in all. Data from only 11 patients generated the figure of 15mg/g liver dry weight, which has subsequently influenced the chelation treatment and risk assessment of young patients with thalassaemia.

Review of the literature shows that the assumption of an even distribution of iron between organs originates from early autopsy studies performed prior to the introduction of iron chelation therapy [Buja 1971]. MRI facilitates the simultaneous assessment of heart and liver iron levels as well as cardiac function and leads us to question these assumptions in the modern era. The results in the present large cohort of thalassaemic patients have demonstrated a very weak association between heart and liver iron stores and no significant correlation between left ventricular ejection fraction and liver iron. There was no significant difference in left ventricular ejection fraction in patients with liver iron above or below 15mg/g and iron-induced cardiomyopathy can develop even in the presence of very low liver iron levels (figures 6.3 and 6.4). Therefore, although liver biopsy with histological analysis will retain an important role in the assessment of liver cirrhosis in these patients, liver iron measurements alone, by biopsy or quantum interference measurement [Brittenham 1982], should no longer be relied upon to estimate cardiac iron levels.

Part of the disparity between liver and heart iron levels can be explained by the effects of iron chelation therapy. Iron has been shown to clear at differing rates from the liver and the heart

[Anderson 2001b], and the mechanism of uptake of iron chelators varies between organs [Porter 1989]. However there also appears to be substantial inter-patient variation in the predominant site of iron deposition, which remains to be investigated and explained.

The measurement of serum ferritin is the most commonly used indirect estimate of body iron stores [Finch 1986, Pippard 1989]. However, serum ferritin differs structurally from tissue iron-storage ferritin [Halliday 1984] and only reflects the proportion of iron in transit in the blood (<1% of the total iron storage pool). Early studies with immunological techniques indicated that serum ferritin may vary with body iron stores. Ferritin was shown to be decreased in iron deficiency states and raised in haemochromatosis [Jacobs 1972], and a correlation between serum ferritin and liver iron by biopsy and a between serum ferritin and total quantity of blood transfused were shown in 18 patients with thalassaemia [Letsky 1974]. However, the reliability of serum ferritin to indicate even liver iron stores has been questioned [Wands 1976, Crosby 1976]. In a study of thalassaemic and sickle cell patients, only 57% of the variation in serum ferritin was shown to be related to variation in liver iron [Brittenham 1993]. This can be explained by variation of serum ferritin with other factors common in thalassaemia such as inflammation [Lipschitz 1974], hepatocellular damage [Prieto 1975] and ascorbate deficiency [Chapman 1982]. A relationship between serum ferritin and myocardial iron has been assumed from the moderate relationship between serum ferritin and liver iron, although only two studies of the relationship between myocardial iron by biopsy and serum ferritin have been published. The results are not decisive, as both were performed in small groups of patients (15 or less) and one demonstrated a relationship [Lombardo 1995], the other did not [Barosi 1989].

Olivieri at al reported the prognosis for survival without cardiac disease as excellent for thalassaemia major patients whose serum ferritin levels remain below 2500mg/l [Olivieri 1994]. In fact the estimated cardiac disease free survival rate was 91% at 15 years – in a patient group with a mean age of only 23 years after a median of 12 years follow-up. In this large cohort we have shown no significant difference in left ventricular ejection fraction in patients with serum ferritin levels above or below 2500µg/l, and that more than half of

patients (54%) with ferritin levels below 2500μg/l have excess myocardial iron deposition. No relationship could be demonstrated between left ventricular ejection fraction and serum ferritin levels. Therefore although serum ferritin is readily obtainable and likely to retain its value in observing trends in patient compliance to therapy, it should not be relied upon as an accurate gauge for myocardial iron or function.

Conclusions

Neither serum ferritin or liver iron measurements reliably predict those patients with increased myocardial iron deposition or impaired ventricular function. The benchmark figures for increased cardiac risk of a liver iron greater than 15mg/g dry weight and serum ferritin levels above 2500μg/l are misleading in many patients and should now be abandoned. Direct assessment of myocardial iron is necessary to guide chelation therapy in thalassaemic patients and to reduce the excessive and preventable cardiac mortality.

CHAPTER 7: THE VARIABILITY OF RETICULO-ENDOTHELIAL AND PARENCHYMAL IRON DEPOSITION IN THALASSAEMIA MAJOR

7.1 INTRODUCTION

Conventional teaching asserts that in transfusional iron overload, reticulo-endothelial iron loading of the spleen and bone marrow occurs first [Finch 1982], and only when these stores are saturated is iron deposited in the parenchymal cells of the liver, heart and endocrine organs [Jandl 1987], which are sensitive to the toxic effects of iron [McLaren 1983, Gordeuk 1987]. Cardiac iron deposition is believed to occur late, and only in the presence of severe spleen and liver iron overload [Buja 1971, Johnston 1989].

On the basis of these theories, liver iron has been considered the gold standard indicator for body iron stores [Pippard 1989] and as serum ferritin correlates with liver iron in normal individuals [Addison 1972, Cazzola 1983], it is widely used as an indirect marker for tissue iron levels in thalassaemia.

With the emergence of advanced MR techniques it is now possible to assess iron levels in the heart, liver, spleen, pancreas and bone during the same scan. We have analysed the data from 210 patients with thalassaemia major in order to examine the pattern of iron deposition in the body and the degree to which serum ferritin and liver iron reflect body iron stores.

7.2 METHODS

7.2.1 Patient Cohort

Two hundred and ten thalassaemia major patients were assessed (104 females and 106 males, mean age 27 ± 7.8 years). All patients received transfusions at 2-4 week intervals to maintain the pre-transfusion haemoglobin concentration between 9- 9.5g/dl and all have received long-term iron chelation therapy with a broad range of compliance to treatment (serum ferritin 215-10341µg/l, mean 2109 ± 1517µg/l). Eighty-three patients had not undergone splenectomy, and spleen T2* could be determined in these patients.

7.2.2 MR Assessments of Myocardial, Liver, Spleen, Pancreas and Bone Iron

All patients were scanned using the same T2* sequence with a Picker 1.5T Edge Scanner (Marconi Medical Systems, Cleveland, Ohio). The full protocol is described in section 4.5. Due to the size of the pancreas, it is difficult to image in every scan and T2* measurements were considered inaccurate. High levels of iron in the bone marrow of many patients also led to inaccuracies in T2* measurement. Therefore the pancreas and bone marrow were assessed using signal intensity ratios to paraspinous skeletal muscle from a multi-slice image through the upper abdomen (echo time 4.47ms). Signal intensity ratios have been shown to be inversely proportional to tissue iron concentration [Gandon 1994, Ernst 1997].

7.2.3 Serum Ferritin Measurements

Measurements of serum ferritin were carried out by enzyme immunoassay and all values are referable to the WHO Ferritin 80/602 First International Standard (normal range 15-300μg/l).

7.2.4 Statistical Analysis

Summary data are presented as means ±1 standard deviation. As organ T2* and SIR values were positively skewed, logarithmic transformation was performed in order to allow parametric analysis. Pearson's coefficient of correlation was used to assess the degree of association between organ log T2* and log SIR values. Pearson's coefficient of determination was used to estimate the proportion of variation in log pancreas SIR that could be accounted for by variations in log liver T2* and log myocardial T2*. Pearson's coefficient of correlation was also used to assess the degree of association between serum ferritin and log T2* for the liver, heart and spleen and the log SIR for the pancreas and bone marrow, and Pearson's coefficient of determination was used to estimate the proportion of variation in serum ferritin that could be accounted for by variations in log T2* and log SIR of these organs. In order to determine whether splenectomy was an independent predictor of log myocardial T2*, we performed multiple regression followed by stepwise backward regression

analysis, including liver iron, serum ferritin, age, diabetes and presence of the spleen as covariates. A p value of less than 0.05 was considered to indicate statistical significance.

7.3 Results

7.3.1 Reticulo-endothelial and Parenchymal Iron Stores

A significant correlation was demonstrated between reticulo-endothelial iron stores in the spleen and bone marrow ($r=0.79$, $p<0.0001$; figure 7.1). However no significant relationships were found between the iron levels in the spleen and the iron in the parenchymal organs of the liver, heart or pancreas (log spleen T2* and log liver T2*, $r=0.21$, $p=0.06$, figure 7.2; log spleen T2* and log myocardial T2*, $r=0.06$, $p=0.57$, figure 7.3; log spleen T2* and log pancreas SIR, $r=0.07$, $p=0.52$, figure 7.4).

Figure 7.1 Relationship between Log Spleen T2* and Log Bone SIR

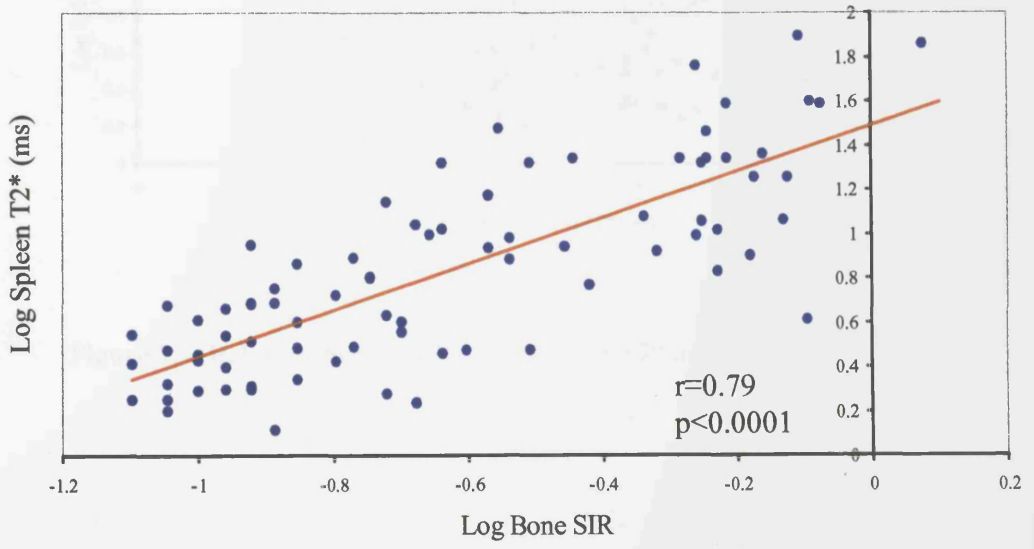

Figure 7.2 Relationship between Log Spleen T2* and Log Liver T2*

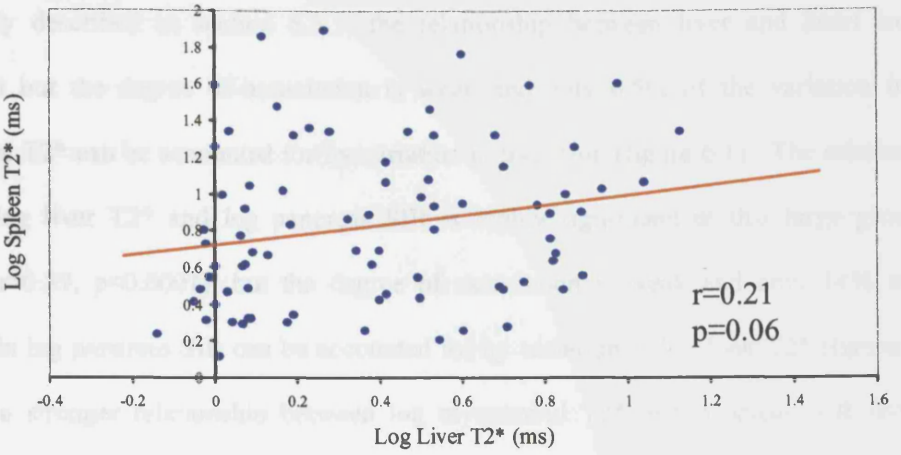

Figure 7.3 Relationship between Log Spleen T2* and Log Myocardial T2*

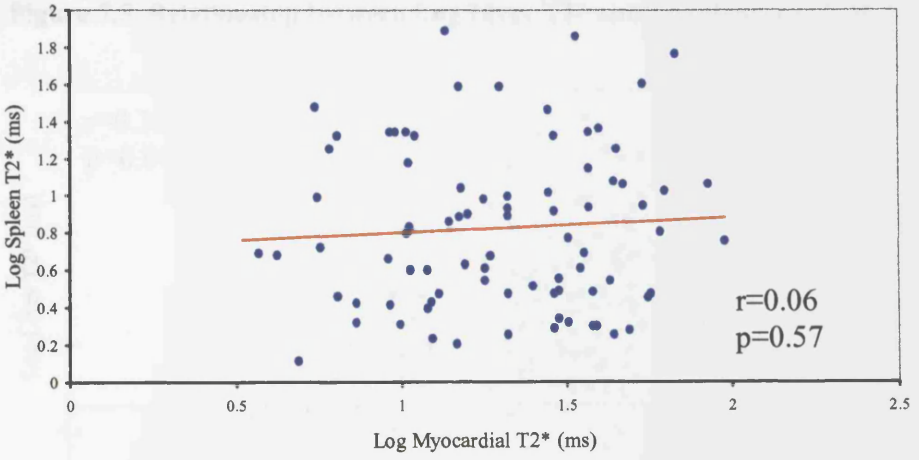

Figure 7.4 Relationship between Log Spleen T2* and Log Pancreas SIR

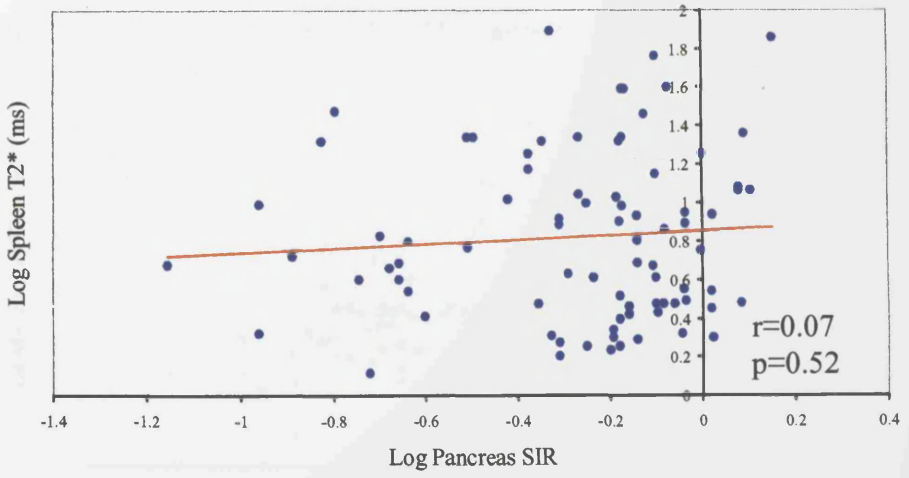

7.3.2 Iron Stores in the Parenchymal Organs of the Liver, Heart and Pancreas

As already described in section 6.3.1, the relationship between liver and heart iron is significant but the degree of association is weak and only 6.5% of the variation in log myocardial T2* can be accounted for by variation in liver iron (figure 6.1). The relationship between log liver T2* and log pancreas SIR is highly significant in this large group of patients (r=0.39, p<0.0001), but the degree of association is weak and only 14% of the variation in log pancreas SIR can be accounted for by variation in log liver T2* (figure 7.5). There is a stronger relationship between log myocardial T2* and pancreas SIR (r=0.59, p<0.0001) and 35% of the variation in log pancreas SIR can be accounted for by variation in log myocardial T2* (figure 7.6).

Figure 7.5 Relationship between Log Liver T2* and Log Pancreas SIR

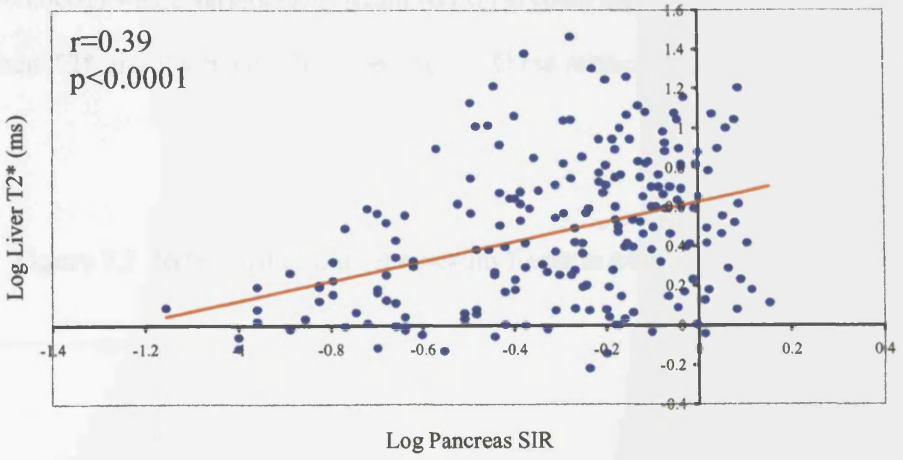

Figure 7.6 Relationship between Log Myocardial T2* and Log Pancreas SIR

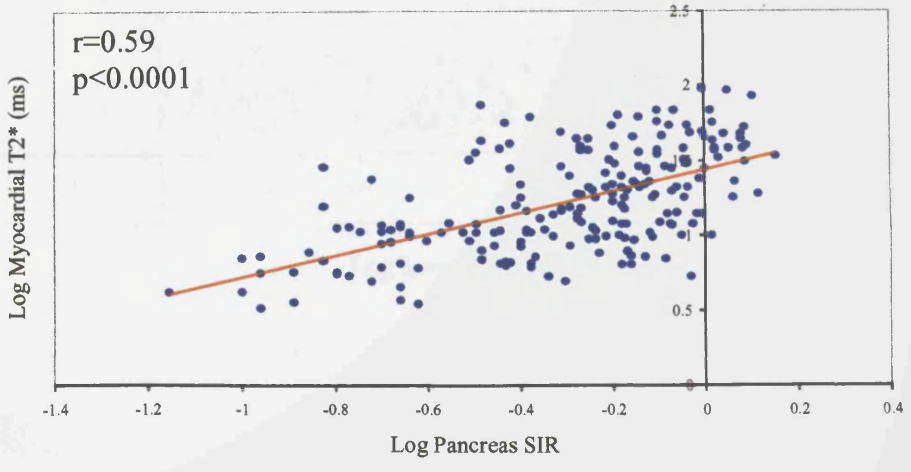

7.3.3 Serum Ferritin and Iron Stores in the Parenchymal and Reticulo-endothelial Organs

We have already shown that although there is a significant correlation between serum ferritin and log myocardial T2*, the degree of association is negligible and only 3.4% of the variation in log myocardial T2* can be accounted for by variation in serum ferritin (figure 6.2). The degree of association between serum ferritin and log pancreas SIR is also weak ($r=0.29$, $p<0.0001$) and only 8.1% of the variation in log pancreas SIR can be accounted for by variation in serum ferritin. A stronger relationship exists between serum ferritin and log liver T2* ($r=0.56$, $p<0.0001$) yet variations in serum ferritin account for only 31% of the variation in log liver T2* levels. The strongest relationship between serum ferritin and tissue iron exists for the reticulo-endothelial organs of the spleen (($r=0.70$, $p<0.0001$) and bone marrow ($r=0.64$, $p<0.0001$) where variations in serum ferritin account for 48 and 40% of the variation in log spleen T2* and log bone SIR respectively. These relationships are shown in figures 7.7-7.10.

Figure 7.7 Relationship between Serum Ferritin and Log Liver T2*

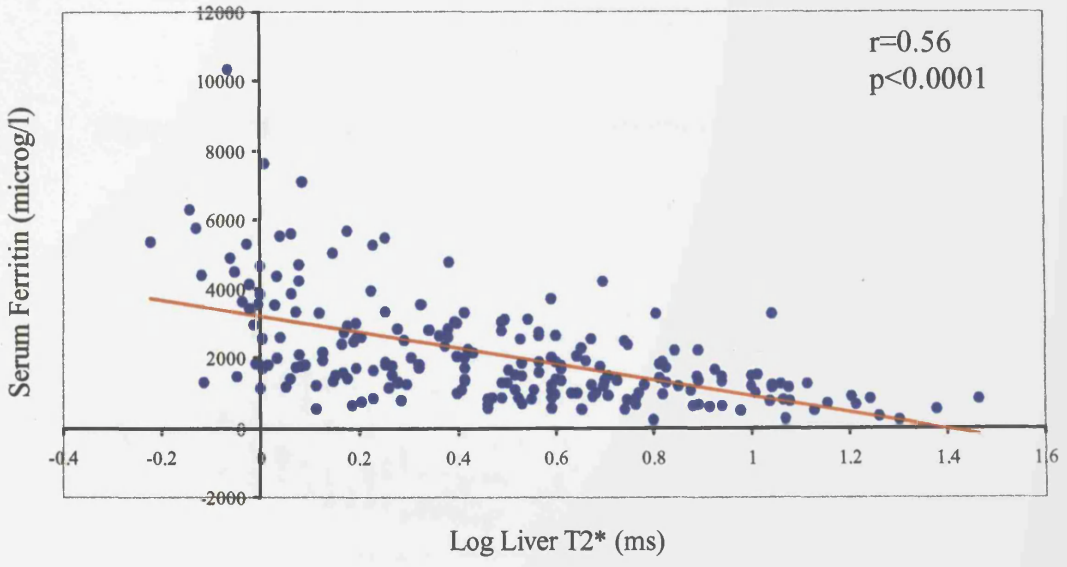

Figure 7.8 Relationship between Serum Ferritin and Log Pancreas SIR

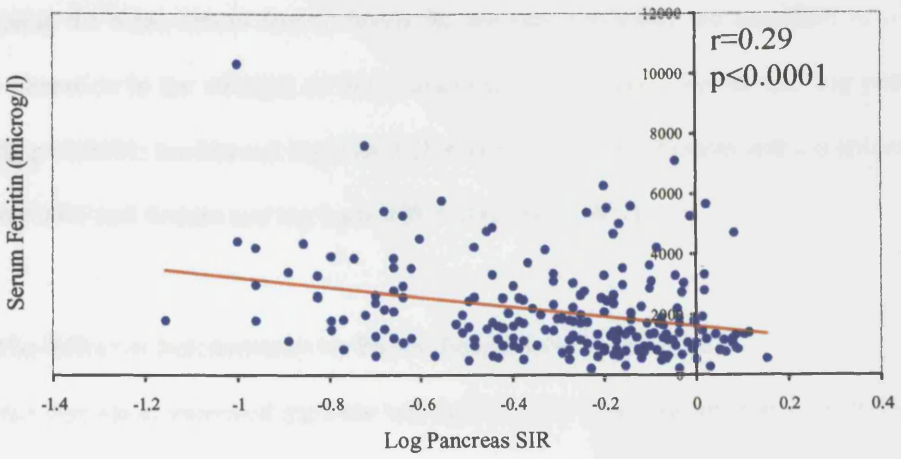

Figure 7.9 Relationship between Serum Ferritin and Log Spleen T2*

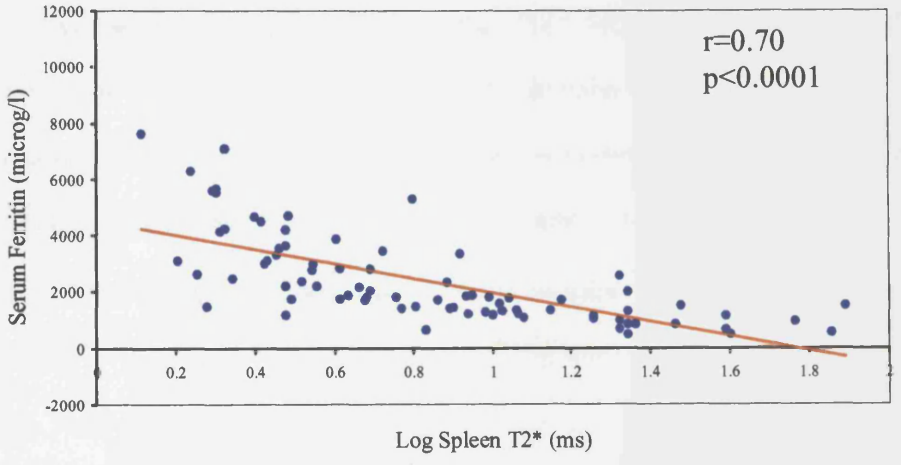

Figure 7.8 Relationship between Serum Ferritin and Log Pancreas SIR

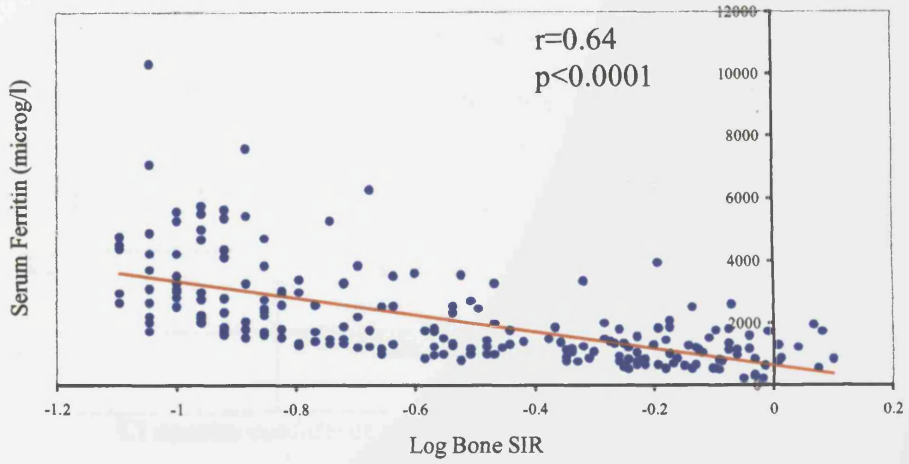

As individual measurements of serum ferritin can give spurious results, we repeated these analyses using the mean serum ferritin levels for the year preceding the magnetic resonance scan. No alteration in the strength of the relationships was found (ferritin and log pancreas SIR r=0.30, p<0.0001; ferritin and log liver T2* r=0.55, p<0.0001; ferritin and log spleen T2* r=0.71, p<0.0001 and ferritin and log bone SIR r=0.63, p<0.0001).

7.3.4 The Effect of Splenectomy on Parenchymal Iron Deposition

It was noted that splenectomised patients had significantly lower serum ferritin (1878±1408 versus 2469±1615μg/l, p=0.006) and significantly lower liver iron (higher liver T2*, 5±4.9 versus 3.2±2.6ms, p=0.002), than non-splenectomised patients. This may be expected as transfusion requirement, and hence iron loading often falls post splenectomy, due to prolongation of red cell survival. However, despite the lower ferritin and liver iron levels, splenectomised patients have significantly higher heart iron (lower myocardial T2*) than non-splenectomised patients (20±17 versus 26±19ms, p<0.0001). In order to determine whether splenectomy was an independent predictor of log myocardial T2*, we performed multiple regression followed by stepwise backward regression analysis. We included liver iron, serum ferritin, age, diabetes and presence of the spleen as covariates. Using p=0.05 to add and p=0.1 to remove variables, we found that liver iron, age and the presence of the spleen were all independent predictors of myocardial T2*

Table 7.1 Model for Prediction of Myocardial T2*

VARIABLE	ODDS RATIO (95% CI)	P VALUE
Liver Iron (mg/g dry weight)	0.96 (0.94, 0.98)	<0.001
Spleen Present	0.61 (0.48, 0.78)	<0.001
Age (years)	1.01 (1.00, 1.03)	0.06

CI denotes confidence interval, adjusted R-squared 12%

7.4 DISCUSSION

Iron overload is the commonest cause of mortality and morbidity in thalassaemia major [Olivieri 1997]. The toxic effects of iron excess become apparent when iron is deposited in the parenchymal cells of the heart [Engle 1964, Anderson 2001a], liver [Risdon 1973], pancreas [Lassman 1974] and endocrine system [Grundy 1994]. In order to guide chelation therapy it is essential to gauge iron levels in the organs sensitive to iron. Until now the most commonly used indicators for body iron stores were liver iron concentration and serum ferritin.

It has been proposed that parenchymal iron deposition occurs only when the iron-storage capacity of the reticulo-endothelial system is exceeded [Finch 1982]. The iron capacity of the reticulo-endothelial cell system has been estimated at 10g, which is the amount of iron in 40 units of blood [Jandl 1987]. However, the results of this study show that very high levels of liver and heart iron deposition can occur without splenic iron deposition (Figures 7.2 and 7.3), and that there is no significant relationship between iron levels in the spleen and iron in the parenchymal organs of the heart, liver and pancreas. This variability in organ iron deposition may be partly explained by the effects of chelation therapy, which is now routinely administered to regularly transfused patients with thalassaemia. Desferrioxamine causes iron to clear at differing rates from the liver and the heart [Anderson 2001b], and the mechanism of uptake of iron chelators varies between organs [Porter 1999].

Serum ferritin is also assumed to reflect body iron stores. Ferritin has a molecular weight of 460,000, and it is comprised of 24 subunits that form a hollow sphere capable of holding up to 4000 atoms of iron. Plasma ferritin differs from intracellular iron-storing ferritin in that it has a very low iron content and is synthesised by the rough rather than the smooth endoplasmic reticulum and glycosylated prior to secretion into the plasma. A correlation between serum ferritin and liver iron by biopsy has been documented in thalassaemic patients [Letsky 1974], but subsequently only 57% of the variation in serum ferritin was found to be associated with variations in liver iron in thalassaemic patients [Brittenham 1993]. Entirely normal serum ferritin levels have also been reported in some haemochromatosis families despite proven

tissue iron overload [Wands 1976, Crosby 1976], and the authors suggested that this might reflect the low levels of reticulo-endothelial iron deposition in haemochromatosis. In the present study the best correlation between serum ferritin and tissue iron occurs with the reticulo-endothelial organs of the spleen and bone marrow. This finding may not be surprising if, as has been suggested, plasma ferritin arises mainly from reticulo-endothelial rather than parenchymal tissues [Siimes 1974, Jacobs 1975].

The influence of splenectomy on myocardial iron deposition is an interesting finding and concurs with earlier work in which increased parenchymal rather than reticulo-endothelial iron deposition was found in patients who had undergone splenectomy [Berry 1967, Risdon 1974]. The authors concluded that these findings may indicate a contraindication to removal of the spleen.

Conclusion

There is substantial variability in iron deposition between organs in patients with thalassaemia major. The theory of gradual loading of reticulo-endothelial followed by parenchymal tissue and late iron loading of the heart is invalid in many patients undergoing chronic chelation therapy. Serum ferritin is a better indicator of the reticulo-endothelial than parenchymal iron stores, and cannot reliably predict iron levels in the organs most sensitive to iron toxicity. Assessment of iron levels in individual organs is necessary to optimise management of iron chelation therapy in thalassaemia and to improve the morbidity and mortality associated with tissue iron overload.

CHAPTER 8: REVERSAL OF IRON-INDUCED CARDIOMYOPATHY: PROSPECTIVE STUDY WITH CARDIOVASCULAR MAGNETIC RESONANCE

8.1 INTRODUCTION

Heart failure due to iron overload can occur secondary either to excess dietary absorption in hereditary hemochromatosis, or to transfusional siderosis. The potential reversibility of iron-induced cardiomyopathy was first documented in case reports of patients with hereditary haemochromatosis treated with recurrent venesection [Easley 1972, Short 1981, Rivers 1987]. Subsequently, improvements in ventricular dysfunction with chelation therapy have been reported in a patient with megaloblastic anaemia [Rahko 1986], thalassaemia major [Wacker 1993] and three patients with transfusional iron overload [Marcus 1984]. However, the reversibility of iron-induced cardiac failure has not been universally accepted, partly due to the high mortality of patients presenting with advanced cardiac failure despite chelation treatment [Marcus 1984] and more recently by those questioning the role of iron in thalassaemic cardiomyopathy [Krematinos 1995 and 1999]. In order to examine the reversibility of iron induced cardiomyopathy, we have prospectively studied 7 thalassaemia major patients with cardiac involvement undergoing intensive intravenous iron chelation. Myocardial and liver T2* levels and ventricular function were assessed at baseline and after 3, 6 and 12 months of treatment.

8.2 METHODS

8.2.1 Study Patients

All patients commencing intensive intravenous desferrioxamine for the treatment of severe iron overload with cardiac involvement were included in the study. One female and 6 male patients with thalassaemia major were studied (mean age 26±5.8 years). Each patient had complied poorly with standard subcutaneous desferrioxamine treatment for a period of at least 2 years prior to the development of cardiac symptoms. Two patients complained of palpitations only and indices of ventricular function, although depressed, remained within

normal limits. Three patients presented with paroxysmal atrial fibrillation associated with a dilated cardiomyopathy. Two patients had overt left and right ventricular failure with intermittent atrial fibrillation. One of these patients (patient 5) died soon after the initial assessment. Clinically relevant characteristics are displayed in table 8.1.

Table 8.1 Patient Characteristics

Characteristic	Patient 1	Patient 2	Patient 3	Patient 4	Patient 5	Patient 6	Patient 7
Age (Years)	21	22	22	23	26	32	36
Sex	Male	Female	Male	Male	Male	Male	Male
Cardiac Symptoms	Palpitations	AF, CCF	PAF, DCM	PAF, DCM	AF, CCF	PAF, DCM	Palpitations
Baseline LVEF (%)	59	41	55	53	41	47	60
Baseline Serum Ferritin (µg/l)	3438	1700	1481	1306	600	2597	3043
Desferrioxamine Dose (mg/kg/day)	50	51	43	47	42	43	48
Diabetes Mellitus	Absent	Absent	Absent	Present	Absent	Present	Absent

LVEF - left ventricular ejection fraction, AF - atrial fibrillation, CCF - congestive cardiac failure, PAF - paroxysmal atrial fibrillation, DCM - dilated cardiomyopathy

8.2.2 Study Protocol

Desferrioxamine was administered continuously via an indwelling central venous catheter in all patients at a mean dose of 46 ± 3.6mg/kg/day. Clinical and MR assessment was performed at baseline and after 3, 6 and 12 months of treatment.

8.2.3 MR Assessments of Myocardial and Liver Iron and Ventricular Function

All patients were scanned using the same sequence with a Picker 1.5T Edge Scanner (Marconi Medical Systems, Cleveland, Ohio). Each scan included the measurement of liver and heart iron using T2*, and the measurement of ventricular volumes, mass and ejection fraction as described in section 4.5.

8.2.4 Statistical Analysis

Summary data are presented as means ±1 standard deviation. A summary measures analysis was performed to assess for significant changes in heart and liver T2* as well as indices of ventricular function over time. Paired Student's t-tests were used to compare heart and liver T2* and left ventricular function in the six patients who survived, between the start and after 12 months of treatment. A p value of <0.05 was considered significant in all tests.

8.3 Results

8.3.1 Summary Measures Analysis

Severe heart and liver iron overload was present in all patients at baseline. A summary measure was created for each patient and the individual slopes for each subject were analysed over time (table 8.2). The slopes for each variable including heart and liver T2*, and left ventricular ejection fraction, end systolic volume and mass were calculated and then averaged across all subjects. There were significant improvements in heart T2* (p=0.012), left ventricular ejection fraction (p=0.017), left ventricular end systolic volume (p=0.037) and left ventricular mass (p=0.007) over time. Myocardial T2* increased by 0.24ms, left ventricular ejection fraction improved by 0.85%, left ventricular end systolic volume decreased by 2.3ml, and left ventricular mass decreased by 1.4g on average per month.

Mean values for each parameter at 0, 3, 6 and 12 months are displayed in table 8.3.

Table 8.2 Results from Analysis of Individual Slopes

Parameter	Average Slope (change per month)	95% CI for slope	P-value
Myocardial T2* (ms)	0.24	0.08 to 0.39	0.012
Liver T2* (ms)	0.71	-0.04 to 1.46	0.060
LVEF (%)	0.85	0.23 to 1.47	0.017
LVESV (ml)	-2.29	-4.38 to -0.20	0.037
LV Mass (g)	-1.36	-2.15 to -0.57	0.007

CI - confidence interval, LVEF - left ventricular ejection fraction, LVESV - left ventricular end systolic volume, LV Mass - left ventricular mass

Table 8.3 Mean values for Myocardial and Liver T2* and Ventricular Function over Time

	Myocardial T2* (ms)	Liver T2* (ms)	LVEF (%)	LVESV (ml)	LV Mass (g)
Baseline (n=7)	5.2±1.8	2.0±1.0	51±7.8	95±36	171±35
3 months (n=6)	7.1±2.1	3.4±1.8	61±8.1	61±14	150±23
6 months (n=6)	7.5±2.5	6.9±5.3	62±7.9	62±16	148±22
12 months (n=6)	8.1±2.8	10.3±9.2	63±6.4	55±8.6	145±23

8.3.2 Left Ventricular Function, Heart and Liver T2* in the Six Surviving Patients

Left Ventricular Function

There was a gradual improvement in left ventricular ejection fraction (LVEF) in all 6 surviving patients over the course of treatment. There was a significant improvement in LVEF from a baseline mean of 52±7.1ml to 63±6.4ml at 12 months (P=0.013). Left ventricular end systolic volume fell from a mean of 84±24ml at baseline to a mean of 55±8.6ml at 1 year (p=0.027) and left ventricular mass fell significantly from a mean of 161±26g at baseline to a mean of 144±24g at 12 months (p=0.006).

Heart and Liver Iron

There was a progressive improvement in myocardial T2*, which is inversely related to myocardial iron, from a baseline mean of 5.1±1.9ms to a mean of 8.1±2.8ms by 1 year (p=0.012). However, considerable myocardial iron remains at 1 year and only one patient had a myocardial T2* greater than 10ms (normal myocardial T2* >20ms). Liver iron fell more quickly during intravenous iron chelation, from a baseline mean of 1.8±0.9ms (9.6±4.3mg/g liver dry weight) to 10.3±9.2ms (2.1±1.5mg/g liver dry weight – normal level 0.35-1.36mg/kg liver dry weight) at 1 year (p=0.05). By 6 months, liver iron content had normalised in three patients.

8.3.3 Cardiac Symptoms and Medication

Patient 5 died soon after the initial scan, but in the surviving patients improvements in ventricular function and myocardial iron were associated with improved cardiac symptoms. Patients 1 and 7 were free of palpitations after 3 months of treatment. Patient 2 improved from New York Heart Association (NYHA) class 4 at baseline to NYHA 2 by 6 months, and to NYHA class 1 by 12 months. ACE inhibitors, diuretics and digoxin were discontinued by 1 year and the patient complained of occasional palpitations only. Patient 3 had no further palpitations after 3 months and β-blockers were stopped at 1 year. Although less frequent, occasional paroxysmal atrial fibrillation persisted in patients 4 and 6 and both remained on β-blockers at 1 year.

8.3.4 Complications of Intensive Intravenous Iron-chelation Treatment

Problems Related to Indwelling Central Line Catheters

Line thrombosis occurred in 1 patient after 3 weeks of treatment and a second line was inserted which was functioning well at 12 months. Line displacement occurred in a second patient after 1 week. The replacement line worked well for the duration of treatment.

Desferrioxamine Toxicity

Symptoms of desferrioxamine auditory neurotoxicity occurred in 3 of the patients, all associated with low ferritin levels. In patient 2, symptoms of tinnitus settled after the dose of desferrioxamine was reduced (ferritin level 600μg/l). In patient 3, serum ferritin levels fell to 146μg/l at 12 months, associated with high frequency sensorineural hearing loss on audiogram. Symptoms improved after discontinuation of the desferrioxamine. Patient 6 complained of tinnitus at 6 months when the ferritin level had fallen to 441μg/l. Despite reducing the dose of desferrioxamine, symptoms recurred and desferrioxamine was discontinued. The patient received oral deferiprone only for the next six months. Myocardial

iron continued to fall in this patient, associated with improving ventricular function and results at 12 months have been included in the final analysis.

8.4 Discussion

These results confirm the reversibility of the iron-induced cardiomyopathy when it is treated aggressively with iron chelation therapy. Although one patient died at the start of the study, all other patients showed a steady improvement in cardiac iron and ventricular function. After 1 year of treatment, all surviving patients had left ventricular ejection fractions within the normal range. The outlook for patients presenting in advanced cardiac failure remains poor [Ehlers 1991, Felker 2000], but if a patient survives the hazardous initial months of therapy, the outlook is good and a return to normal lifestyle and normalisation of systolic ventricular function is achievable. The potential reversibility of this cardiomyopathy, once iron is removed, influences its treatment. Despite the high mortality in advanced cases, management should be active and aggressive including mechanical assistance during the acute initial presentation if necessary. Although cardiac medication, in the form of antiarrhythmics, ACE inhibitors and diuretics, are essential during the initial management, the main aim of treatment should be to remove iron rapidly from the myocardium in order to reverse the cardiomyopathy and eventually render cardiac medication unnecessary whenever possible. Although cardiac transplantation has been performed in thalassaemic and haemochromatosis patients [Perrimond 1991, Jensen 1993, Koerner 1997], this option should only be considered in cases where effective iron removal cannot be achieved.

The exact mechanism by which iron overload causes a reversible reduction in cardiac function is not known. At normal body iron levels, plasma iron is bound to transferrin, preventing catalytic activity and free radical production. However, when transferrin becomes fully saturated, the non-transferrin bound fraction of iron becomes detectable in plasma, accelerating the formation of free hydroxyl radicals and facilitating the uptake of iron by tissues [Gutteridge 1985]. Excess iron is gradually deposited as ferritin and haemosiderin within intracellular lysosomes. In these forms the iron is relatively non-toxic but it is likely

that the myocardial cell begins to fail once a critical concentration is reached and the iron storage capacity is exhausted, releasing free iron into the cell. In the heart, this results in impaired function of the mitochondrial respiratory chain and is manifested clinically as heart failure [Hershko 1998]. However, the relatively mild degree of fibrosis in most autopsy studies suggests that even when advanced, the cardiomyopathy may be potentially reversible [Buja 1971]. The oxidative state plays an important role in iron toxicity [Hershko 1987b], as it affects both the uptake of iron into the cell and the release of free iron. In this study, it was sepsis related to cholecystitis that precipitated the rapid deterioration of patient 5, resulting in death in low output cardiac failure.

Removal of iron from the heart is a slow process and even after one year, five of the remaining six patients have high levels of myocardial iron (T2*<10ms). Conversely, liver iron appears to clear more rapidly with desferrioxamine treatment, and liver iron levels had normalised in three patients by six months (figure 8.1). The difference in iron clearance rates between organs may in part be due to the larger, more crystalline structure of cardiac ferritin [St-Pierre 1991], or due to an active uptake mechanism for desferrioxamine into hepatic cells [Porter 1989]. Differing rates of iron clearance can result in large variations in iron concentration between organs. Although liver biopsy was used in the past to guide management in iron overloaded patients, these results demonstrate that liver iron alone cannot be used to gauge the cardiac risk of the patient as liver iron normalises far more quickly than myocardial iron. This slow clearance of iron from the heart may be important in haemochromatosis patients, where liver iron and serum ferritin are still used as the main guides to venesection regimes.

Limitations

At 1 year, significant myocardial iron remained in the majority of patients and further assessments are necessary to determine whether myocardial iron continues to fall and whether this is associated with ongoing improvements in cardiac function.

Figure 8.1 Iron Deposition before and during Intravenous Chelation Therapy

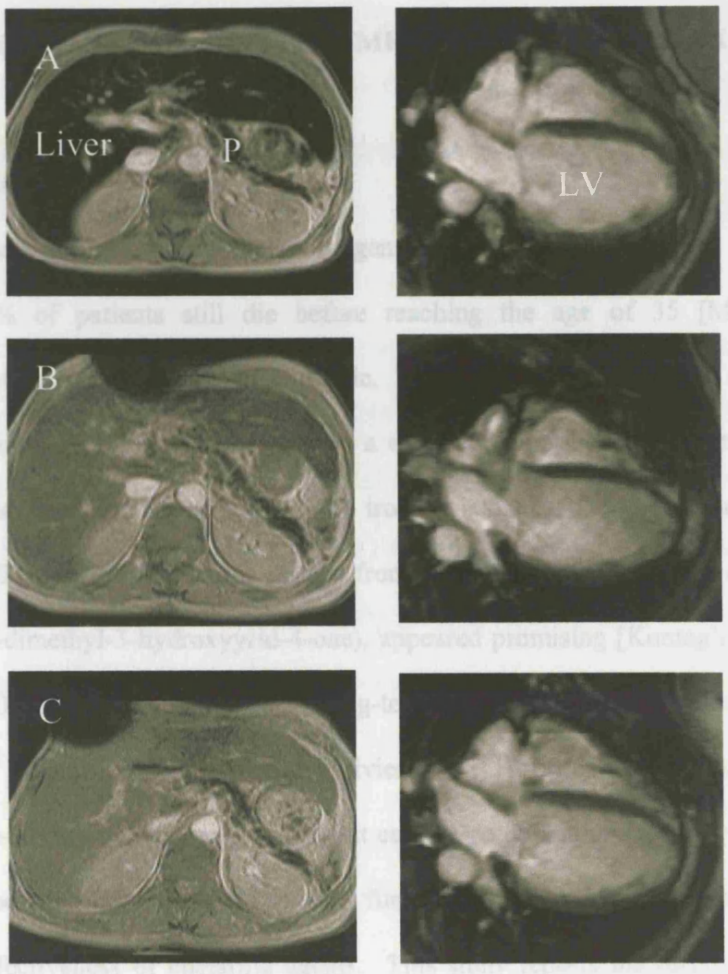

Before treatment (panel A), after 3 months (panel B) and after 6 months of treatment (panel C). There is severe iron loading (dark tissue signal) in the liver, pancreas (P) and heart prior to treatment. By 3 months, liver iron is almost normal, but there is less improvement in cardiac iron. By 6 months, liver iron is normal but significant myocardial iron remains.

Conclusions

Iron-induced heart failure is reversible when iron overload is treated. Clinical management should therefore be aggressive, with the primary objective being the swift removal of myocardial iron. Due to differing rates of iron clearance between organs, liver biopsy alone is insufficient to guide treatment.

CHAPTER 9: IMPROVED CARDIOPROTECTION WITH DEFERIPRONE COMPARED TO STANDARD TREATMENT WITH DESFERRIOXAMINE

9.1 INTRODUCTION

Despite the introduction of the iron-chelating agent desferrioxamine more than 20 years ago in the UK, 50% of patients still die before reaching the age of 35 [Modell 2000]. Administration of desferrioxamine is problematic. The drug requires prolonged subcutaneous or intravenous infusions on at least 4 to 6 days a week and compliance to treatment is often inadequate. The need for an effective oral iron-chelator has long been acknowledged [Weatherall 1983], and medium-term results from prospective trials of the oral chelator, deferiprone (1,2-dimethyl-3-hydroxyyrid-4-one), appeared promising [Kontoghiorghes 1990, Agarwal 1992, Olivieri 1995], however, its long-term effectiveness has been questioned due to high levels of liver iron in some patients [Olivieri 1998, Hoffbrand 1998]. As the primary objective of iron–chelation therapy is to prevent cardiac complications from myocardial iron deposition, myocardial iron and ventricular function should also be considered when assessing the effectiveness of chelating agents. This study reports the results of heart and liver iron and ventricular function after long-term chelation with deferiprone and compare these results with a set of age, sex, and ferritin-matched control patients receiving standard therapy with subcutaneous desferrioxamine.

9.2 METHODS

9.2.1 Study Patients

Fifteen thalassaemia major patients have received chelation with deferiprone alone for more than three years (mean duration 5.7 ± 1.8 years). We assigned 2 age-, sex- and ferritin-matched thalassaemia major controls receiving standard subcutaneous desferrioxamine therapy to each deferiprone patient in order to compare the effectiveness of iron chelation. All patients received transfusions at 2-3 week intervals to maintain the pre-transfusion

haemoglobin concentration between 9- 9.5g/dl and all have received long-term iron chelation therapy (since the late 1970s or from early childhood in patients born after this time). The reason for commencing deferiprone was the refusal or inability to comply with the subcutaneous regime in 12 patients and desferrioxamine toxicity in 3 patients (auditory neurotoxicity in 2 and growth impairment in 1). Clinically relevant characteristics for both groups are compared in table 9.1.

The mean administered dose of deferiprone was 80.5±10.1mg/kg body weight divided into 3 separate doses and the drug was prepared by Pfertec Pharmaceuticals, Essex, UK. The mean dose of desferrioxamine was 37.4±7.9 mg/kg body weight on 5.1±0.8 days per week, having commenced desferrioxamine a mean of 18.3±2.8 years earlier. At the time of the MR assessment, 13 patients were administered the drug via 24-hour infusors and 17 patients via overnight infusors. As this study is a comparison of current iron status, patients were matched for current ferritin readings.

Table 9.1 Patient Characteristics

	Deferiprone Cohort	**Desferrioxamine Controls**	**P Value**
Number of Patients	15	30	-
Mean Age (years)	29.0 ± 6.3	29.4 ± 7.1	0.62
Sex	3 female, 12 male	6 female, 24 male	-
Serum Ferritin (µg/l)	1236 ± 651	1250 ± 508	0.81
Diabetes Mellitus	6 patients (40%)	11 patients (36.7%)	>0.99
Hypopituitary Hypogonadism	7 patients (46.7%)	20 patients (66.7%)	0.22
Hypothyroidism	2 patients (13.3%)	2 patients (6.6%)	0.59
Hepatitis C	4 patients (26.7%)	9 patients (30%)	>0.99

9.2.2 MR Assessments of Myocardial and Liver Iron and Ventricular Function

All patients were scanned using the same sequence with a Picker 1.5T Edge Scanner (Marconi Medical Systems, Cleveland, Ohio). Each scan included the measurement of liver and heart iron using T2*, and the measurement of ventricular volumes, mass and ejection fraction as described in section 4.5.

As liver T2* has been validated against liver biopsy iron concentration, we have converted all liver T2* measurements into milligrams per gram liver dry weight as described in section 4.3.3. Myocardial T2* has not been converted into tissue iron concentrations because although the relationship is likely to be similar to that for liver iron, the precise correlation awaits confirmation with a right ventricular biopsy study. Myocardial T2* values measured in healthy volunteers showed a normal distribution with a mean value of 52ms, and a lower 95% confidence interval of 20ms.

9.2.3 Echocardiographic Data

Follow-up echocardiographic data in the form of M-Mode left ventricular dimensions and shortening fractions were available for 9/15 deferiprone patients and 20/30 desferrioxamine controls.

9.2.4 Statistical Analysis

Summary data are presented as means ±1 standard deviation. Paired Student's t-tests were used to assess comparisons of heart and liver iron and left ventricular function between the deferiprone and the desferrioxamine groups. Each deferiprone patient was paired to the mean value of the two matched desferrioxamine patients. As left ventricular volumes and mass vary with the height and weight of a patient, left ventricular volume and mass indices were calculated by dividing end systolic and end diastolic volumes and left ventricular mass by the patient's surface area. Comparisons between the 30 desferrioxamine control patients and the larger population of 160 patients receiving subcutaneous desferrioxamine were assessed using unpaired Student's t-tests. Comparisons of proportions of patients with excess

myocardial iron deposition in the three groups were assessed using Fisher's exact tests. The risk ratio for the prevalence of excess myocardial iron in the deferiprone versus the desferrioxamine group is calculated with a 95% confidence interval. A p value of <0.05 was considered significant in all tests.

9.3 RESULTS

9.3.1 Myocardial Iron and Ventricular Function

The deferiprone-treated group had significantly less myocardial iron (myocardial T2* 37 ± 19.3ms) than the desferrioxamine treated group (myocardial T2* 21 ± 14.5ms, p=0.012). This corresponded with significantly higher left ventricular ejection fractions (p=0.004) and significantly less left ventricular dilatation in both systole (p=0.035) and diastole (p=0.015) in the deferiprone patients. There was a trend towards lower left ventricular mass index in the deferiprone patients but the difference was not significant (p=0.094). Excess myocardial iron (myocardial T2* value <20ms) was found in 27 % of deferiprone patients versus 67% desferrioxamine patients (p=0.025). The likelihood ratio for the prevalence of excess myocardial iron in the deferiprone versus the desferrioxamine group was 0.4 (95% confidence interval 0.19 to 0.83).

9.3.2 Liver Iron

Despite the superior results for both myocardial iron and left ventricular function in the deferiprone-treated patients (table 9.2), this group was found to have significantly higher levels of liver iron (mean 6.5 ± 4.5mg/g liver dry weight) than the desferrioxamine group (mean 3.9 ± 2.5 mg/g liver dry weight, p=0.024).

Table 9.2 Comparisons of Heart and Liver Iron and Indices of Left Ventricular Function between the Deferiprone and Desferrioxamine Treated Patients

	Deferiprone Treated Patients	Desferrioxamine Treated Patients	Mean Difference	95% Confidence Interval	P Value
Myocardial T2* (ms)	37 ± 19	21 ± 14.5	16	4.1 to 27.8	0.012
Left Ventricular Ejection Fraction (%)	70 ± 6.5	63 ±6.9	7.5	2.8 to 12.2	0.004
Left Ventricular End Systolic Index (ml/m^2)	24 ± 10	36 ± 11	-11	-17 to -5	0.015
Left Ventricular End Diastolic Index (ml/m^2)	81 ± 19	94 ± 13	-12	-23 to -1	0.035
Left Ventricular Mass Index (g/m^2)	87 ± 18	94 ± 11	-6.9	-15 to 1.3	0.094
Liver Iron (mg/g liver dry weight)	6.5 ± 4.5	3.9 ± 2.5	2.6	0.4 to 4.8	0.024

9.3.3 Comparison of Desferrioxamine-treated Group to a Larger Population of Patients Treated with Subcutaneous Desferrioxamine

To ensure that the myocardial iron and ventricular function in the desferrioxamine group were representative of the general thalassaemia major population we compared the results of the control group with 160 patients receiving standard subcutaneous treatment with desferrioxamine. Both sets of desferrioxamine treated patients were similar in age and there was no significant difference in mean myocardial iron or left ventricular ejection fraction. Serum ferritin and liver iron were found to be higher in the large desferrioxamine population (Table 9.3). The proportion of patients with excess myocardial iron deposition (T2*<20ms) was similar in both desferrioxamine groups (67% in the 30 desferrioxamine controls and 63% in the larger desferrioxamine population, p=0.84, not significant).

Table 9.3 Comparison of the Desferrioxamine Control Group to a Larger Population of Thalassaemia Major Patients Treated with Subcutaneous Desferrioxamine

	Desferrioxamine Controls	Large Desferrioxamine Population	P Value
Number of Patients	30	160	-
Age (years)	29 ± 7.1	27 ± 8.1	0.16
Myocardial T2* (ms)	21 ± 14.5	22 ± 17	0.70
Left Ventricular Ejection Fraction (%)	63 ± 6.9	65 ± 9.3	0.21
Serum Ferritin (µg/l)	1250 ± 508	2034 ±1252	0.0004
Liver Iron (mg/g dry weight)	3.9 ± 2.5	6.7 ± 5.1	0.03

9.3.4 Retrospective Echocardiographic Data

Retrospective echocardiographic data were available in 9 of the 15 deferiprone patients and 20 of the 30 desferrioxamine controls. The mean follow-up times were 3 ± 1.8 years and 2.3 ± 1.3 years respectively. The initial and final shortening fractions in the deferiprone group were 33 ± 9.3% and 36 ± 6.2% respectively (mean improvement 3.1%, p=0.15 non-significant). The initial and final shortening fractions in the desferrioxamine group were 32 ± 6.8% and 33 ± 5.4% respectively (mean improvement 0.7% p=0.61 non-significant). Although there was no significant difference in end systolic dimensions between the groups at the initial scan (deferiprone patients 3.4cm, desferrioxamine patients 3.5cm, p=0.42), end systolic dimensions were significantly smaller in the deferiprone group at the final scan (deferiprone patients 3.1cm, desferrioxamine patients 3.6cm, p=0.019).

9.4 Discussion

The iron chelator desferrioxamine was first introduced more than 30 years ago [Sephton-Smith 1964, Barry 1974] and remains the only chelator approved for regular use in North America, and the only first line agent approved for use in Europe. Desferrioxamine improves hepatic, cardiac and endocrine dysfunction and prolongs survival in patients with iron

overload [Modell 1982, Wolfe 1985]. The disadvantages of desferrioxamine are its high cost [Karnon 1999], the requirement for daily parenteral administration and its local and systemic toxicity, which include visual [Arden 1984] and auditory neurotoxicity [Olivieri 1986], skeletal abnormalities [Brill 1991] and growth retardation [De Virgilis 1988]. Despite the administration of this arduous regime for more than 20 years, or from early childhood in younger patients, many still die of iron-induced heart failure [Aldouri 1990, Olivieri 1994] with only 50% surviving to the age of 35 years in the UK [Modell 2000].

To date, only deferiprone has been introduced for clinical use as an orally effective substitute for desferrioxamine. Deferiprone is a bidentate chelator, binding iron in a 3:1 ratio, whereas desferrioxamine is a larger hexadentate molecule binding iron in a 1:1 ratio. Although formal dose response studies have shown that iron excretion with deferiprone is inferior to that with desferrioxamine, intermediate term clinical trials have demonstrated its effectiveness [Tondury 1990, Al-Refaie 1992, Agarwal 1992, Olivieri 1995], possibly as a result of improved compliance with the oral agent. However a longer term trial of 18 patients over 4.6 years [Olivieri 1998], showed that 8 patients had hepatic iron concentrations above 80μmol/g liver wet weight, a value previously believed to be associated with an increased risk of cardiac disease [Brittenham 1994b]. The authors concluded that deferiprone did not adequately control body iron burden. This conclusion is arguable: All patients had previously been treated with desferrioxamine yet 10 had hepatic iron concentrations >80μmol/g liver wet weight at the beginning of the trial. During treatment with deferiprone, the mean liver iron fell from a mean of 88.7±12.1 to a mean of 65.5±7.9μmol/g liver wet weight. Therefore, although the number of patients with high liver iron levels was disappointing, treatment with deferiprone appeared to be more effective than prior standard therapy with desferrioxamine.

The primary role of iron chelation therapy is to prevent premature death from myocardial iron overload. With the emergence of advanced MRI techniques it is now possible to accurately assess both liver and cardiac iron in the same study. This has revealed that myocardial iron cannot be predicted from liver iron concentration and that left ventricular ejection fraction is

unrelated to liver iron or serum ferritin levels in thalassaemic patients [Anderson 2000]. The results of the present study show a significantly lower incidence of excess myocardial iron in the deferiprone group compared to the desferrioxamine controls (p=0.025, likelihood ratio 0.4, 90% confidence interval 0.19 to 0.83), corresponding to improved left ventricular ejection fractions despite significantly higher liver iron levels. These results emphasise the importance of inter-organ variation of iron deposition and the lack of correlation between liver iron and cardiac function.

A possible mechanism for improved cardioprotection from deferiprone compared to desferrioxamine is its enhanced ability to penetrate myocardial cells, where excess iron is stored in lysosomes as ferritin and haemosiderin. Deferiprone is able to penetrate cell membranes more effectively than desferrioxamine because of its lower molecular weight and lipophilicity [Shalev 1995, de Franceshi 1999]. Conversely, in the liver, desferrioxamine has the advantage of facilitated transport into cells via an active uptake mechanism [Porter 1989]. Although our results indicate better myocardial iron levels with deferiprone and better hepatic iron levels with desferrioxamine, there is considerable variability between patients, which remains to be explained. An individualised approach to guiding iron chelation therapy with assessment of iron in each target organ may optimise patient care in the future.

Limitations

This is a retrospective analysis using a technique that was not available when treatment with deferiprone was instituted. Ideally the two groups would be matched for baseline myocardial iron deposition, but this is unknown for either group. Although all patients on long-term deferiprone were included, the number of patients is small and a larger, randomised, prospective study, assessing both tissue iron and ventricular function is required to confirm these findings. In such a small group it is possible that all patients had low myocardial iron even before deferiprone was started. However the echocardiographic data that is available demonstrates marked improvement in ventricular function in two of these patients following the introduction of deferiprone (figure 9.1). Alternatively, the desferrioxamine controls could have had unusually high myocardial iron compared to the larger population of patients

receiving standard therapy with desferrioxamine but our comparison with 160 such patients shows that myocardial iron levels and left ventricular ejection fractions are similar in both groups.

Figure 9.1 Improvement in Ventricular Function in Deferiprone-treated Patients

Panel A

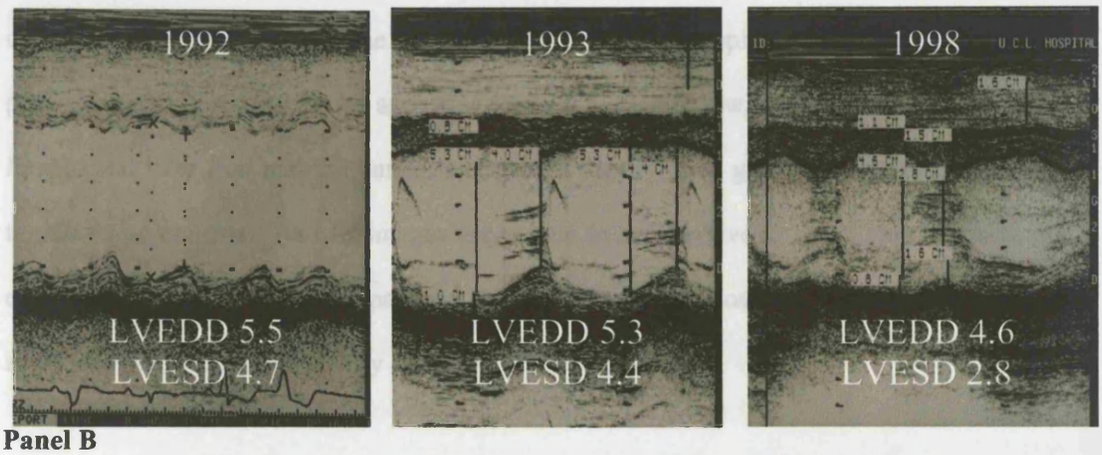

Panel B

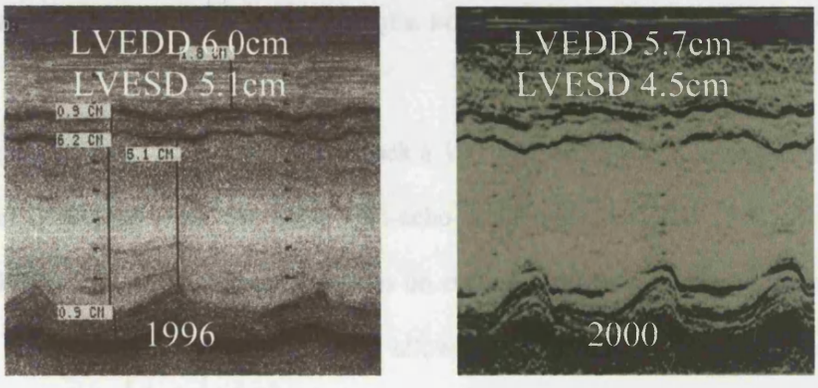

A) M-mode echocardiogram images from a 24-year-old man at the start of treatment with deferiprone and after 1 and 6 years of treatment. The initial scan showed severely impaired ventricular function with a dilated ventricle. There is some improvement by 1 year and after 6 years, ventricular dimensions and systolic function have normalised. B) M-mode echocardiogram images from a 21-year-old male at the start of treatment with deferiprone and after 4 years of treatment. The initial image shows a dilated, impaired left ventricle. After 4 years the ventricular dimensions have improved but have not yet normalised.

Conclusions

Excess myocardial iron develops in more than half of thalassaemia major patients treated with long-term subcutaneous desferrioxamine. Oral deferiprone may be more effective than subcutaneous desferrioxamine in removing iron from the myocardium and a larger prospective trial is needed to confirm these results.

CHAPTER 10: GENERAL DISCUSSION AND CONCLUSIONS

10.1 THESIS OBJECTIVES

Iron-induced cardiac failure remains the commonest cause of death (60%) in young patients with thalassaemia. Despite the potential reversibility of the cardiomyopathy, the introduction of iron-chelation therapy and the availability of echocardiographic monitoring, only 50% of patients currently survive to the age of 35 in the UK. Until now, the indirect markers, serum ferritin and liver iron and the patient's chelation history have guided chelation treatment in thalassaemic patients. As MR images are known to be sensitive to tissue iron deposits, and expertise in CMR is rapidly expanding, it was theoretically possible to develop a clinically applicable technique for the early detection of cardiac iron.

10.2 MAGNETIC RESONANCE T2* TECHNIQUE FOR THE ASSESSMENT OF MYOCARDIAL IRON

The use of gradient-echo techniques, which lack a 180^0 rephasing pulse, improves sensitivity to tissue iron deposition over the older spin-echo techniques [Gandon 1993, Ernst 1997, Bonkovsky 1999]. The T2* method improves on earlier gradient-echo signal intensity ratio methods by using an array of echo times to allow measurement of iron deposition over a broad range of concentrations from normal to severe iron loads. In addition, inter-study and inter-observer reproducibility are improved as the measurement of small regions of interest in paraspinal skeletal muscle is avoided (See section 4.3.7). Signal intensity ratio methods are highly sequence-dependent – with ratios varying with echo time used. A further theoretical advantage of the T2* technique is the potential for the sequence to be used in different models of scanner. This benefit remains to be confirmed.

The use of a gradient-echo technique lends itself to imaging of the beating heart as acquisitions are rapid and respiratory and cardiac motion artefacts are reduced. This results in

the good interstudy reproducibility of the T2* technique in both the liver and the heart (3.3% and 5.0% coefficient of variation respectively).

The technique was validated by comparing liver T2* measurements with iron concentration from liver biopsy. A highly significant correlation was demonstrated, allowing the estimation of liver iron concentration from non-invasively determined T2* values. We anticipate a similar correlation in myocardial tissue but as this remains to be confirmed with a myocardial biopsy study, myocardial iron assessments are currently graded as levels of T2* (with a lower limit of normal of 20ms).

10.3 Myocardial Iron and Ventricular Function

Although thalassaemic cardiomyopathy is generally acknowledged to result from myocardial iron deposition, the aetiology has recently been questioned and it has been suggested that the rapid deterioration in these patients may be caused by an infective or autoimmune myocarditis [Kremastinos 1995, 1999]. The arguments supporting this theory are the impaired immune status of thalassaemic patients, the apparently normal ventricular dimensions and function, preserved until late in the course of the disease and the rapid and dramatic deterioration frequently observed once heart failure develops. The pattern of the relationship between myocardial T2* and ejection fraction was recognised early in the clinical application of the technique and has clarified over the successive scanning of more than 200 thalassaemic patients. At normal myocardial iron levels (T2*>20ms), ventricular ejection fractions are predominantly in the upper normal range. Once cardiac iron deposition occurs and the myocardial T2* falls below 20ms, there is a steep fall in left ventricular ejection fraction ($r=0.61$, $p<0.0001$). Although the decline in ventricular function is obvious however, only a few patients (<10%) are detected by an ejection fraction below the normal range, indicating that abnormal ventricular function alone is a poor and late indication of myocardial iron overload. Once cardiac iron deposition commences, there is also a precipitous increase in dimensions and mass, although once again, only a few patients fall outside the normal ranges.

Therefore as cardiac iron overload progresses, the ventricle dilates, thickens and function deteriorates.

These relationships demonstrate clear evidence for the aetiological role of iron in the development of thalassaemic cardiomyopathy. The technique enables the detection of myocardial iron before overt ventricular dysfunction occurs, thereby facilitating early diagnosis and treatment. Lastly, despite the ubiquitous use of iron-chelation therapy it is evident that more than 60% of thalassaemia major patients have excess myocardial iron deposition (T2*<20ms). Current chelation regimes are therefore ineffective in preventing cardiac iron deposition, the major cause of death in this patient group. Potential causes are inadequate treatment or patient compliance (or a combination of both factors).

10.4 Serum Ferritin and Liver Iron as Indicators of Cardiac Risk

Serum ferritin is the most commonly used marker of response to iron-chelation therapy in thalassaemia and is believed to reflect total body iron stores. However, in our analysis of 205 patients with thalassaemia major, we have shown that the correlation between serum ferritin and myocardial T2* is negligible and that there is no significant correlation between serum ferritin and left ventricular ejection fraction. These findings illustrate that serum ferritin readings should no longer be relied upon to detect those patients at greatest risk of cardiac failure in thalassaemia.

The measurement of liver iron has been considered the gold standard guide to the estimation of body iron stores [Pippard 1989]. Cardiac iron deposition was believed to occur late and only in the presence of severe liver iron overload [Buja 1971]. However in the 205 patients studied, there was a weak correlation between liver T2* and myocardial T2* and no significant relationship was demonstrated between liver iron and left ventricular ejection fraction. It is possible for a patient to have severe cardiac iron overload and impaired ventricular function with normal levels of liver iron, and many patients with high liver iron levels have no demonstrable myocardial iron. Liver iron levels >15mg/g liver dry weight were previously believed to be associated with increased cardiac risk in thalassaemia, but in

this large cohort we have shown that this measure is unhelpful in identifying those patients with excess myocardial iron or ventricular dysfunction.

Myocardial T2* was found to be the only independent predictor of left ventricular ejection fraction (of the clinical covariates; serum ferritin, liver iron, age and diabetes). We conclude therefore that direct monitoring of myocardial iron stores is necessary to detect patients at risk of developing iron-induced cardiomyopathy in order to direct appropriate iron-chelation therapy and reduce the mortality from this reversible condition.

10.5 The Variability of Tissue Iron Stores in Patients with Thalassaemia

Early in the clinical application of this technique, it became obvious that there was substantial variability in the inter-organ deposition of tissue iron. We compared the relationships in tissue iron between the liver, heart, spleen and pancreas in order to try and detect any identifiable patterns for iron deposition. In the past it was believed that transfusional siderosis resulted firstly in reticulo-endothelial iron deposition and that it was only when these stores were replete that iron spilled over into the parenchymal tissue of the liver, pancreas heart and endocrine organs. Cardiac iron overload was believed to occur late and only in combination with considerable liver iron loading. Analysis of these 210 patients with thalassaemia major demonstrated no correlation between iron loading in the reticulo-endothelial tissues of the spleen and the parenchymal organs of the liver, heart and pancreas. Additionally, there was no obvious progression of iron loading in the parenchymal organs with only weak correlations between liver T2* and myocardial T2* or pancreas SIR.

The conventional theory of progressive iron loading beginning in the spleen, then the liver before iron is deposited in the heart and pancreas needs therefore to be re-examined. Iron chelation treatment is likely to have affected this relationship due to altered rates of iron clearance between organs [Anderson 2001] and differential uptake of iron chelators in the liver, heart and pancreas [Porter 1989].

10.6 The Reversibility of Iron-Induced Cardiomyopathy

There have been several case reports in the past documenting cardiac function improvement in iron-overloaded patients following venesection or iron-chelation therapy. However the high mortality rates in patients with overt cardiac failure has resulted in the questioning of the degree of reversibility of the cardiomyopathy. We performed a prospective trial of patients commencing intensive chelation therapy for cardiac involvement and monitored both ventricular function and myocardial and liver T2* over time. We demonstrated a gradual improvement in indices of ventricular function (left ventricular ejection fraction, left ventricular end-systolic volume and left ventricular mass). These changes were paralleled by a decrease in myocardial iron deposition, although after one year significant myocardial iron stores remained and intensive chelation therapy was continued in all patients. Liver iron cleared more quickly, normalising in 3 of the patients by 6 months. The differing rates of iron clearance between the liver and the heart re-emphasise the importance of monitoring changes in iron deposition in individual organs. If iron-chelation had been guided by liver iron and ferritin alone, intensive therapy would have been discontinued in these 3 patients long before iron had cleared from the myocardium, leaving the patients at continued cardiac risk.

This study therefore confirms the reversibility of iron-induced cardiomyopathy and emphasises the need for aggressive management of these young patients. Although the mortality in advanced cases is high, there is the potential to not only improve but also reverse the cardiomyopathy once cardiac iron has been removed.

10.7 Magnetic Resonance T2* Imaging in the Comparison of Effectiveness of Chelation Regimes

We have used the T2* sequence in conjunction with assessment of ventricular function to compare the outcome in 2 groups of patients after long-term treatment with either standard subcutaneous desferrioxamine therapy or oral deferiprone. Until now, the effectiveness of chelation therapies has been determined by the effect on serum ferritin or liver iron only. As heart failure remains the commonest cause of death in thalassaemia, it is appropriate that

effectiveness in myocardial tissue should also be examined. Early trials of oral deferiprone therapy appeared promising [Agarwal 1992, Olivieri 1995] but the long-term effectiveness of deferiprone has been questioned [Olivieri 1998, Hoffbrand 1998].

Liver iron was indeed found to be significantly higher in the deferiprone patients but myocardial iron was significantly lower than the desferrioxamine controls and this was associated with better left ventricular ejection fractions in the deferiprone patients. Excess myocardial iron deposition was found in 27% of the deferiprone patients compared to 67% of the desferrioxamine controls and 63% of the larger cohort of 160 patients receiving standard treatment with desferrioxamine. We conclude that oral deferiprone may be more effective than subcutaneous desferrioxamine in removing iron from the myocardium and that future trials of iron chelators should monitor both cardiac iron and ventricular function in addition to liver iron, as heart failure remains the commonest cause of death in these patients.

10.8 Clinical Application of the T2* Technique

The T2* technique has been rapidly adopted as part of the clinical management of iron-loaded patients by haematologists and paediatricians. Since May 1999, when the first patient was scanned as part of the initial validation study, more than 300 patients at risk of iron overload have been assessed. This ready acceptance of a new technique can be partly explained by non-invasive nature of the test, which is well tolerated by patients, but largely because previous patient management was problematic, as only indirect markers were available to guide therapy. It will be some time before a benefit to cardiac mortality rates in this patient group can be proved, but it is hoped that in the meantime other centres will adopt this simple technique as it is believed that it provides a definite advance in the management of thalassaemic patients.

10.9 Conclusions

This MR T2* technique provides a simple, robust assessment of tissue iron in the heart, liver, spleen and pancreas. Conventional markers of body iron deposition are unreliable for the

assessment of myocardial iron or cardiac risk. As myocardial iron levels increase, the ventricle dilates, thickens and ejection fraction falls. With intensification of iron-chelation therapy, iron can be slowly removed from the heart and the cardiomyopathy is reversed. As tissue iron deposition is extremely variable, trials of chelating-agents should monitor iron levels in individual organs, particularly the heart, as cardiomyopathy remains the major cause of death. With early identification and treatment of patients with severe myocardial iron overload, the mortality and morbidity from this reversible cardiomyopathy should fall.

CHAPTER 11: FUTURE DIRECTIONS

11.1 ONGOING SUPPORT

The British Heart Foundation has recently granted funds for a second Junior Fellowship to Dr Mark Westwood (Junior Fellowship FS/2001048) to continue the development of the T2* technique and the study of cardiomyopathy in iron overloaded patients with an 18-month prospective, controlled randomised trial of the oral chelator deferiprone combined with desferrioxamine versus standard treatment with desferrioxamine alone.

11.2 QUANTITATIVE EVALUATION OF MYOCARDIAL T2* WITH MYOCARDIAL BIOPSIES

At present we are able to provide clinicians with an estimate of liver iron concentration in mg/g liver dry weight as this has been validated by the liver biopsy study. For full validation of this T2* technique it is necessary to demonstrate that myocardial T2* is correlated to myocardial iron concentration. However, unlike liver biopsies, myocardial tissue sampling is not a routine part of patient management. In order to minimise the risk and distress to patients it is proposed that consenting patients who require insertion of indwelling central lines for intensification of chelation therapy, undergo myocardial biopsy via the same central access. Ethical approval is awaited for this study to take place at the Middlesex Hospital under the supervision of Dr Malcolm Walker, consultant cardiologist.

11.3 INTER-VENDOR, INTER-SCANNER REPRODUCIBILITY OF THE T2* TECHNIQUE

In order for the T2* technique to be readily replicated and performed elsewhere it is necessary to determine the reproducibility of the technique between scanners. The scanner used for all the analysis in this thesis was a Picker 1.5T Edge Scanner (Marconi Medical Systems, Ohio, USA). A new Siemens Sonata 1.5T scanner was installed at the same unit in August 2000. Twenty patients have since been scanned in both scanners and the reproducibility of T2* measurements in the heart and liver between scanners is due to be published shortly.

11.4 Application of the MR T2* Technique in Other Iron-overload Diseases

Other iron-overload diseases scanned to date include hereditary haemochromatosis, sickle cell anaemia, paroxysmal nocturnal haematuria, sideroblastic anaemia and patients undergoing chemotherapy with multiple transfusions. Studies planned include the assessment of newly diagnosed haemochromatosis patients at the Royal Free Hospital to determine the prevalence of myocardial involvement at the time of diagnosis and a study of tissue iron distribution in patients with sickle cell anaemia. The value of follow-up in haemochromatosis patients needs to be assessed as until now, venesection therapy has been guided by liver iron and serum ferritin alone.

11.5 A Future MR Screening Program for Thalassaemic Patients

At present the MR assessment is only available to patients referred by their haematology or paediatric consultants. The major centres for the treatment of thalassaemia in the UK are the Whittington, University College and Great Ormond Street Hospitals in London. Around half of UK thalassaemia major patients are cared for at these centres. However many patients attend smaller units around the country and do not have access either to this technique or to the major centres of expertise. It has been shown that the mortality rate for these patients is higher than for patients under the care of the major centres [Modell 2000]. The care of thalassaemic patients is already expensive [Karnon 1999] and the additional cost of routine MR scanning may exceed the budget of some hospitals – particularly those caring for a large number of thalassaemic patients. An ambitious hope for the future would be a formal screening program, to allow the detection of the highest risk patients and facilitate their review at specialist centres when appropriate.

CHAPTER 12: REFERENCES

Addison GM, Beamish M, Hales CN, Hodgkins M, Jacobs A, Llewellyn P. An Immunoradiometric assay for ferritin in the serum of normal subjects and patients with iron deficiency and iron overload. J Clin Pathol 1972; 25:326-329

Agarwal MB, Gupte SS, Viswanathan C, Vasandani D, Ramanathan J, Desai N, Puniyani RR, Chhablani AT. Long-term assessment of efficacy and safety of L1, an oral iron chelator, in transfusion dependent thalassaemia: Indian trial. Br J Haematol 1992;82:460-6

Aldouri MA, Wonke B, Hoffbrand AV, Flynn DM, Ward SE, Agnew JE, Hilson AJ. High incidence of cardiomyopathy in beta-thalassaemia patients receiving regular transfusion and iron chelation: reversal by intensified chelation. Acta Haematol 1990;84:113-7

Al-Refaie FN, Wonke B, Hoffbrand AV, Wickens DG, Nortey P, Kontoghiorghes GJ. Efficacy and possible adverse effects of the oral iron chelator 1,2-dimethyl-3-hydroxypyrid-4-one (L1) in thalassemia major. Blood 1992;80:593-9

Ambu R, Crisponi G, Sciot R, Van Eyken P, Parodo G Ianelli S, Marongiu F, Silvagni R, Nurchi V, Costa V et al. Uneven hepatic iron and phosphorus distribution in beta-thalassaemia. J Hepatol 1995;23:544-549

Anderson L, Porter JB, Wonke B, Walker JM, Holden S, Davis BA, Prescott E, Charrier C, Firmin DN, Pennell DJ. Cardiac iron deposition is not predicted by conventional markers of iron overload in homozygous beta-thalassaemia (abstract). Blood 2000; 96 (suppl I):606a

Anderson L, Holden S, Davis B, Prescott E, Charrier C, Bunce N, Firmin D, Wonke B, Porter J, Walker JM, Pennell D. Cardiovascular T2* magnetic resonance for the early diagnosis of myocardial iron overload. European Heart Journal 2001a;20 (23): In press

Anderson L, Bunce N, Davis B, Charrier C, Porter J, Firmin D, Holden S, Prescott E, Wonke B, Walker JM, Pennell D. Reversal of siderotic cardiomyopathy: A prospective study with cardiac magnetic resonance (CMR). Heart 2001b; 85(suppl 1):33

Arden GB, Wonke B, Kennedy C, Huehns ER. Ocular changes in patients undergoing long-term desferrioxamine treatment. Br J Ophthalmol 1984;68:873-7

Baron MG, Flint R, Pettigrew RI. Phasic variations in T2 relaxation times of myocardium. Radiol Suppl 1987; 237:165

Barosi G, Arbustini E, Gavazzi A, Grasso M, Pucci A. Myocardial iron grading by endomyocardial biopsy. A clinico-pathologic study on iron overloaded patients. Eur J Haematol. 1989; 42:382-8.

Barry M, Sherlock S. Measurement of liver-iron concentration in needle-biopsy specimens. Lancet 1971; 1:100-3

Barry M, Flynn D, Letsky E, Risdon RA. Long term chelation therapy in thalassaemia major: Effect on liver iron concentration, liver histology and clinical progress. Br Med J 1974; 2:16–20

Baynes R, Bezwoda W, Bothwell T, Khan Q, Mansoor N. The non-immune inflammatory response; serial changes inplasma iron, iron-binding capacity, lactoferrin, ferritin, and C-reactive protein. Scand J Clin Lab Invest 1986; 46:695-704

Berry CL, Marshall WC. Iron distribution in the liver of patients with thalassaemia major. Lancet 1967; 1: 1031-3

Bellenger NG, Francis JM, Davies CL, Coats A, Pennell DJ. Establishment and performance of a magnetic resonance cardiac function clinic. J Cardiovasc Magn Reson 2000; 2: 15-22

Blankenberg F, Eisenberg S, Scheinman MN, Higgins CB. Use of gradient echo (GRE) MR in the imaging of cardiac haemochromatosis. J Comput Assist Tomogr 1994; 18:136-8

Bonkovsky HL RR, Cable EE, Davidoff A, Rijcken TH, Stark DD. Hepatic iron concentration: noninvasive estimation by means of MR imaging techniques. Radiology. 1999; 212: 227-34

Bottomley PA, Foster TH, Argersinger RE, Pfeifer LM. A review of normal tissue hydrogen NMR relaxation times and relaxation mechanisms from 1-100 MHz: dependence on tissue type, NMR frequency, temperature, species, excision, and age. Med Phys 1984; 11:425-48

Brasch RC. Methods of contrast enhancement for NMR imaging and potential applications. Radiology 1983; 147: 781-8

Brasch RC, Wesbey GC, Gooding CA, Koerper MA. Magnetic resonance imaging of transfusional haemosiderosis complicating thalassaemia major. Radiology 1984;150:767-771

Brill PW, Winchester P, Giardina PJ, Cunningham-Rundles S. Deferoxamine-induced bone dysplasia in patients with thalassemia major. AJR Am J Roentgenol 1991;156:561-5

Brittenham GM, Farrell DE, Harris JW, Feldman ES, Danish EH, Muir WA, Tripp JH, Bellon EM. Magnetic-susceptibility measurement of human iron stores. N Engl J Med 1982; 307:1671-5

Brittenham GM, Cohen AR, McLaren CE, Martin MB, Griffith PM, Nienhuis AW, Young NS, Allen CJ, Farrell DE, Harris JW. Hepatic iron stores and plasma ferritin concentration in patients with sickle cell anemia and thalassemia major. Am J Hematol 1993; 42: 81-5

Brittenham GM. The Red Cell Cycle. In: Bruck J, Halliday J, Pippard M, Powell L, ed., Iron metabolism in health and disease. Philadelphia: Saunders WB. 1994a:31-62

Brittenham GM, Griffith PM, Nienhuis AW, McLaren CE, Young NS, Tucker EE, Allen CJ, Farell DE, Harris JW. Efficacy of desferrioxamine in preventing complication of iron overload in patients with thalassaemia major. N.Eng.J.Med. 1994b;331:567

Buja LM, Roberts WL . Iron in the heart. Etiology and clinical significance. Am. J. Med. 1971;51:209-21

Cazzola M, Borgna-Pignatti C, deStefano P, Bergamaschi G, Bongo IG, Dezza L, Arato F. Internal distribution of excess iron and sources of serum ferritin in patients with thalassaemia. Scand. J. Haematol. 1983;30:289-96

Cecchetti G, Binda A, Piperno A, Nador F, Fargion S, Fiorelli G. Cardiac alterations in 36 consecutive patients with idiopathic haemochromatosis: polygraphic and echocardiographic evaluation. European Heart Journal 1991; 12: 224-30

Chapman RW, Hussain MA, Gorman A, Lauricht M, Politis D, Flynn DM, Sherlock S, Hoffbrand AV. Effect of ascorbic acid deficiency on serum ferritin concentration in patients with beta thalassaemia major and iron overload. 1982;35:487-491

Chezmar JL, Nelson RC, Malko JA, Bernardino ME. Hepatic iron overload; diagnosis and quantification by MR imaging. Gastrointest Radiol 1990; 15: 27-31

Crosby WH. Serum ferritin fails to indicate haemochromatosis – nothing gold can stay. N Eng J Med 1976;294:333-4

Davis BA, Porter JB. Long-term outcome of continuous 24-hour deferoxamine infusion via indwelling intravenous catheters in high-risk beta-thalassaemia. Blood 2000; 95: 1229-36

de Franceschi L, Shalev O, Piga A, Collell M, Olivieri O, Corrocher R, Hebbel RP, Brugnara C. Deferiprone therapy in homozygous human beta-thalassemia removes erythrocyte membrane free iron and reduces KCl cotransport activity. J Lab Clin Med 1999;133:64-9

De Virgiliis S, Congia M, Frau F, Argiolu F, Diana G, Cucca F, Varsi A, Sanna G, Podda G, Fodde M, et al. Deferoxamine-induced growth retardation in patients with thalassemia major. J Pediatr 1988;113:661-9

DeRees A, Kundel HL, Joseph PM, Kressel HY. Myocardial signal intensity on MR images: influence of cardiac phase and echo delay time. Soc Mag Reson Med 1988; 2:800

Doyle FH, Pennock JM, Banks LM, McDonnell MJ, Bydder GM, Steiner RE, Young IR, Clarke GJ, Pasmore T, Gilderdale DJ. Nuclear magnetic resonance imaging of the liver: initial experience. AJR Am J Roentgenol 1982 Feb;138:193-200

Earley A, Valman HB, Altman DG, Pippard MJ. Microcytosis, iron deficiency and thalassaemia in preschool children. Arch. Dis. Child 1990; 65: 610–4

Easley RM, Schreiner BF, Yu PN. Reversible cardiomyopathy associated with hemochromatosis. N. Eng. J. Med. 1972;287:866-867

Ehlers KH, Levin AR, Klein AA, Markenson AL, O'Loughlin JE Jr, Engle MA. The cardiac manifestations of thalassemia major: natural history, noninvasive cardiac diagnostic studies and results of cardiac catheterization. Cardiovasc Clin 1981;11:171-86

Ehlers KH, Giardina PJ, Lesser ML, Engle MA, Hiltgartner MW. Prolonged survival in patients with beta-thalassemia major treated with deferoxamine.J Pediatr 1991;118:540-545

Emond MJ, Bronner MP, Carlson TH, Lin M, Labbe RF, Kowdley KV. Quantitative study of the variability of hepatic iron concentrations. Clin Chem 1999; 45: 340-6

Engle MA, Erlandson M, Smith CH. Late cardiac complications of chronic, severe, refractory anemia with hemochromatosis. Circulation 1964; 30:698–705

Ernst O SG, Bonvarlet P, Canva-Delcambre V, Paris JC, L'Hermine C. Hepatic iron overload: diagnosis and quantification with MR imaging. Am J Roentgenol. 1997; 168: 1205-8

Felker GM, Thompson RE, Hare JM, Hruban RH, Clemetson DE, Howard DL, Baughman KL, Kasper EK. Underlying causes and long-term survival in patients with initially unexplained cardiomyopathy. N Engl J Med 2000; 342: 1077-84

Finch CA. The detection of iron overload. N Engl J Med 1982 307:1702-4

Finch CA, Bellotti V, Stray SEA. Plasma ferritin as a diagnostic tool. West J Med 1986; 145:657

Fitchett DH, Coltart DJ, Littler WA, Leyland MJ, Trueman T, Gozzard DI, Peters TJ. Cardiac involvement in secondary haemochromatosis: A catheter biopsy study and analysis of myocardium. Cardiovasc. Res 1980;14:719-724

Flint J, Harding RM, Boyce AJ, Clegg JB. The population genetics of the thalassaemias. Baillieres Clin Haematol 1993; 6: 215-62

Floyd RA, Yoshida T, Leigh JS. Changes of tissue water proton relaxation rates during early phases of chemical carcinogenesis. Proc Natl Acad USA 1975; 72:56-8

Freeman AP, Giles RW, Berdoukas VA, Walsh WF, Choy D, Murray PC. Early left ventricular dysfunction and chelation therapy in thalassaemia major. Ann. Intern. Med. 1983;99:450

Gandon Y, Guyader D, Heautot JF, Reda MI, Yaouanq J, Buhe T, Brissot P, Carsin M, Deugnier Y. Hemochromatosis: diagnosis and quantification of liver iron with gradient-echo MR imaging. Radiology 1994;193:533-8

Gomori JM, Grossman RI, Drott HR. MR relaxation times and iron content of thalassemic spleens: an in vitro study. AJR Am J Roentgenol 1988; 150:567-569

Gomori JM HG, Tamary H, Zandback J et al. Hepatic iron overload: quantitative MR imaging. Radiology. 1991; 179: 367-9

Gordeuk VR, Bacon BR, Brittenham GM. Iron overload: causes and consequences. Ann Rev Nutr 1987; 7:485-508

Grundy RG, Woods RA, Savage MO, Evans JPM. Relationship of endocrinopathy to iron chelation status in young patients with thalassemia major. Arch Dis Child 1994; 71:128

Gutteridge JMC, Rowley DA, Griffiths E, Halliwell B. Low-molecular-weight iron complexes and oxygen radical reactions in idiopathic haemochromatosis. Clin Sci 1985;68:463-7

Hall GW, Barneston RA, Thein SL. Beta Thalassaemia in the Indigenous Popualtion. Br. J. of Haematol. 1992; 82: 584–58

Halliday JW, Powell LW. Ferritin metabolism and the liver. Seminars in liver disease 1984; 4: 207-15

Halliwell B, Gutteridge JMC. Role of free radicals and catalytic metal ions in human disease: an overview. Methods Enzymol 1990; 186:1-85

Henry WL NA, Wiener M, Miller DR, Canale VC, Piomelli S. Echocardiographic abnormalities in patients with transfusion-dependent anaemia and secondary myocardial iron deposition. Am J Med 1978; 64: 547-55

Herfkens R, Davis P, Crooks L, Kaufman L, Price D, Miller T, Margulis AR, Watts J, Hoenninger J, Arakawa M, McRee R. Nuclear magnetic resonance imaging of the abnormal live rat and correlations with tissue characteristics. Radiology 1981; 141:211-8

Herschko C, Graham G, Bates CW, Rachmilewitz EA. Non specific serum iron in thalassaemia: An abnormal serum iron fraction of potential toxicity. Br. J. Haematol. 1978:40:255

Hershko C, Peto TEA. Annotation: Non-transferrin plasma iron. Br. J. Haematol. 1987a; 66:149

Hershko C, Link G, Pinson A. Modification of iron uptake and lipid peroxidation by hypoxia, ascorbic acid and α-tocopheryl in iron-loaded rat myocardial cell cultures. J Lab Clin Med 1987b; 110:355-61

Hershko C, Link G, Cabantchik I Pathophysiology of iron overload. Ann N Y Acad Sci 1998; 850: 191-201

Hinshaw WS, Bottomley PA, Holland GN. Radiographic thin-section imaging of the human wrist by nuclear magnetic resonance. Nature 1977; 270: 722-3

Hoffbrand AV, AL-Refaie F, Davis B, Siritanakatkul N, Jackson BF, Cochrane J, Prescott E, Wonke B. V. Long term trial of deferiprone in 51 transfusion dependent iron overloaded patients. Blood 1998;91:295-300

Hou J, Wu M, Lin K, Lue H. Prognostic significance of left ventricular diastolic indexes in β-thalassaemia major. Arch Ped Adolesc Med 1994; 148:862-6

Jacobs A, Miller F, Worwood M, Beamish MR, Wardrop CA. Ferritin in the serum of normal subjects and patients with iron deficiency and iron overload. Br Med J 1972; 4:206-8

James TL. Nuclear magnetic resonance in biochemistry. New York: Academic press 1975: 46-8

James TN. Pathology of the cardiac conduction system in hemochromatosis. N. Eng. J. Med. 1964;271:92-94

Jandl JH. Blood: textbook of hematology. Boston: Little, Brown. 1987; 201-7

Jensen PD, Bagger JP, Jensen FT, Baandrup U, Christensen T, Ellegaard J. Heart transplantation in a case of juvenile hereditary haemochromatosis followed up by MRI and endomyocardial biopsies. Eur J Haematol 1993;51:199-205

Jensen PD, Jensen FT, Christensen T, Ellegaard J. Non-invasive assessment of tissue iron overload in the liver by magnetic resonance imaging. Br. J. Haematol. 1994; 87:171-184

Johnston DL, Rice L, Vick GW, Hedrick TO, Rokey R. Assessment of tissue iron overload by nuclear magnetic resonance imaging. Am. J. Med. 1989;87:40-47

Judd RM, Levy BI. Effects of barium-induced cardiac contraction on large and small vessel intramyocardial blood volume. Circ Res 1991; 68:217-225

Kaltwasser JP GR, Schalk KP, Hartl W. Non-invasive quantitation of liver iron-overload by magnetic resonance imaging. Br J Haematol. 1990; 74: 360-3

Karnon J, Zeuner D, Brown J, Ades AE, Wonke B, Modell B. Lifetime treatment costs of beta-thalassaemia major. Clin Lab Haematol 1999; 21:377-85

Koerner MM, Tenderich G, Minami K, zu Knyphausen E, Mannebach H, Kleesiek K, Meyer H, Koerfer R. Heart transplantation for end-stage heart failure caused by iron overload. Br J Haematol 1997;97:293-6

Kontoghiorghes GJ, Bartlett AN, Hoffbrand AV, Goddard JG, Sheppard L, Barr J, Nortey P. Long-term trial with the oral iron chelator 1,2-dimethyl-3-hydroxypyrid-4-one (L1). I. Iron chelation and metabolic studies. Br J Haematol 1990;76:295-300

Kremastinos DT, Toutouzas PK, Vyssoulis GP, Venetis CA, Vretou HP, Avgoustakis DG. Global and segmental left ventricular function in β-thalassaemia. Cardiology 1985; 72:129-39

Kremastinos DT, Tsiapras DP, Tsetsos GA, Rentoukas EI, Vretou HP, Toutouzas PK. Left ventricular diastolic doppler characteristics in β-thalassaemia major. Circ 1993; 88:1127-35

Kremastinos DT, Tiniakos G, Theodorakis GN, Katritsis DG, Toutouzas PK. Myocarditis in beta-thalassaemia major. A cause of heart failure. Circ 1995; 91: 66-71

Kremastinos DT, Flevari P, Spyropoulou M, Vrettou H, Tsiapras D, Stavropoulos-Giokas CG. Association of heart failure in homozygous beta-thalassaemia with the major histocompatibility complex. Circ 1999; 100: 2074-8

Lassman MN, Genel M, Wise JK, Hendler R, Felig P. Carbohydrate homeostasis and pancreatic islet-cell function in thalassemia. Ann Intern Med 1974; 80:65

Lattanzi F, Bellotti P, Picano E, Chiarella F, Mazzarisi A, Melevendi C, Forni G, Landini L, Distante A, Vecchio C. Quantitative ultrasonic analysis of myocardium in patients with thalassaemia major and iron overload. Circ 1993; 87:748-54

Leon MB, Borer JS, Bacharach SL, Green MV, Benz EJ, Griffith P, Nienhuis AW. Detection of early cardiac dysfunction in patients with severe β-thalassaemia and chronic iron overload. N Engl J Med 1979; 301:1143-8

Letsky EA, Miller F, Worwood M, Flynn DM. Serum ferritin in regularly transfused children with thalassaemia. J Clin Path 1974; 27:652-5

Lewis BS, Rachmilewitz EA, Amitai N, Halon DA, Gotsman MS. Left ventricular function in β-thalassaemia and the effect of multiple transfusions. Am Heart J 1978; 96:636-45

Li D, Dhawale P, Rubin PJ, Haacke EM, Gropler RJ. Myocardial signal response to dipyridamole and dobutamine : Demonstration of the BOLD effect using a double echo gradient echo sequence. Magn Reson Med 1996; 36: 16-20

Link G, Pinson A, Hershko C. Heart cells in culture: a model of iron overload and chelation. J Lab Clin Med 1985; 106:147-53

Link G, Pinson A, Kahane I, Hershko C. Iron loading modifies the fatty acid composition of cultured rat myocadial cells and liposomal vesicle; Effect of ascorbate and α-tocopheryl on myocardial lipid peroxidation. J Lab Clin Med 1989a; 114:243-9

Link G, Athias P, Grynberg A, Pinson A, Hershko C. Effect of iron loading on transmembrane potential, contraction and automaticity of rat ventricular muscle cells in culture. J Lab Clin Med 1989b; 113:103-111

Link G, Pinson A, Hershko C. Iron loading of cultured cardiac myocytes modifies sarcolemmal structure and increases lysosomal fragility. J Lab Clin Med 1993;121:127-34

Link G, Pinson A, Hershko C. Ability of the orally effective iron chelators dimethyl- and diethyl-hydroxypyrid-4-one and of deferoxamine to restore sarcolemmal thiolic enzyme activity in iron-loaded heart cells. Blood 1994;83:2692-7

Link G, Tirosh R, Pinson A, Hershko C. Role of iron in the potentiation of anthracycline cardiotoxicity: identification of heart cell mitochondria as a major site of iron-anthracycline interaction. J Lab Clin Med 1996;127:272-8

Lipschitz DA, Cook JD, Finch CA. A clinical evaluation of serum ferritin as an index of iron stores. N Eng J Med 1974; 290: 1213-6

Liu PP, Henkelman M, Joshi J, Hardy P, Butany J, Iwanochko M, Clauberg M, Dhar M, Mai D, Waien S, Olivieri N. Quantification of cardiac and tissue iron by nuclear magnetic resonance relaxometry in a novel murine thalassaemia – cardiac iron overload model. Can J Cardiol. 1996;12:155-164

Lombardo T, Tamburino C, Bartoloni G, Morrone ML, Frontini V, Italia F, Corduro S, Privitera A, Calvi V. Cardiac iron overload in thalassaemic patients. An endomyocardial biopsy study. Ann Hematol 1995; 71:135-141

Longmore DB, Klipstein RH, Underwood SR, Firmin DN, Housfield GN, Watanabe M, Bland C, Fox K, Poole-Wilson PA, Rees RSO, Denison DM, McNeilly AM, Burman ED. Dimensional accuracy of magnetic resonance in studies of the heart. Lancet 1985; 1: 1360-2

Lorenz CH, Walker ES, Morgan VL, Klein SS, Graham TP. Normal human right and left ventricular mass, systolic function, and gender differences by cine magnetic resonance imaging. J Cardiovascular Magn Reson 1999; 1: 7-21

Lukens JN The Thalassaemias and related disorders: Quantitative Disorders of Hemoglobin Synthesis 39:1102-45

MacDonald RA, Mallory GK. Hemochromatosis and hemosiderosis; study of 211 autopsied cases. Arch Intern Med 1960; 105: 686

Marcus RE, Davies SC, Bantock HM, Underwood SR, Walton S, Huehns ER. Desferrioxamine to improve cardiac function in iron-loaded patients with thalassaemia major. Lancet 1984;1:392

Mavrogeni SI, Maris T, Gouliamos A, Vlahos L, Vretou E, Kremastinos D. MRI of heart function and tissue characterisation in beta-thalassaemia major with heart failure. Proc ISMRM 1997; 905

Mavrogeni SI, Gotsis ED, Markussis V, Tsekos N, Politis C, Vretou E, Kremastinos D. T2 relaxation time study of iron overload in β-thalassemia. MAGMA. 1998a; 6: 7-12

Mavrogeni SI, Maris T, Gouliamos A, Vlahos L, Kremastinos DT. Myocardial iron deposition in beta-thalassemia studied by magnetic resonance imaging. Int J Card Imaging 1998b;14:117-22

McLaren GD, Muir WA, Kellermeyer RW. Iron overload disorders: natural history, pathogenesis, diagnosis and therapy. Crit Rev Clin Lab Sci 1983; 19:205-66

Modell B, Letsky EA, Flynn DM, Peto R, Weatherall DJ. Survival and desferrioxamine in thalassaemia major. Br Med J 1982;284:1081

Modell B Khan M, Darlison M. Survival in beta thalassaemia major in the UK: Data from the UK Thalassaemia Register. Lancet 2000; 355: 2051-2

Nienhuis AW, Griffith P, Strawczynski H et al. Evaluation of cardiac function in patients with thalassaemia major. Ann N Y Acad Sci 1980; 344: 384-96

Nienhuis AW. Vitamin C and iron. N Engl Med J 1981; 304:170-1

Olivieri NF, Buncic JR, Chew E, Gallant T, Harrison RV, Keenan N, Logan W, Mitchell D, Ricci G, Skarf B, et al. Visual and auditory neurotoxicity in patients receiving subcutaneous deferoxamine infusions. N Engl J Med 1986;314:869-73

Olivieri NF, Nathan DG, MacMillan JH et al. Survival in medically treated patients with homozygous beta-thalassaemia. N Engl J Med 1994; 331:574-8

Olivieri NF, Brittenham GM, Matsui D, Berkovitch M, Blendis LM, Cameron RG, McClelland RA, Liu PP, Templeton DM, Koren G. Iron-chelation therapy with oral deferiprone in patients with thalassemia major. N Engl J Med 1995;332:918-22

Olivieri NF, Brittenham GM. Iron chelating therapy and the treatment ogf thalassaemia. Blood 1997; 89:2621

Olivieri NF, Brittenham GM, McLaren CE, Templeton DM, Cameron RG, McClelland RA, Burt AD, Fleming KA. Long-term safety and effectiveness of iron-chelation therapy with deferiprone for thalassemia major. N Engl J Med 1998;339:417-23

Olson LJ, Edwards WD, McCall JT, Ilstrup DM, Gersch BJ. Cardiac iron deposition in idiopathic hemochromatosis: Histologic and analytic assessment of 14 hearts from autopsy. JACC 1987;10:1239-1243

Olson LJ, Edwards WD, Holmes DR, Miller FA, Nordstrum LA, Baldus WP. Endomyocardial biopsy in hemocheomatosis: clinicopathological correlates in six cases. J Am Coll Cardiol 1989; 13:116-20

Overmoyer BA, McLaren CE, Brittenham GM. Uniformity of liver density and nonheme iron distribution. Arch Pathol Lab Med 1987;111:549

Papakonstantinou OG, Maris TG, Kostaridou V, Gouliamos AD, Koutoulas GK, Kalovidouris AE, Papavassiliuo GB, Kordas G, Kattamis C, Vlahos LJ, Papavassiliou CG. Assessment of liver iron overload by T2 quantitative magnetic resonance imaging: correlation of T2 QMRI measurements with serum ferritin concentration and histoligical grading of siderosis. MRI 1995; 13: 967-977

Parkes JG, Hussain RA, Olivieri NF, Templeton DM. Effects of iron loading on uptake, speciation, and chelation of iron in cultured myocardial cells. J Lab Clin Med 1993; 122:36-47

Pattynama PM, De Roos A, Van der Wall EE, Van Voorthuisen AE. Evaluation of cardiac function with magnetic resonance imaging. Am Heart J 1994; 128:595-607

Perrimond H, Michel G, Orsini A, Kreitmann B, Metras D. First report of a cardiac transplantation in a patient with thalassaemia major. Br J Haematol 1991;78:467

Pippard MJ. Measurement of iron status. Prog Clin Biol Res 1989; 309:85

Porter JB. Development of primary hepatocyte cultures for the preclinical evaluation of iron chelators. MD Thesis, University of Cambridge 1999

Prieto J, Barry M, Sherlock S. Serum ferritin in patients with iron overload and with acute and chronic liver diseases. Gastroenterology1975; 68: 525-33

Rahko PS, Salermi R, Uretsky BF. Successful reversal by chelation therapy of congestive cardiomyopathy due to iron overload. J. Am. Coll. Cardiol. 1986; 8:436

Reeder SB, Faranesh AZ, Boxerman JL, McVeigh ER. In vivo measurement of T2* and field inhomogeneity maps in the human heart at 1.5T. Magn Reson Med 1998; 39: 988-98

Risdon RA, Flynn DM, Barry M. The relation between liver iron concentration and liver damage in transfusional iron overload in thalassemia and the effect of iron-chelating therapy. Gut 1973; 14:421

Risdon RA, Barry M, Flynn DM. Transfusional iron overload: the relationship between tissue iron concentration and hepatic fibrosis in thalassaemia. J Path 1975; 116: 83-95

Rivers J, Garrahy P, Robinson W, Murphy A. Reversible cardiac dysfunction in hemochromatosis. Am. Heart J. 1987:216-217

Rozanski A, Diamond GA, Berman D, Forrester JS, Morris D, Swan HJ. Declining specificity of exercise radionuclide ventriculography. N Engl J Med 1983;309 1671-5

Schellhammer PF, Engle MA, Hagstrom JWC. Histochemical studies of the myocardium and conduction system in acquired iron storage disease. Circ 1967; 35:631-637

Sechtem U, Pflugfelder PW, Gould RG, Cassidy MM, Higgins CB. Measurement of right and left ventricular volumes in healthy individuals with cine MR imaging. Radiology 1987; 163: 697

Semelka RC, Tomei E, Wagner S, Mayo J, Kondo C, Suzuki J, Capulo GR, Higgins CB. Normal left ventricular dimensions and function: interstudy reproducibility of measurements with cine MR imaging. Radiology 1990;174:763-8

Shalev O, Repka T, Goldfarb A, Grinberg L, Abrahamov A, Olivieri NF, Rachmilewitz EA, Hebbel RP. Deferiprone (L1) chelates pathologic iron deposits from membranes of intact thalassemic and sickle red blood cells both in vitro and in vivo. Blood 1995;86:2008-13

Short EM, Winkle RA, Billingham ME. Myocardial involvement in idiopathic hemochromatosis. Morphological and clinical improvement following venesection. Am. J. Med. 1981; 70:1275-9
Smith RS. Chelating agents in the diagnosis and treatment of iron overload in thalassaemia. Ann.N.Y. Acad. Sci. 1964; 119:776–88

Spirito P, Lupi G, Melevendi C, Vecchio C. Restrictive diastolic abnormalities identified by doppler echocardiography in patients with thalassaemia major. Circ 1990; 82:88-94

St Pierre TG, Tran KC, Webb J, Macey DJ, Heywood BR, Sparks NH, Wade VJ, Mann S, Pootrakul P Organ-specific crystalline structures of ferritin cores in beta-thalassemia/hemoglobin E. Biol Met 1991;4:162-5

Stark DD BN, Moss AA, Bacon BR et al. Nuclear magnetic resonance imaging of experimentally induced liver disease. Radiology 1983; 148:743-51

Stark DD, Moseley ME, Bacon BR, Moss AA, Goldberg HI, Bass NM, James TL. Magnetic resonance imaging and spectroscopy of hepatic iron overload. Radiology 1985; 154: 137-42

Stark DD. Hepatic iron overload: paramagnetic pathology. Radiology 1991; 179: 333-5

Steudel A, Krahe T, Becher H, Steudel H. Kardiomyopathie bei idiopathischer hamochromatose; diagnostische moglichkeiten mit der kernspintomographie. DMW 1987; 112:590-2

Tondury P, Kontoghiorghes GJ, Ridolfi-Luthy A, Hirt A, Hoffbrand AV, Lottenbach AM, Sonderegger T, Wagner HP. L1 (1,2-dimethyl-3-hydroxypyrid-4-one) for oral iron chelation in patients with beta-thalassaemia major. Br J Haematol 1990;76:550-3

Trent RJ, Williams BG, Kearney A, Wilkinson T, Harris PC. Molecular and hematologic characterization of Scottish-Irish type (epsilon gamma delta beta) zero thalassaemia. Blood 1990;76:2132-2138

Valdes-Cruz LM, Reinecke C, Rutkowski M, Dudell GG, Goldberg SJ, Allen HD, Sahn DJ, Piomelli S. Preclinical abnormal segmental cardiac manifestations of thalassaemia major in children on transfusion-chelation therapy: Echographic alterations of left ventricular posterior wall contraction and relaxation patterns. Am Heart J 1982; 103:505-11

Villeneuve JP, Bilodeau M, Lepage R, Cote J, Lefebvre M. Variability in hepatic iron concentration measurement from needle-biopsy specimens. J Hepatol 1996; 25: 172-7

Voogd A, Sluiter W, van Eijk HG, Koster JF. Low molecular weight iron and the oxygen paradox in isolated rat hearts. J Clin Invest 1992; 90:2050-5

Wacker CM, Bock M, Hartlep AW, Bauer WR, van Kaick G, Pfleger S, Ertl G, Schad LR. BOLD-MRI in 10 patients with coronary artery disease: Evidence for imaging of capillary recruitment in myocardium supplied by the stenotic artery. MAGMA 1999;8:48-54

Wacker P, Halperin DS, Balmer-Ruedin D, Oberhansli I, Wyss M. Regression of cardiac insufficiency after ambulatory intravenous deferoxamine in thalassaemia major. Chest 1993;103:1276-1278

Wands JR, Rowe JA, Mezey SE. Normal serum ferritin concentrations in precirrhotic haemochromatosis. N Eng J Med 1976; 294:302-5

Waxman S, Eustace S, Hartnell GG. Myocardial involvement in primary hemochromatosis demonstrated by magnetic resonance imaging. AHJ 1994; 128 1047-49

Weatherall DJ, Pippard MJ, Callender ST. Editorial retrospective. Iron loading in thalassemia--five years with the pump. N Engl J Med 1983;308:456-8

Weatherall DJ. Common genetic disorders of the red cell and the "malaria hypothesis". Ann Trop Med Parasitol 1987; 81:539-48

Weatherall DJ. The thalassaemias. In: The molecular basis of blood diseases. 2nd edition. WB Saunders 1994:157-205

WeatherallDJ, Clegg JB. Thalassaemia – a global public health problem. Nat Med 1996a; 2:847-9

Weatherall DJ. Anaemia as a World Health Problem. Oxford Textbook of Medicine. Oxford University Press 1996b; 22. 3463–82

Weatherall DJ. Fortnightly Review. The Thalassaemias. BMJ 1997; 314: 1675-8

Wolfe l, Olivieri N, Sallan D, Colan S, Rose V, Propper P, Freedman H, Nathan D. Prevention of cardiac disease by subcutaneous deferoxamine in patients with thalassaemia major. N Eng J Med. 1985; 312:1600-1603

Zurlo MG, De Stefano P, Borgna-Pignatti C, Di Palma A, Piga A, Melevendi C, Di Gregorio F, Birattini MG, Terzoli S. Survival and causes of death in thalassaemia major. Lancet 1989; 2: 27-30

CHAPTER 13: APPENDICES

13.1 PUBLICATIONS ARISING FROM THIS WORK

PEER REVIEWED PAPERS

Anderson L, Holden S, Davis B, Prescott E, Charrier C, Bunce N, Firmin D, Wonke B, Porter J, Walker JM, Pennell D. Cardiovascular T2* magnetic resonance for the early diagnosis of myocardial iron overload. European Heart Journal 2001; 20 (23). In press.

Anderson L, Wonke B, Holden S, Prescott E, Walker JM, Pennell D. Improved Cardioprotection in Thalassaemia with the Oral Iron Chelator Deferiprone Compared to Standard Treatment with Subcutaneous Desferrioxamine. Submitted to the Lancet.

Anderson L, Holden S, Davis B, Prescott E, Wonke B, Porter J, Walker JM, Pennell D. Reversal of Iron-induced Cardiomyopathy: a Prospective Study with Cardiac Magnetic Resonance. In preparation for Circulation

Anderson L, Holden S, Davis B, Prescott E, Wonke B, Porter J, Walker JM, Pennell D. Conventional Markers of Iron Overload cannot Predict Cardiac Risk in Thalassaemia Major. In preparation for JAMA.

Anderson L, Holden S, Davis B, Prescott E, Charrier C, Bunce N, Firmin D, Wonke B, Porter J, Walker JM, Pennell D. The Variability of Reticulo-endothelial and Parenchymal Iron Deposition in Thalassaemia Major. In preparation for the British Journal of Haematology.

REVIEW PAPERS

Rajappan K, Bellenger NG, Anderson L, Pennell DJ. The role of cardiovascular magnetic resonance in heart failure. European Journal of Heart of Heart Failure 2000;2:241

ABSTRACTS

Anderson LJ, Holden S, Davis BA, Prescott E, Charrier C, Bunce NH, Firmin DN, Porter JB, Wonke B, Walker JM, Pennell DJ. A novel method of cardiac iron measurement using magnetic resonance T2* imaging in thalassemia: Validation and clinical application. Circulation 2000; 102 (suppl II):403

Anderson L, Porter JB, Wonke B, Walker JM, Holden S, Davis BA, Prescott E, Charrier C, Firmin DN, Pennell DJ. Cardiac iron deposition is not predicted by conventional markers of iron overload in homozygous beta-thalassaemia. Blood 2000; 96 (suppl I):606a

Anderson L, Porter JB, Wonke B, Walker JM, Holden S, Davis BA, Prescott E, Charrier C, Firmin DN, Pennell DJ. Relationship of myocardial iron overload to right and left ventricular function in homozygous beta-thalassemia. Blood 2000; 96 (suppl I); 605a

Anderson L, Holden S, Davis B, Prescott E, Charrier C, Firmin D, Wonke B, Porter J, Walker JM, Pennell DJ. The aetiology of heart failure in iron overload. JACC 2001;37 (suppl 2):161A

Anderson L, Wonke B, Prescott E, Holden S, Walker JM, Pennell DJ. Improved cardioprotection with the oral iron-chelator L1, over standard therapy with subcutaneous deferoxamine in iron overload cardiomyopathy. JACC 2001;37 (suppl 2):218A

Anderson L, Charrier C, Firmin D, Porter J, Wonke B, Walker JM, Holden S, Davis B, Prescott E, Pennell DJ. Cardiac magnetic resonance for the early diagnosis of myocardial iron overload. JCMR 2001;5:

Anderson L, Bunce N, Davis B, Charrier C, Porter J, Firmin D, Holden S, Prescott E, Wonke B, Walker JM, Pennell D. Reversal of siderotic cardiomyopathy: A prospective study with cardiac magnetic resonance (CMR). Heart 2001; 85(suppl 1):33

Vogel MF, Anderson L, Deanfield JE, Walker JM. Quantitative assessment of global and regional myocardial function in patients with thalassemia major with and without myocardial iron overload. JACC 2001;37(2):168A

13.2 PERSONAL CONTRIBUTION TO THE RESEARCH

This project stemmed from a grant application made to the British Heart Foundation in 1998 entitled "Assessment of Myocardial Iron using Magnetic Resonance T2 – Relaxometry. Optimization of Chelation Therapy in Thalassaemia for Prevention of Cardiac Mortality". I wrote the first draft for this application and was subsequently awarded a 2-year British Heart Foundation Junior Fellowship, commencing in November 1998, under the supervision of Professor Dudley Pennell at the Cardiovascular Magnetic Resonance Unit at the Royal Brompton Hospital. This was subsequently extended to a 3-year BHF Junior Fellowship ending in September 2001.

I initiated the T2* technique after spin-echo and fast-spin-echo techniques proved to have poor reproducibility in the heart. Following early promising results with this technique, the sequence was enhanced on my behalf by the physics team at the Cardiovascular MR Unit (Clare Charrier and David Firmin). Using the T2* sequence. I personally scanned and analysed the results from all patients included in this thesis. The patients all come from one of two sources.

1. The Thalassaemia Cardiomyopathy Clinic at University College Hospital, London, under the supervision of Dr J Malcolm Walker, myself and Sr Sally Holden.

2. Recruitment by the hematology teams at the Whittington hospital, London (Dr Beatrix Wonke, Sr Emma Prescott) and University College Hospital, London (Professor John Porter, Dr Bernard Davis).

Validation of the T2* technique was accomplished by using liver iron measurements in patients undergoing liver biopsy. Sr Emma Prescott performed these biopsies at The Whittington Hospital, London.

I have compared and analyzed all the results personally, and have sought statistical advice from Melissa Wright, based initially at the statistical unit at The Hammersmith Hospital, London, now based at Bristol University Statistical Unit. Reproducibility data was analyzed by Dr Nicholas Bunce of the Cardiovascular Magnetic Resonance Unit, Royal Brompton Hospital, London.

13.3 SUPERVISION

My supervisor for this research was Professor Dudley Pennell, director of the Cardiovascular Magnetic Resonance Unit at the Royal Brompton Hospital, London. The development of the T2* sequence, scanning of all patients and analysis of results was carried out at the Cardiovascular MR Unit.

I received additional supervision and advice from Dr J Malcolm Walker, consultant cardiologist and head of the Thalassaemia Cardiomyopathy Clinic, University College Hospital, London, Dr Beatrix Wonke, consultant haematologist at the Whittington Hospital, London and Professor John Porter, consultant haematologist at University College Hospital, London.

13.4 RESEARCH FUNDING

This project was funded by a Junior Fellowship grant from the British Heart Foundation (FS/98064).